OCCURRENCE AND STABILITY OF GLACIATIONS IN GEOLOGIC TIME

A Dissertation

by

KELIN ZHUANG

Submitted to the Office of Graduate Studies of
Texas A&M University
in partial fulfillment of the requirements for the degree of

DOCTOR OF PHILOSOPHY

August 2010

Major Subject: Geology

OCCURRENCE AND STABILITY OF GLACIATIONS IN GEOLOGIC TIME

A Dissertation

by

KELIN ZHUANG

Submitted to the Office of Graduate Studies of
Texas A&M University
in partial fulfillment of the requirements for the degree of

DOCTOR OF PHILOSOPHY

Approved by:

Co-Chairs of Committee,	John Giardino
	Jerry North
Committee Members,	Robert Korty
	Steven Quiring
	John Vitek
Head of Department,	Andreas Kronenberg

August 2010

Major Subject: Geology

ABSTRACT

Occurrence and Stability of Glaciations in Geologic Time.

(August 2010)

Kelin Zhuang, B.S., Nanjing University; M.S., Ocean University of China

Co-Chairs of Advisory Committee: Dr. John Giardino
Dr. Jerry North

Earth is characterized by episodes of glaciations and periods of minimal or no ice through geologic time. Using the linear energy balance model (EBM), nonlinear EBM with empirical ice sheet schemes, the general circulation model coupled with an ice sheet model, this study investigates the occurrence and stability of glaciations in geologic time.

The simulations since the last glacial maximum (LGM) suggest that the summertime thawline of ice sheets conforms closely to the equatorward edge of the ice sheets and implies the relative stability toward deglaciation.

CO_2 levels are indispensable in controlling the initiation of ice sheet in the Cretaceous. At low CO_2 levels, ice sheets exist in all periods no matter LGM or the last interglacial (LIG) orbital elements; however, at high CO_2 levels ice sheets rarely exist.

The simulations agree well with recent geological evidence of the hysteresis of glaciations in the Permo-Carboniferous. Gondwanaland reached its glacial maximum when CO_2 level was roughly the same or slightly higher than the preindustrial value. With a further increase of CO_2, deglaciation dominates and results in an ice free state. Again, if CO_2 decreased to the present level, Gondwanaland would be glaciated once more and start a new cycle of glaciation and deglaciation.

Simulations from five paleogeography maps in Gondwanaland with a suite of CO_2 levels and different orbital elements reveal that paleogeography, CO_2 levels and the Milankovitch cycles all contribute to the glaciations of Gondwanaland.

This study shows that orbital elements alone are insufficient to account for the evolution of ice sheets. Net radiative forcing caused by greenhouse gases, such as CO_2 and solar constant change are the primary drivers to glacial inception or demise. Continental geography, CO_2 levels, solar constant change, and the Milankovitch cycles complicate the glacial history of Earth.

DEDICATION

To my wife Jiying and son Kevin

ACKNOWLEDGEMENTS

I gratefully acknowledge my advisors Dr. John Giardino and Dr. Jerry North for their encouragement, guidance, patience, and extraordinary support during this research. Dr. Jerry North has kindly instructed my modeling step by step and broadened my scope of paleoclimatology. I would also like to express my gratitude to Dr. Robert Korty for his constructive advice. I thank the other members of my committee, Dr. Quiring for his weather and climate seminar, and Dr. John Vitek for his talk on the history of paleoclimate research in geology.

I would like to thank Dr. David Pollard for his guidance of the general circulation model, Dr. Ralph Greve for his assistance of the ice sheet model for this research, and Dr. Ethan Grossman for his reference recommendation of the Paleozoic time.

I also want to extend my gratitude to Steve Tran, who coordinated the Sunfire linux server which made the simulation highly efficient. Thanks also go to my friends and the department faculty and staff for making my time at Texas A&M University a great experience.

Finally, thanks go to my wife and son for their patience and love.

NOMENCLATURE

EBM	The Energy Balance Climate Model
GCM	The General Circulation Model
GENESIS	The Global and Environmental and Ecological Simulation of Interactive Systems Climate Model
L2DEBM	The 2-Dimensional Energy Balance Model
LGM	The Last Glacial Maximum
LIG	The Last Interglacial
Ma	Million Years Ago
PAL	The Preindustrial Level of CO_2
SICOPOLIS	The Simulation Code for Polythermal Ice Sheets

TABLE OF CONTENTS

CHAPTER Page

LIST OF FIGURES

Page

Page

Page

Page

LIST OF TABLES

CHAPTER I

INTRODUCTION

Glaciations interspersed between non-glaciations are common features of the history of Earth (e.g., Frakes, 1979; Fisher, 1982; Frakes and Francis, 1988; Crowley and North, 1991; Frakes et al., 1992; Crowell, 1999; Veizer et al., 2000; Crowley and Berner, 2001). Many theories have been proposed to explain glaciations such as the Milankovitch cycles, radiative forcing changes, including solar output and greenhouse effect, polar land shifts, biogeochemical interplay and even bolide impacts (e.g., Hays et al, 1976; Berger, 1978; Imbrie and Imbrie, 1980; Berner et al., 1983; Crowley et al., 1987; Crowley et al., 1992; Berner and Kothavala, 2001; Huybers, 2006; Drysdale et al., 2009).

With this knowledge, could we use climate models to reconstruct glaciations in geologic time? Further, could we investigate the occurrence and stability of glaciations in geologic time using climate models and have the simulation results consistent with geological evidence? A basic problem here is if net radiative forcing, paleogeography, paleobotany induced albedo, orbital elements, geothermal heat flux and other associated parameters are given, could we reconstruct the glacial and deglacial history on Earth and reconcile the model results with evidence in the geologic record?

This dissertation follows the style of Quaternary Research.

The objective of this study is to reconstruct the occurrence and stability of glaciations in geologic time by the nonlinear two dimensional energy balance model (EBM) with ice sheet schemes based on seasonal temperature under the scenario of various CO_2 levels. The linear EBM, nonlinear EBM, the general circulation model GENESIS (the global and environmental and ecological simulation of interactive systems climate model) and the ice sheet model SICOPOLIS (the simulation code for polythermal ice sheets) are used.

A suite of numerical schemes is applied to investigate the possibility and stability of glaciations in geologic time. A nonlinear energy balance model (EBM) from Stevens' linear version (Stevens and North, 1996) with ice sheet schemes based on seasonal temperature has been developed for this study. A linear EBM and a general circulation model GENESIS (the global and environmental and ecological simulation of interactive systems climate model) coupled with an ice sheet model SICOPOLIS (the simulation code for polythermal ice sheets) are also employed to explore glacial developments.

In Chapter II, the CO_2-induced radiative forcing and the Milankovitch cycles are investigated in detail. Is the Milankovitch cycle alone sufficient to cause the evolution of ice sheets in geologic time? Are net radiative forcing caused by greenhouse gases, such as CO_2 and solar constant change important to glacial inception or demise? Through the demonstration of a series of iteration steps, the robustness of the model is discussed as well.

In Chapter III, deglaciation since the last glacial maximum (LGM) using a linear EBM is discussed. Does the summertime thawline of ice sheets conform closely to the equatorward edge of the ice sheets? A common sense is that ice sheets should stay within the thawline of summer temperature. Is this phenomenon well presented in the EBM?

In Chapter IV, the possibility of glaciation in the Cretaceous is explored. The Cretaceous is generally considered to be warm and ice free; however, recently more and more geological evidence has questioned this viewpoint. What does the nonlinear EBM contribute to this discussion?

In Chapter V, the author delves into the hysteresis of glaciations in the Permo-Carboniferous. The Permo-Carboniferous is not glacial all the time as previously considered; it has deglacial intervals called lacuna. How does the nonlinear EBM explain the hysteresis of glaciations? Could a similar glacial picture develop using GENESIS and SICOPOLIS?

In Chapter VI, the occurrence and stability of Gondwanaland is simulated in detail from the Pre-Cambrian until the early Triassic. What factors control the development of ice sheets in Gondwanaland? Continental geography, CO_2 levels, and the Milankovitch cycles will be discussed in the nonlinear EBM model.

Finally, the major findings of this research will be summarized in Chapter VII. This study shows that orbital elements alone are insufficient to account for the evolution of ice sheets. Net radiative forcing caused by greenhouse gases, such as CO_2 and solar constant change are the primary drivers to glacial inception or demise. Continental geography, CO_2 levels, solar constant change, and the Milankovitch cycles complicate the glacial history of Earth.

CHAPTER II

CO_2-FORCED CLIMATE AND THE MILANKOVITCH CYCLE

Synopsis

A nonlinear EBM with empirical ice sheet scheme is developed and applied to the LGM and presented to explore the robustness of the model. The sensitivity tests show that the model is capable of investigating the occurrence and stability of glaciations in geologic time. The CO_2 level and the Milankovitch cycles contribute to the glaciation process. Lower CO_2 lowers the global temperature and the nonlinear iteration finally builds up the ice sheets from ice-albedo feedback. The high ice albedo enhanced the growth of ice sheets. Net radiative forcing caused by greenhouse gases such as CO_2 and solar constant change are the primary drivers to glacial inception or demise. The Milankovitch cycles adjust the waxing and waning of ice sheets.

Introduction

EBM was first proposed by Budyko (1969) and Sellers (1969). Later North and his colleagues developed this annual average model into seasonal and nonlinear (e.g., North et al., 1983; Crowley and North, 1988; Crowley and North, 1991). Calculating the seasonal cycle as a function of solar input, longwave radiation and geography, EBM has been successfully applied in paleoclimatology (e.g., Crowley and North, 1991; Baum

and Crowley, 1991; Hyde et al., 1990; North et al., 1983). The accuracy of EBM was tested in the 1970s and 1980s using the present climate (e.g., North et al, 1983; Hyde et al., 1990; Crowley and North, 1991). Previous studies have revealed that EBM agrees well with the present climate and can reach the accuracy of GCMs in terms of surface temperature (Crowley and North, 1991; Hyde et al., 1989). The present study originated from the linear EBM which was consistent with the present climate responded with natural and anthropogenic forcings (Stevens and North, 1996).

The problem set out to study is how satisfactory and consistent is the simulation of the seasonal cycle of the surface temperature field, given the values of the various changes in the driving agents from the present values. I will explore what the summer temperature field would be in geologic time with the known distribution of albedo because of the placement of ice, the value of the orbital elements (eccentricity, obliquity and seasonal time of perihelion), and the concentrations of the greenhouse gases. Changes in aerosols or elevation of the ice sheet surface will not be taken into account. The objective of the study is to test if the results of EBM simulations agree with the distributions of ice sheets in geologic time. In a strict sense, EBM can only give us a sensitivity study about the geologic past (e.g., North et al., 1983; Crowley and North, 1991); The conceptual modeling, however, may shed light on some of the more robust features that leads to significant questions in more sophisticated modeling experiments.

A seasonal two-dimensional EBM (Stevens and North, 1996) will be extended with a simple ice sheet scheme to simulate the glacial and deglacial possibility. CO_2 was established as an important radiative forcing variable with a formula introduced by Myhre et al. (1998). The simple ice sheet buildup scheme was similar to Hyde et al. (1990). Any land with monthly average temperature less than -2ºC is defined as ice covered; meanwhile, any sea with monthly average temperature less than -4ºC is stipulated as having sea ice. The nonlinear EBM with ice sheet feedback mechanism with orbital elements and CO_2 will test the occurrence and distribution of glaciation with a seasonal ice sheet scheme (Hyde et al., 1990; Hyde et al., 2006).

Model Description

The energy balance model is expressed as:

$$C(\theta,\phi)\frac{\partial T(\theta,\varphi,t)}{\partial t} - \nabla\cdot[D(\theta,\phi)\nabla T(\theta,\varphi,t)] + A + BT(\theta,\varphi,t) = QS(\theta,t)[1-\alpha(\theta,t)] \qquad (1)$$

where the independent variables are the latitude, θ, longitude, φ, and time, t. $C(\theta,\varphi)$ is the heat capacity, $D(\theta,\varphi)$ is the diffusion coefficient, A and B are the longwave radiation parameters with values of 210.3 Wm^{-2} and 2.15 $Wm^{-2}℃^{-1}$, respectively, for present climate, Q is solar constant with a value of 1371.75 Wm^{-2} for present climate (Stevens and North, 1996) , $S(\theta,t)$ is the solar insolation where orbital elements including the eccentricity, obliquity and longitude of the perihelion are calculated based on Berger (1978). $\alpha(\theta,t)$ is planetary albedo.

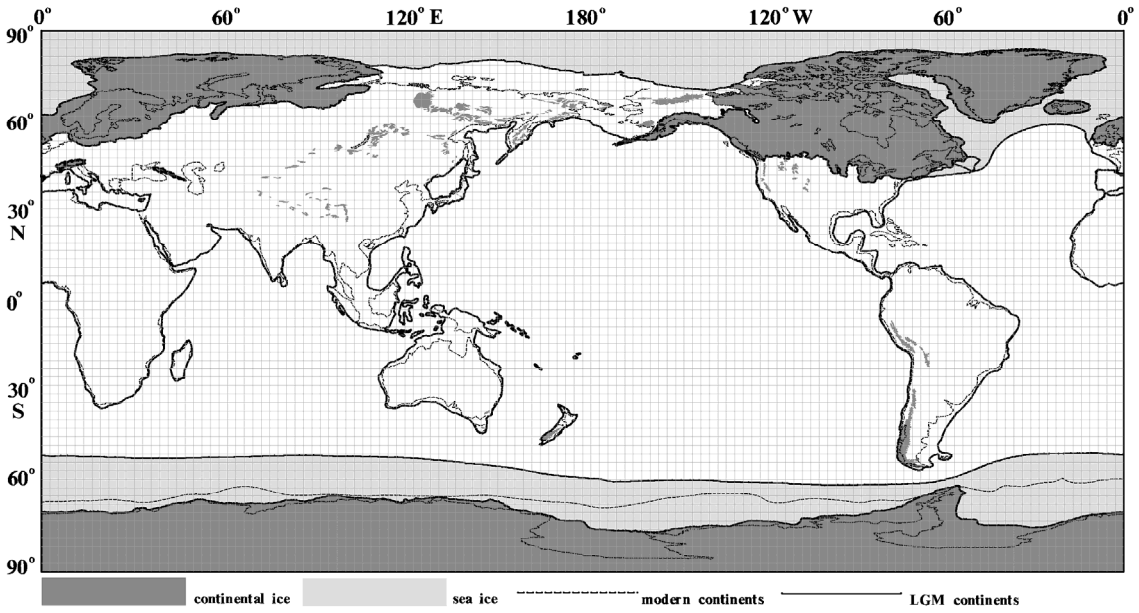

Figure 1. EBM calculation grid points in LGM paleogeography. EBM divides the globe into 128 longitudinal x 65 latitudinal grid points on the globe including the poles with a space interval of 2.8125° x 2.8125° with a resolution is similar to that of a spectral GCM with T42 truncations.

48 time steps occur in a year; hence, each time step is equal to 7.6 days. The first time step is at the vernal equinox. Four time steps occur in each month. The astronomical year instead of the calendar year is used in the model. 128 longitudinal x 65 latitudinal grid points occur on the globe including the poles with a space interval of 2.8125° x 2.8125° and a resolution is similar to that of a spectral GCM with T42 truncations (Fig. 1). The

full multigrid algorithm is used to numerically solve the above equation (Huang and Bowman, 1992; Stevens and North, 1996).

Simulation Results

An albedo scheme is applied similar to Hyde et al. (1990) and Mengel et al. (1988). Whenever temperature is greater than ice thresholds which are -2ºC for land and -4ºC for sea, land albedo is $0.30+0.09\times P_2(x)$, where $P_2(x)$ is the second-order Legendre polynomial, $(3x^2-1)/2$, x is the sine of latitude; sea albedo $0.29+0.09\times P_2(x)$; sea ice albedo 0.40, and land ice 0.68. If temperature at the time is lower than ice thresholds, land turns into ice and sea into sea ice and the albedos change accordingly. Based on the successful simulation of present climate, the model is extended to the last glacial maximum (LGM) with a set of CO_2 levels and orbital elements. The nonlinear iteration is as follows: Start with zero ice state, the monthly temperature stipulates the ice existence: T< -2 ºC, land ice; T< -4 ºC, sea ice (Hyde et al., 1990). At each run ice/land and sea/sea ice boundary and albedo changed based on the previous run until equilibrium reached.

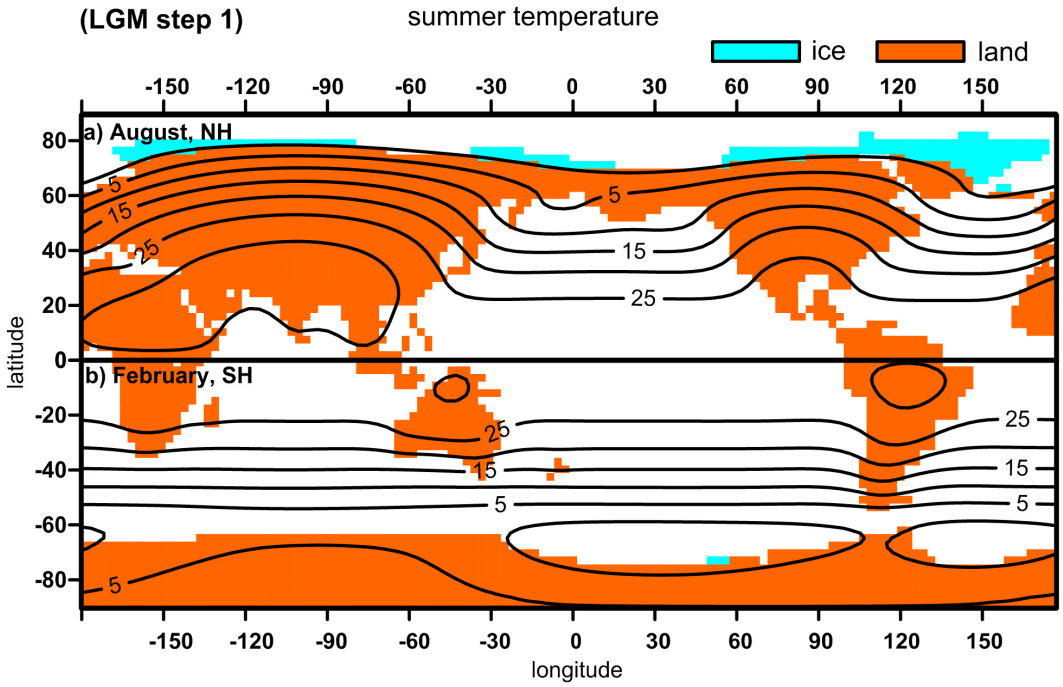

Figure 2. The stability of ice sheets at iteration step 1. The orbital elements are the LGM and CO_2 level is the LGM level as well. Start with ice free state, the EBM has the first convergent run. Based on the summer temperature of previous run, an ice albedo feedback is introduced by stipulating land ice if summer temperature of the given land grid point is less than -2℃ and sea ice if summer temperature of the given sea grid point is less than -4℃. The newly changed geography is input into the next run of the EBM calculation until the final equilibrium state. This shows the first step. Ice sheets stay within the 0℃ isotherms of summer temperature and imply their stability.

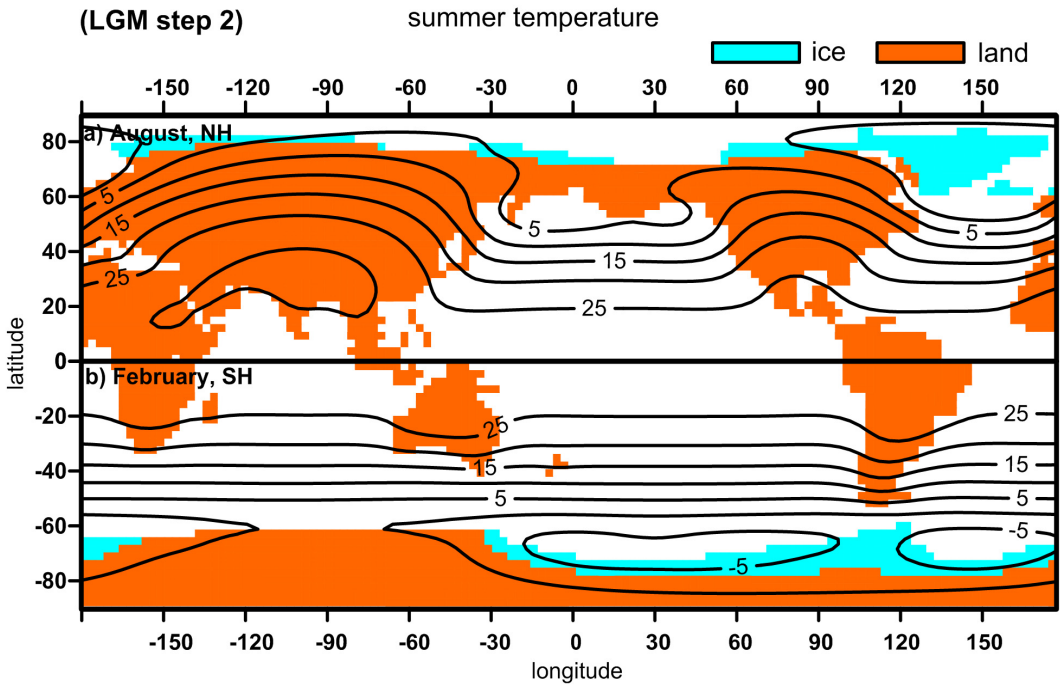

Figure 3. The stability of ice sheets at iteration step 2. The orbital elements are the LGM and CO_2 level is the LGM level as well. Start with ice free state, the EBM has the first convergent run. Based on the summer temperature of previous run, an ice albedo feedback is introduced by stipulating land ice if summer temperature of the given land grid point is less than -2℃ and sea ice if summer temperature of the given sea grid point is less than -4℃. The newly changed geography is input into the next run of the EBM calculation until the final equilibrium state. This shows the second step. Ice sheets stay within the 0℃ isotherms of summer temperature and imply their stability.

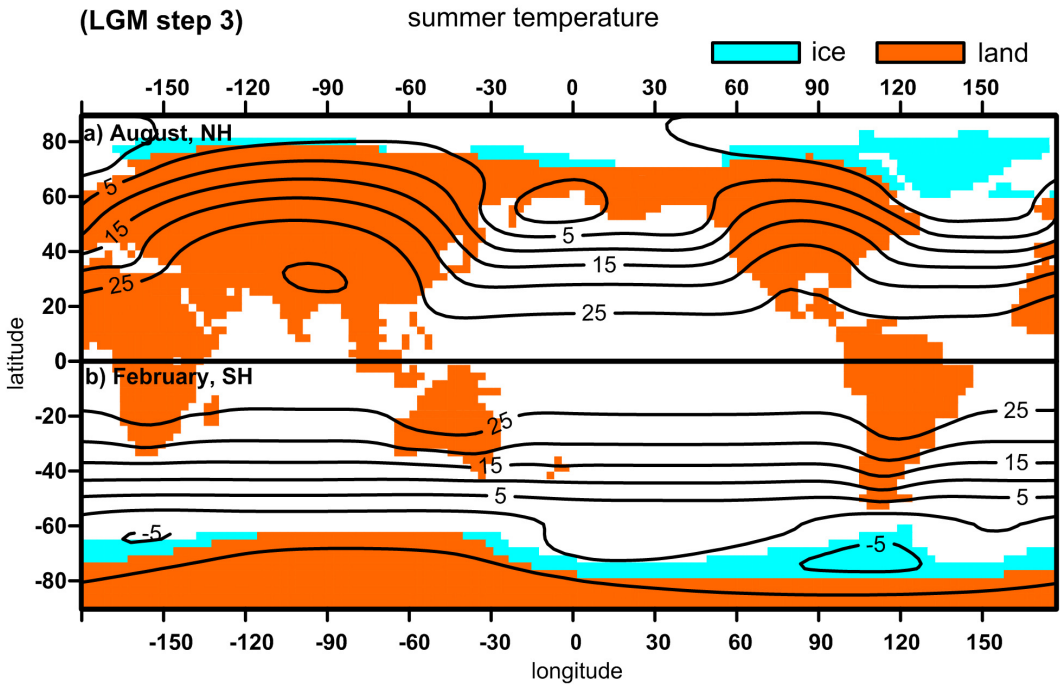

Figure 4. The stability of ice sheets at iteration step 3. The orbital elements are the LGM and CO_2 level is the LGM level as well. Start with ice free state, the EBM has the first convergent run. Based on the summer temperature of previous run, an ice albedo feedback is introduced by stipulating land ice if summer temperature of the given land grid point is less than -2℃ and sea ice if summer temperature of the given sea grid point is less than -4℃. The newly changed geography is input into the next run of the EBM calculation until the final equilibrium state. This shows the third step. Ice sheets stay within the 0℃ isotherms of summer temperature and imply their stability.

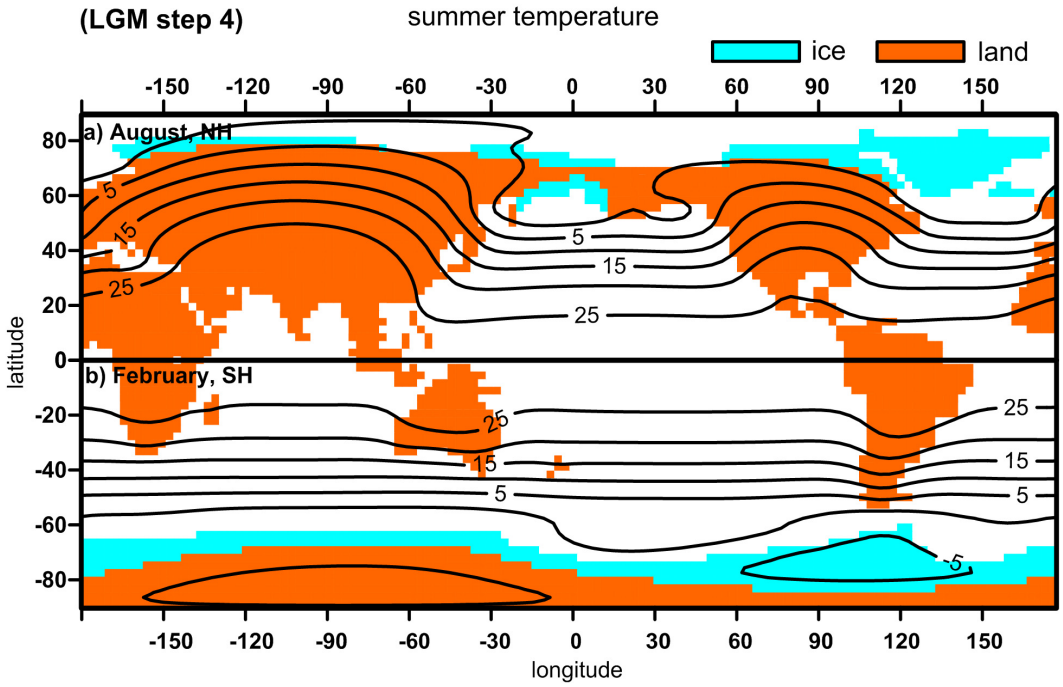

Figure 5. The stability of ice sheets at iteration step 4. The orbital elements are the LGM and CO_2 level is the LGM level as well. Start with ice free state, the EBM has the first convergent run. Based on the summer temperature of previous run, an ice albedo feedback is introduced by stipulating land ice if summer temperature of the given land grid point is less than -2℃ and sea ice if summer temperature of the given sea grid point is less than -4℃. The newly changed geography is input into the next run of the EBM calculation until the final equilibrium state. This shows the fourth step. Ice sheets stay within the 0℃ isotherms of summer temperature and imply their stability.

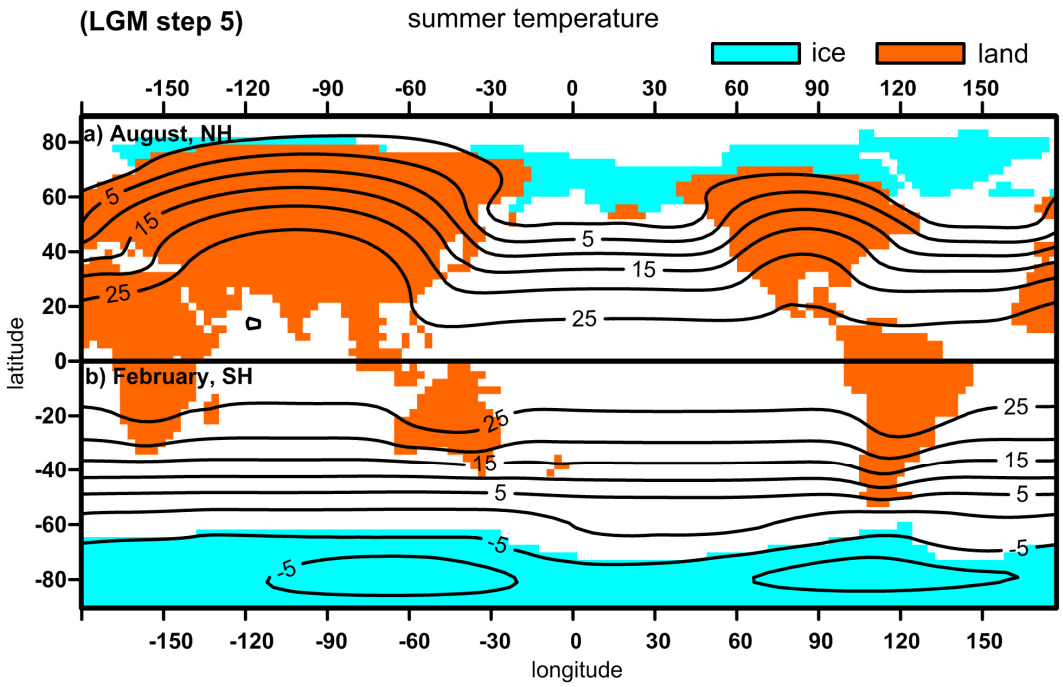

Figure 6. The stability of ice sheets at iteration step 5. The orbital elements are the LGM and CO_2 level is the LGM level as well. Start with ice free state, the EBM has the first convergent run. Based on the summer temperature of previous run, an ice albedo feedback is introduced by stipulating land ice if summer temperature of the given land grid point is less than -2℃ and sea ice if summer temperature of the given sea grid point is less than -4℃. The newly changed geography is input into the next run of the EBM calculation until the final equilibrium state. This shows the fifth step. Ice sheets stay within the 0℃ isotherms of summer temperature and imply their stability.

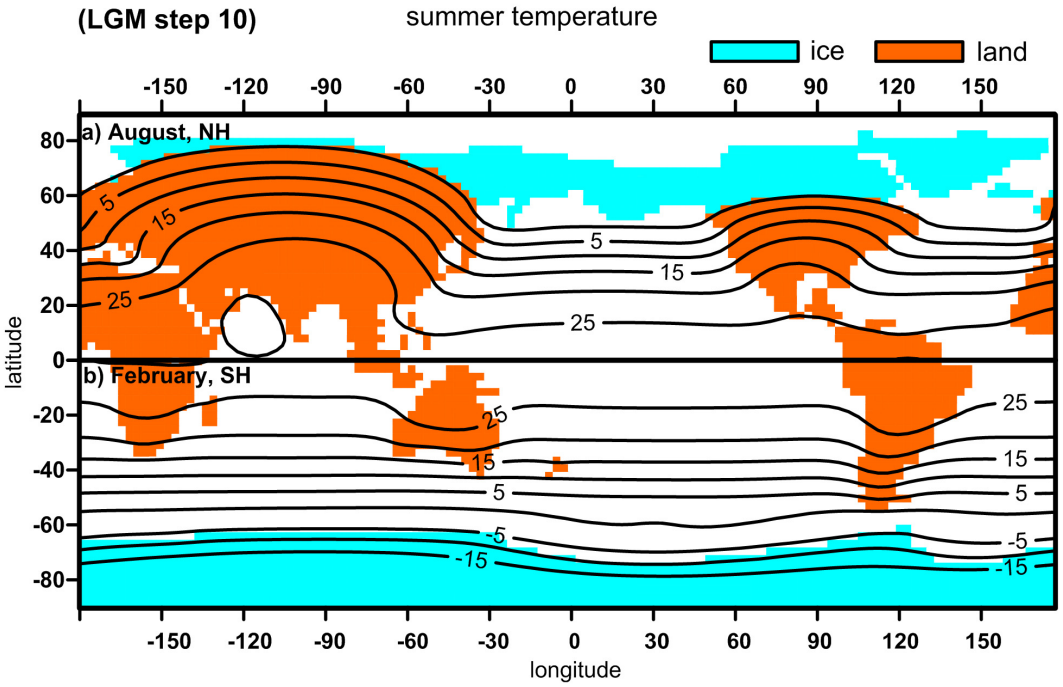

Figure 7. The stability of ice sheets at iteration step 10. The orbital elements are the LGM and CO_2 level is the LGM level as well. Start with ice free state, the EBM has the first convergent run. Based on the summer temperature of previous run, an ice albedo feedback is introduced by stipulating land ice if summer temperature of the given land grid point is less than -2℃ and sea ice if summer temperature of the given sea grid point is less than -4℃. The newly changed geography is input into the next run of the EBM calculation until the final equilibrium state. This shows the tenth step. Ice sheets stay within the 0℃ isotherms of summer temperature and imply their stability.

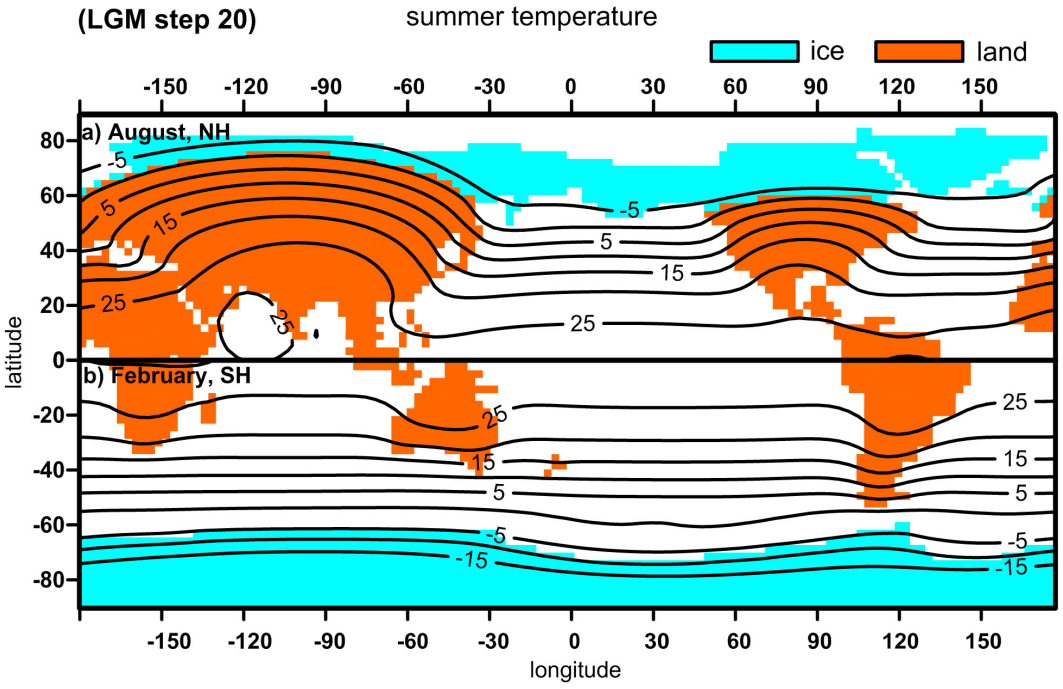

Figure 8. The stability of ice sheets at iteration step 20. The orbital elements are the LGM and CO_2 level is the LGM level as well. Start with ice free state, the EBM has the first convergent run. Based on the summer temperature of previous run, an ice albedo feedback is introduced by stipulating land ice if summer temperature of the given land grid point is less than -2℃ and sea ice if summer temperature of the given sea grid point is less than -4℃. The newly changed geography is input into the next run of the EBM calculation until the final equilibrium state. This shows the twentieth step which is the final equilibrium state. Ice sheets stay within the 0℃ isotherms of summer temperature and imply their stability.

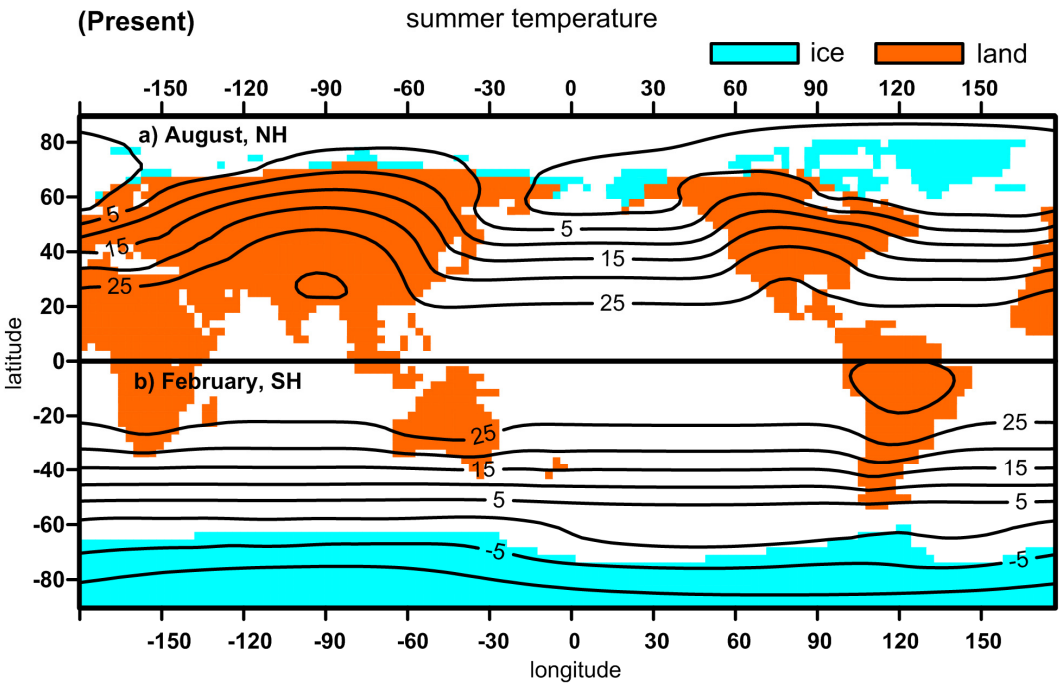

Figure 9. The final equilibrium state with present geography and present CO_2 level. The orbital elements are the LGM. Start with ice free state, the EBM has the first convergent run. Based on the summer temperature of previous run, an ice albedo feedback is introduced by stipulating land ice if summer temperature of the given land grid point is less than -2℃ and sea ice if summer temperature of the given sea grid point is less than -4℃. The newly changed geography is input into the next run of the EBM calculation until the final equilibrium state. This shows the final equilibrium state. Ice sheets stay within the 0℃ isotherms of summer temperature and imply their stability.

The simulations show that at each step ice sheets remain within the thawline of 0ºC isotherm during summer which means they are preserved even in summer.

Discussion

The simulations have shown that at each iteration step (Fig. 2 through Fig. 8) the ice sheet stays within the 0℃ isotherms of summer temperature and it demonstrates that the nonlinear algorithm is robust to apply to the study of occurrence and stability of glaciations in geologic time.

The simulations also show that under the same CO_2 level, ice sheet areas have similar results with high, low, or middle obliquity parameters without much difference. For example, at the same LGM CO_2 level, the area of ice sheets is 34.5 x 10^6 km^2 in high obliquity of 24.5°, the area of ice sheet is 36.7 x 10^6 km^2 in medium obliquity of 23.5°, and the area of ice sheet is 41.2 x 10^6 km^2 in low obliquity of 22.5°. But if we use the present CO_2 level, the ice sheet area even in low obliquity can only have a value slightly higher than the present ice sheet area (Fig. 9) which means that CO_2 induced radiative forcing plays a predominant role in the buildup of ice sheets and the orbital elements are secondarily important.

The CO_2 level and the Milankovitch cycle contribute to the glaciation process. Lower CO_2 lowers the global temperature and the nonlinear iteration finally builds up the ice sheets from ice-albedo feedback. The high ice albedo enhanced the growth of ice sheets.

Now the question is: how was the ice albedo feedback iteration possible? CO_2-induced global temperature is the answer. That is why at the same ice albedo condition a great ice sheet in the northern hemisphere can grow at the LGM and only Greenland at present.

So net radiative forcing caused by greenhouse gases such as CO_2 and solar constant change are the primary drivers to glacial inception or demise. The Milankovitch cycles adjust the waxing and waning of ice sheets. Figure 8 and Figure 9 have the same geography and orbital elements but different CO_2 levels, one can see a different glacial scenario.

CHAPTER III

DEGLACIATION SINCE THE LAST GLACIAL MAXIMUM IN A SIMPLE SEASONAL CLIMATE MODEL

Synopsis

A simple linear two dimensional energy balance model (L2DEBM) is applied to the present, the last glacial maximum (LGM), 15ka, 12ka and 9ka BP, respectively, with corresponding geography, albedo, concentrations of greenhouse gases and orbitally forced changes in seasonal insolation. The simulation results show that the summertime thawline conformed closely to the equatorward edge of the ice sheets and implied the relative stability toward deglaciation.

Introduction

Ice sheets on the surface of Earth at the LGM were not uniformly distributed around latitude belts. The ice at LGM was more plentiful in North America, Greenland and northwestern Europe compared to Siberia and eastern Asia. The apparent reason for this zonal inhomogeneity was the warmer summers over the larger continent of Asia (North et al., 1983). The locations of sea surface in the polar regions of North America tend to moderate the summer maximum temperatures and, therefore, make the persistence of winter and spring snow cover through the summer more likely. Recognition of the

importance of summer insolation (actually surface temperature) in the onset and growth of ice sheets dates back to Milankovitch (e.g., Crowley and North, 1991; Huybers, 2006). This chapter examines the distribution of ice and its stability within the context of the simple L2DEBM that includes a seasonal cycle. This class of climate models has a long history of successful applications in paleoclimate and modern climate problems (e.g., North et al., 1981; North et al., 1983; Stevens and North, 1996). Not all of these papers will be reviewed here, but note that the present model is simply a replica of those that were discussed in several of the earlier papers. The essential feature is its ability to simulate the two dimensional geographical seasonal cycle of temperatures for the present climate with a minimum number of phenomenological coefficients. This model can incorporate different levels of driving agents such as orbitally forced changes in seasonal insolation, changes in albedo and concentrations of greenhouse gases. The most compelling feature of the model is its simplicity.

The seasonal EBM has achieved remarkable progress in modeling glaciation throughout geologic time and provided significant insight into the role of seasonality, especially summer temperature, in the initiation and buildup of ice sheets (e.g., North et al., 1983; Crowley et al., 1986; Crowley et al., 1987; Crowley et al., 1989; Crowley and North, 1990; Crowley and Baum, 1992; Huybers, 2006; Crowley and Hyde, 2008); However, deglaciation in a sequence such as the decay of ice sheets since the LGM has been little discussed before. The problem set out to study is how satisfactory and consistent is the simulation of the seasonal cycle of the surface temperature field, given the values of the

various changes in the driving agents from the present values. What would the late summer temperature field be at the LGM with known distribution of albedo because of the placement of ice, the value of the orbital elements (eccentricity, obliquity and seasonal time of perihelion), and the concentrations of the greenhouse gases? Changes in aerosols or elevation of the ice sheet surface were not taken into account. These parameters are easily incorporated into the L2DEBM, and steady repeating seasonal cycles extracted. Moreover, how well was the model able to simulate the same field at different periods since the LGM at which appropriate parameter values are also known (CLIMAP, 1976; CLIMAP, 1981; Barnola et al., 1987)?

Another explored question was whether more than one climate solution with different ice sheet configurations was possible for the same external forcings. For example, might it be possible with the same parameter values (except albedo) to have a solution with the present ice configuration but associated with the LGM values of orbital and greenhouse parameters? The answer to this question turned out to be affirmative, which suggests that the ice sheet at the LGM might have been unstable and on its way to disintegration, limited only by the time constants necessary for its demise.

Why use the energy balance model when coupled ocean-atmosphere general circulation models (GCM) are available? Such experiments are costly and require considerable investment of human capital. The conceptual modeling may shed light on some of the more robust features that leads us to ask good questions in more sophisticated modeling

experiments. Indeed, the simulation results will show that such experiments would be very interesting.

Description of the L2DEBM

The model is physically the same as that described by North et al. (1983), a two dimensional energy balance model whose solution is the seasonal cycle of the surface temperature field. It is governed by the equation

$$C(\hat{r})\frac{\partial T}{\partial t} + A + BT = \nabla \cdot (D(\hat{r})\nabla T) + QS(\hat{r},t)a(\hat{r}) \qquad (2)$$

where C is an effective heat capacity as a function of position for a column of air over the land surface, but over ocean it refers to the much larger mixed layer of the ocean; A and B are phenomenological coefficients that can be estimated from satellite data. These parameters were all taken from Stevens and North (1996) for the present climate. B with a value of 2.15 $Wm^{-2o}C^{-1}$ (Kyle et al., 1995) is very important in determining the sensitivity of the seasonal cycle and mean annual changes in the forcing agents; its value incorporates all the feedbacks such as water vapor, lapse rate and cloud cover. A is adjusted using the well known logarithmic dependence on the concentration of CO_2 (Myhre et al., 1998) for paleoclimate simulations. It is worth mentioning that the value of B leads to a sensitivity to doubling CO_2 (~2.5K). The local thermodynamic relaxation time scale is C/B and varies from land to sea. The heat is transported horizontally by the simple mechanism of diffusion across isotherms. D has a parabolic dependence on sine of latitude which is slightly smaller near the poles and larger over the oceans. Q with a

value of 342 Wm^{-2} is the solar constant divided by four. *S* is the seasonal and latitudinal distribution of insolation which depends on the orbital parameters. The local coalbedo is given by 1-*a*, which has a small value over ice and a mild latitude (mostly zenith angle) dependence otherwise.

In the parlance of climate modeling this is a mixed layer model which allows some transport in the oceans via prescribing a heat flux at the ocean surface in some simulations to see how robust the solutions are. It turns out that none of the conclusions are sensitive to this detail. In solving the model a finer grid than most of the earlier investigators is employed with the same spatial resolution as the T42 truncation GCM.

Whereas the whole seasonal cycle is interesting, I focus on the summer temperature field because of the polar extent of the thaw line. The model does not include a seasonal snow line that would introduce a nonlinearity tending to enhance the amplitude of the cycle. This omission may not be so important in this study because the sun is overhead mostly in summer when the snow cover is least. Even in winter the sun is low in the sky when snow cover is largest.

The working hypothesis is that the summer thaw line determines the propensity for an ice sheet to grow or not (North et al., 1983; Huybers, 2006). No matter how much snow falls in winter, if the thaw line moves over the snow in summer no ice sheet can grow. Once ice is established and is thick such as at the LGM, many years may be required for

total removal. On the millennial time scales collapse (~10ka) is short compared to ice sheet buildup (~90ka), because the mechanisms for growth (cool summers for eligibility, but limited by lack of moisture in the form of snow) and decay (glacial flow, rapid melting and calving, etc.). The L2DEBM does not attempt to simulate an ice sheet budget because such an effort is far beyond the scope of this simple model without significant augmentation. Such a modeling effort may not even be justified. The simulations and the comparison with the available data serve as a check for consistency with the working hypothesis.

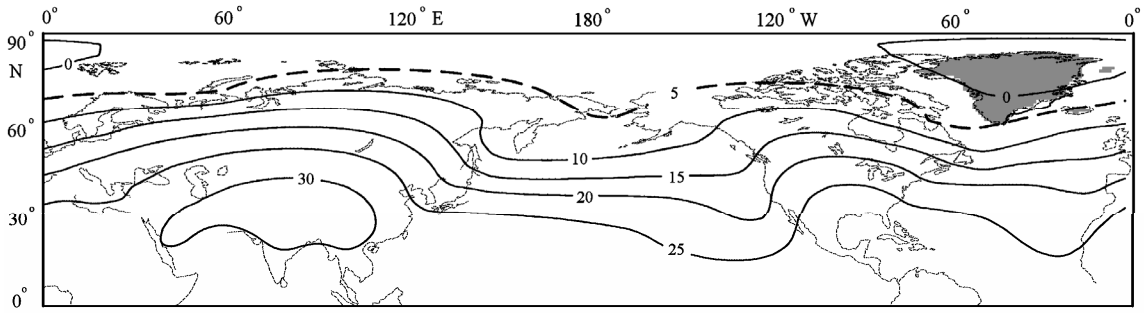

Figure 10. The present summertime surface temperature. The L2DEBM runs on the whole globe; only the northern hemisphere is shown here. The thawline defined as 5°C conforms well to the southern edge of the Greenland ice sheet which is gray-shaded.

Figure 10 shows the summertime temperature field for the present climate with the current ice sheets darkly shaded. The thaw line conforms rather snugly just outside the shores of Greenland and suggests that the ice configuration today is in very good agreement with the hypothesis. This was also noted in North et al. (1983) even without the high albedo on Greenland.

Simulations of LGM Climate

Now consider the placement of ice at the LGM. After A is altered to include the lower values of CO_2 of the LGM, the orbital elements and coalbedo of the ice sheets are changed to those of the LGM, the simulated summer temperature is shown in Figure 2a. Once again the thaw line is rather tightly conforming to the southern ice edge in North America and in Europe. Crowley (2000) and Kim et al. (2007) have shown that for the globe as a whole the global temperature cooler was by 2.5 - 4.5K. The simulation of this study shows that the changes are consistent with the global average changes (3.5K), and in addition the L2DEBM provides a summer thaw line that reaches right up to the edge of the LGM ice sheets.

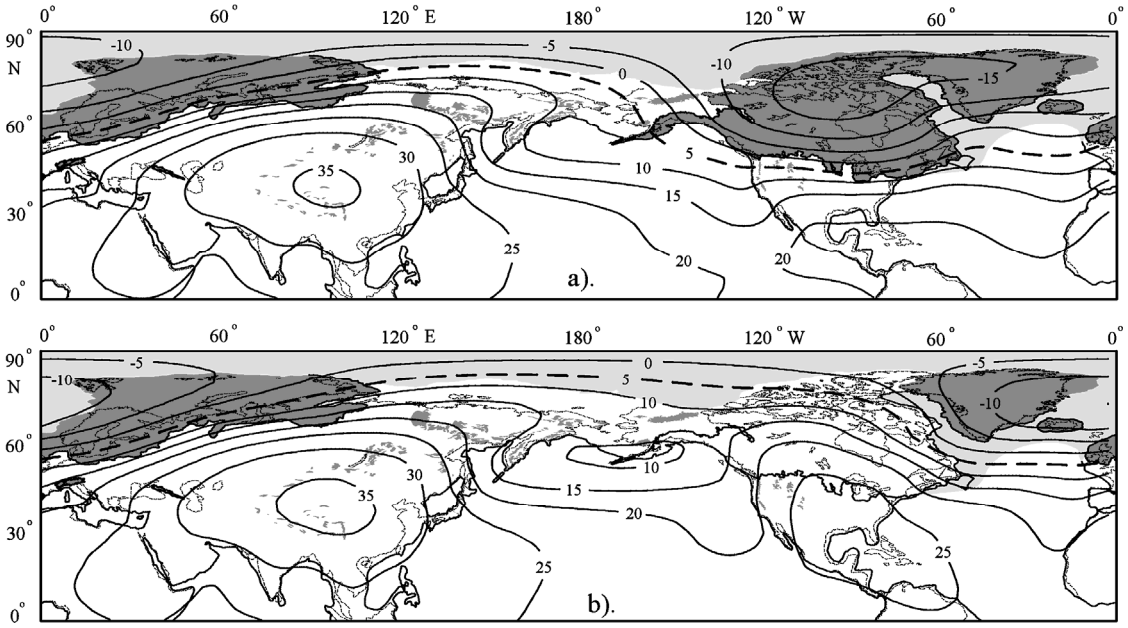

Figure 11. The summertime surface temperature distribution at the LGM with Laurentide ice sheet. (a) and without Laurentide ice sheet (b). The thawline of 5^{o}C tightly conforms to the southern edges of ice sheets both in North America and in Europe. If the Laurentide ice sheet were artificially removed, the surface temperature had a different distribution pattern in the regions of North America and Greenland. It is much warmer where the southern edge of the LGM ice sheet could reach 25ºC and proves that deglaciation trend since the LGM was irreversible.

An additional simulation with LGM parameters is designed except that the Laurentide Ice Sheet in North America is removed. The simulated summer temperature field is shown in Figure 11b. Curiously the thaw line now runs essentially to its present day simulated location. The linear model of this study cannot tell the stability of these two solutions (Laurentide and no-Laurentide), but it appears that two distinct solutions occur where the summer thaw line is consistent with both. It is suggested that the icy solution is unstable and on the way to decaying ice. In these cases the disintegration may not progress very far before another cool period sets in and the growth resumes. This may have happened many times in the long growth of the ice sheet between the last interglacial and the LGM.

Simulations of Post-LGM Climates

Next the summer temperature fields for 15ka, 12ka and 9ka BP are included in Figure 12. The ice sheet distributions of these three separate periods are based on Peltier (2004). In each case the same close conformity of the summer thaw line with the equatorward edge of the ice sheets is found in the Northern Hemisphere. Consistent with the deglaciation, the summer thaw line is well onto the ice sheet.

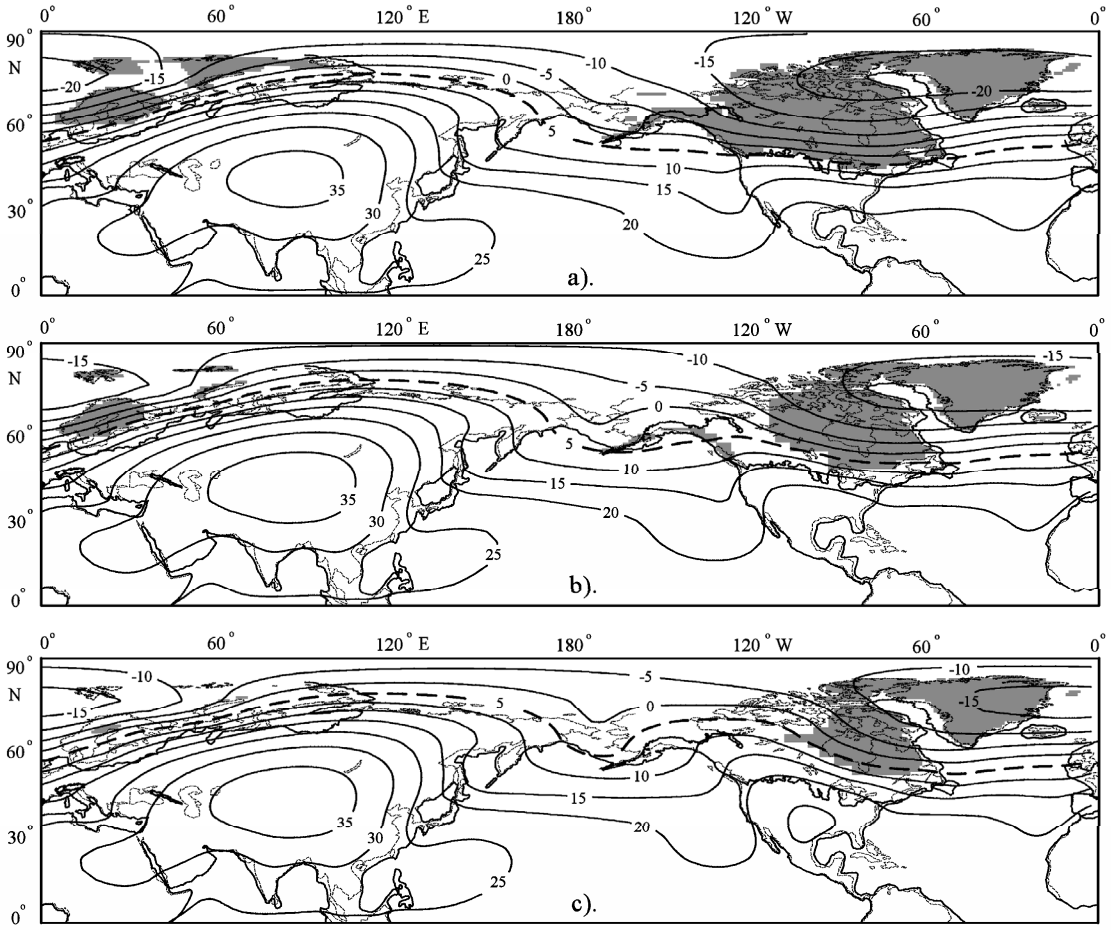

Figure 12. The summertime surface temperature at 15ka (a), 12ka (b) and 9ka BP (c). Compared with LGM, the ice sheets gradually decay but the southern edges are still coincident with the 5ºC thawline.

Some may ask that if an ice sheet were put in Siberia or any other place, then the summertime thawline would also conform to its southern edge. To test this hypothesis, an ice patch is added artificially in the Siberian region at the LGM, 15ka, 12ka and 9ka

BP. The results show that the summertime temperature in the ice patch area would reach more than 20ºC and the thawline lies far north of the ice patch and implies that it would melt rapidly.

Discussion

The L2DEBM was applied to present, the LGM, 15ka, 12ka and 9ka BP conditions with the result that the summertime thaw line conformed closely to the equatorward edge of the ice sheets, except that in the later 15ka, 12ka, and 9ka simulations the thaw line was well onto the ice sheet consistent with those configurations trending towards total disintegration.

Whereas the rather crude hypotheses seem to hold up at least to the level of consistency, many caveats are in order, and further experiments are warranted. On the other hand, the L2DEBM has been tested against GCMs elsewhere under some rather severe conditions (North and Wu, 2001). The failures of the model are likely to be worse in the tropics, but in an EBM, where dynamic interactions are absent, the tropics are not important to this study. The simulation results do seem to suggest further experiments with an ice budget may not be beyond the reach of the credulity. If so, a study might be envisioned along the lines of those in a recent paper utilizing only zonal averages by Huybers and Tziperman (2008). If so, the ice volume could be suggested as a function of time as the driving parameters evolve.

Experiments with GCMs are also of interest, but it must be kept in mind that the EBM is simulating perhaps 1000 years of average seasonal cycle, whereas the GCM has to go day by day. It is not clear *a priori* which would do the better job on such a problem.

CHAPTER IV

OCCURRENCE OF GLACIATIONS IN THE CRETACEOUS AND TRIASSIC

Synopsis

The energy balance model with an empirical ice scheme was applied to the Cretaceous. The simulation results support the idea of glaciation during this time of supergreenhouse. About half to a full size of the modern Antarctic ice sheet is reconstructed corresponding with 20~40m of sea level change which agrees well with recent isotopic discoveries.

Introduction

Controversy exists as whether ice sheets existed during the Cretaceous greenhouse climate (Miller, 2009). So far, no unequivocal Cretaceous glacial deposits have been found and this complicates the debate though some possible glacially derived sediments and glendonites have been discovered (Kemper, 1987; Frakes and Francis, 1988; Frakes, 1990; Crowley and North, 1991a; Frakes et al., 1992; Price, 1999; De Lurio and Frakes, 1999; Selleck et al., 2007). More and more isotopic evidence supports the possibility of ephemeral polar glaciations during this supergreenhouse period (Stoll and Schrag, 1996; Stoll and Schrag, 2000;Steuber et al., 2005; Galeotti et al., 2009) though some researchers are still against the glaciation during this time (Ando et al, 2009; Miller, 2009) based on correlation between isotopic data and sea level curve. Miller and his

colleagues inferred a sea level change of 100±50 m in the Cretaceous from ephemeral Antarctic ice sheets using stratigraphy and isotope techniques (Miller et al., 2003; Miller et al., 2004; Miller et al., 2005).

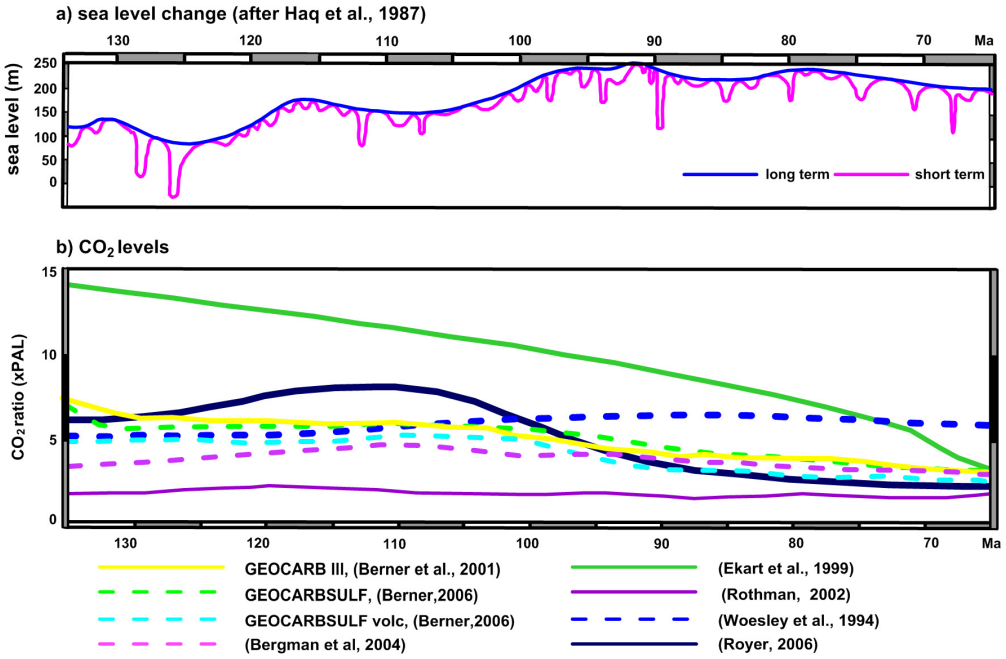

Figure 13. Sea level and CO_2 level changes in the Cretaceous. a) The Cretaceous has a long-term sea level change of more than 100m and the short-term changes are frequent and oscillation with amplitudes more than 100m; b) CO_2 levels differ greatly from different authors ranging from 2x to 12x PAL.

In the sea level curve of Haq et al. (1987) and Hallam (1992), the sea level change of the Cretaceous is about 100m (Fig. 13). Sea floor spreading and sedimentation process cannot wholly cover the million-year scale sea level change in addition to the short-term fluctuations in this period and glaciation is a possible mechanism to explain it (Miller et al., 2005).

Recent studies have revealed a direct link between climate and CO_2 (e.g., Crowley and Berner, 2001; Kump, 2002; Holbourn et al., 2005; Tripati et al., 2009). CO_2 levels varied during the Cretaceous (Fig. 13; Royer, 2006; Breecker et al., 2010; Royer, 2010). The question here is if ephemeral ice sheets and ice-free Cretaceous are two bifurcated stable states during this period? That is to say, under varied CO_2 levels and the Milankovitch cycles (Berger, 1978), the Cretaceous was ice-free in high CO_2 levels and also the polar areas are glaciated if CO_2 level reached the threshold sometime.

The purpose of this chapter is to check the occurrence of glaciations in the Cretaceous within the framework of varied CO_2 levels and the Milankovitch cycles using a nonlinear energy balance model (EBM) with an empirical ice sheet scheme.

Methods

Calculating the seasonal cycle as a function of solar input, longwave radiation and geography, EBM has been successfully applied in paleoclimatology (e.g., Crowley and

North, 1991; Baum and Crowley, 1991; Hyde et al., 1990; North et al., 1983). A seasonal two-dimensional EBM (Stevens and North, 1996) was extended with an empirical ice sheet scheme to simulate the possibility of glaciations. CO_2 was used as an important radiative forcing with a formula introduced by Myhre et al. (1998). The simple scheme to ice sheet buildup was similar to Hyde et al. (1990). Any land with a monthly average temperature less than -2ºC is defined as ice-covered; meanwhile, any sea with monthly average temperature less than -4ºC is stipulated as having sea ice. The nonlinear EBM with ice sheet feedback mechanism, orbital elements and CO_2, and will test the possibility and distribution of glaciation in a seasonal ice sheet scheme (Hyde et al., 1990; Hyde et al., 2006).

An albedo scheme similar to Hyde et al. (1990) and Mengel et al. (1988) is applied to this study. Whenever temperature is greater than ice thresholds which are -2ºC for land and -4ºC for sea, land albedo is $0.30+0.09\times P_2(x)$, where $P_2(x)$ is the second-order Legendre polynomial, $(3x^2-1)/2$, x is the sine of latitude; sea albedo $0.29+0.09\times P_2(x)$; sea ice albedo 0.40, and land ice 0.68. If temperature at the time is lower than ice thresholds, land turns into ice and sea into sea ice and the albedo change accordingly. Based on the successful simulation of present climate, the model is extended to the Cretaceous with a set of CO_2 levels and orbital elements. CO_2 levels range from 1x to 18x PAL, which PAL is CO_2 preindustrial level of 280 ppmv. Orbital elements include those of the last glacial maximum (LGM) and the last interglacial (LIG).

Modeling Results

Six periods of the Cretaceous have been selected to be the simulation intervals, namely 130Ma, 120Ma, 118Ma, 94Ma, 88Ma, and 69Ma (Scotese and Golonka, 1992; Blakey, 2008). Tables 1 and 2 list the total ice areas up to 6.0x PAL under LGM and LIG orbital elements. A small ice sheet criterion similar to that of Hyde et al. (2006) is applied which deems climate with <1 million km^3 of ice as ice-free. According to the empirical formula between ice sheet volume and area coverage (Paterson, 1972; Paterson, 1994; Crowley and Baum, 1991; Isbell et al., 2003), the small ice sheet criterion of <1 million km^3 roughly equals to the criterion of <1 million km^2 of area. Here the small ice sheet criterion is extended to both hemispheres: if ice sheet area in either or both of these two hemispheres is <1 million km^2, the climate is defined as ice-free.

One can see (Tables 1 and 2) that if the CO_2 level is lower than 6x PAL, ice sheets might exist on both hemispheres although the sizes may vary in different intervals (Figures 14 through 20). Except 69Ma and 120Ma, little ice occurs if CO_2 levels are greater than 6x PAL. The different temperature patterns are shown in Figures 21 through 24.

Table 1

Ice sheet areas under different CO_2 levels with LGM orbital elements.

CO_2	1.0x	2.0x	3.0x	4.0x	5.0x	6.0x
130Ma	12.28	8.06	6.90	6.41	6.45	5.82
120Ma	17.08	13.80	12.21	10.00	10.16	9.95
118Ma	12.49	9.41	8.00	6.65	6.63	6.10
94Ma	9.61	10.65	7.50	7.06	6.91	6.69
88Ma	20.36	10.25	7.21	10.60	5.93	5.61
69Ma	28.38	25.10	24.03	23.13	22.69	20.45

CO_2 levels in PAL, ice sheet area in 10^6 km^2.

Table 2

Ice area under different CO_2 levels with LIG orbital elements.

CO_2	1.0x	2.0x	3.0x	4.0x	5.0x	6.0x
130Ma	11.88	8.41	7.32	6.18	6.64	6.69
120Ma	16.28	14.05	10.16	11.84	11.68	9.06
118Ma	19.41	13.94	10.87	7.21	7.75	6.44
94Ma	16.13	12.45	10.92	7.89	8.55	6.56
88Ma	21.12	16.29	14.76	6.63	6.91	11.86
69Ma	27.44	25.13	20.49	19.03	18.81	17.67

CO_2 levels in PAL, ice sheet area in 10^6 km^2.

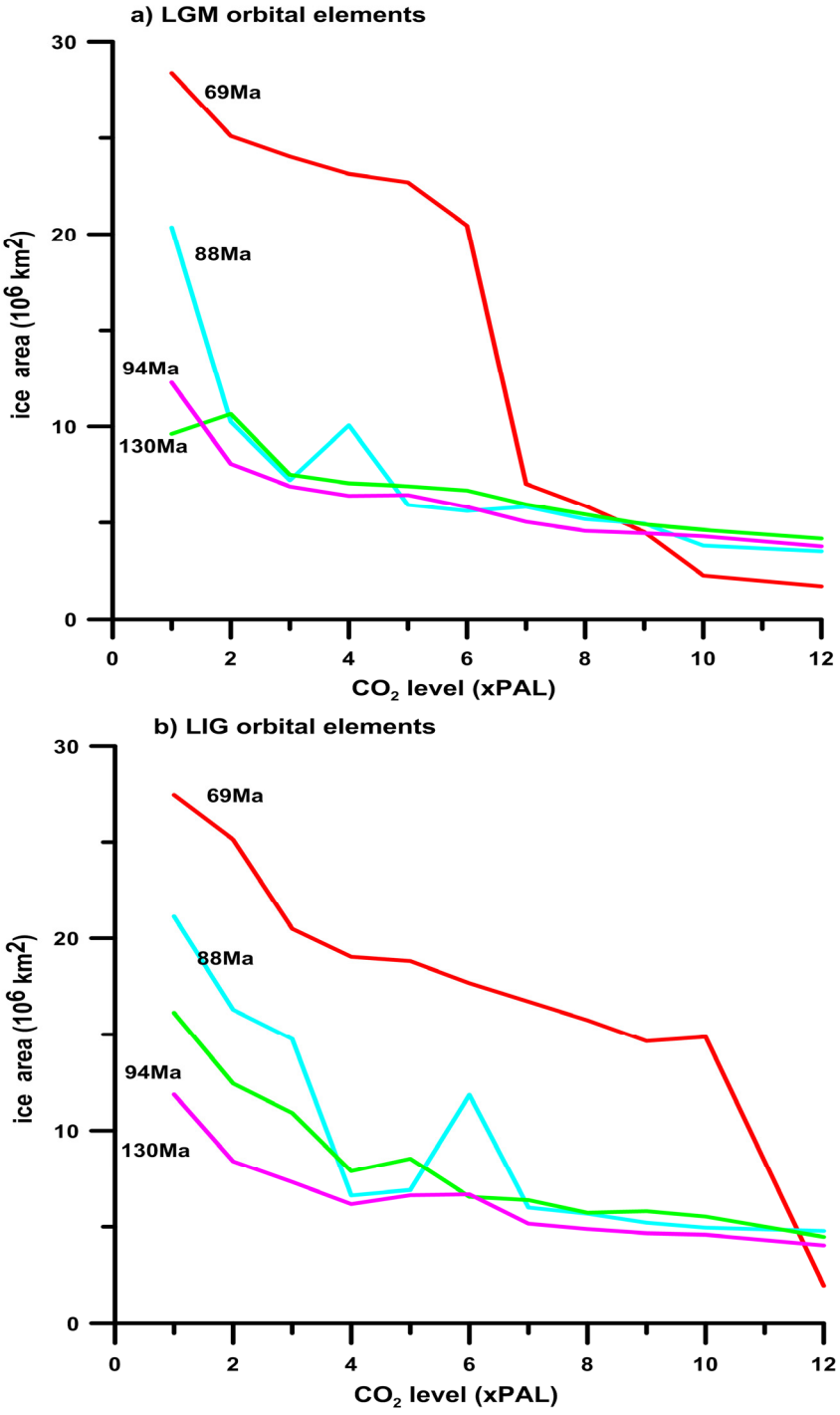

Figure 14. Ice sheet areas at different CO_2 levels with LGM and LIG orbital elements.

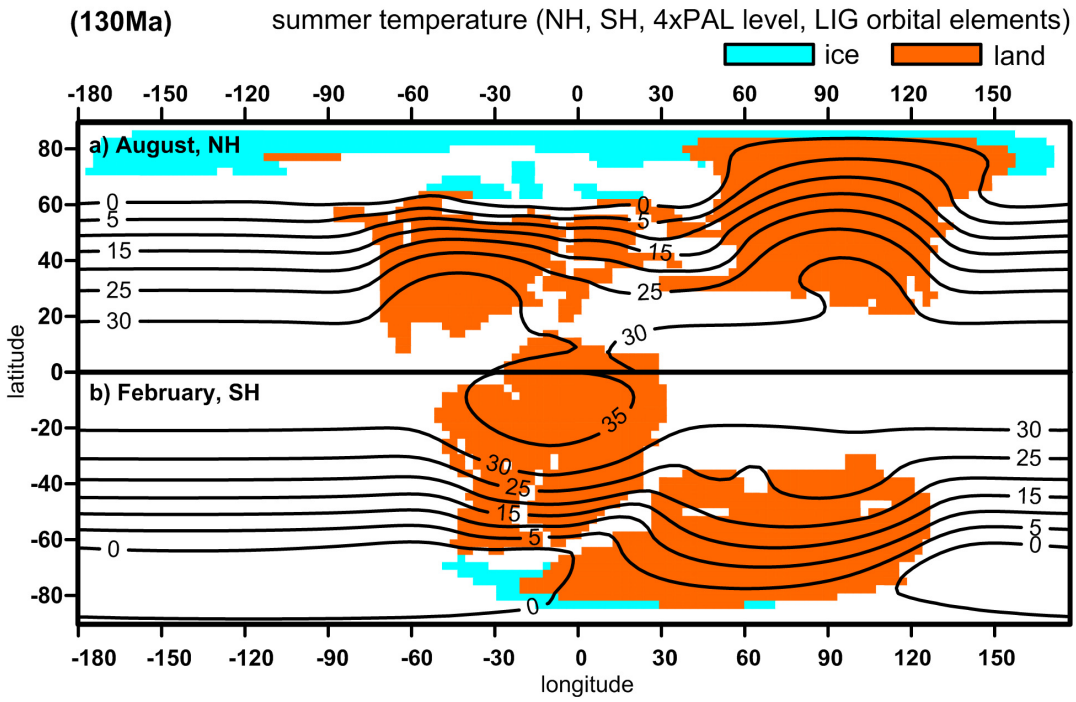

Figure 15. Glacial scenario and summer temperature in 130Ma. Isotherms are in 5ºC intervals. NH and SH refer to the Northern Hemisphere and Southern Hemisphere respectively. Under 4x PAL CO_2 levels and LIG orbital elements, little ice occurs in the SH; whereas NH has about 6 million km^2 of ice.

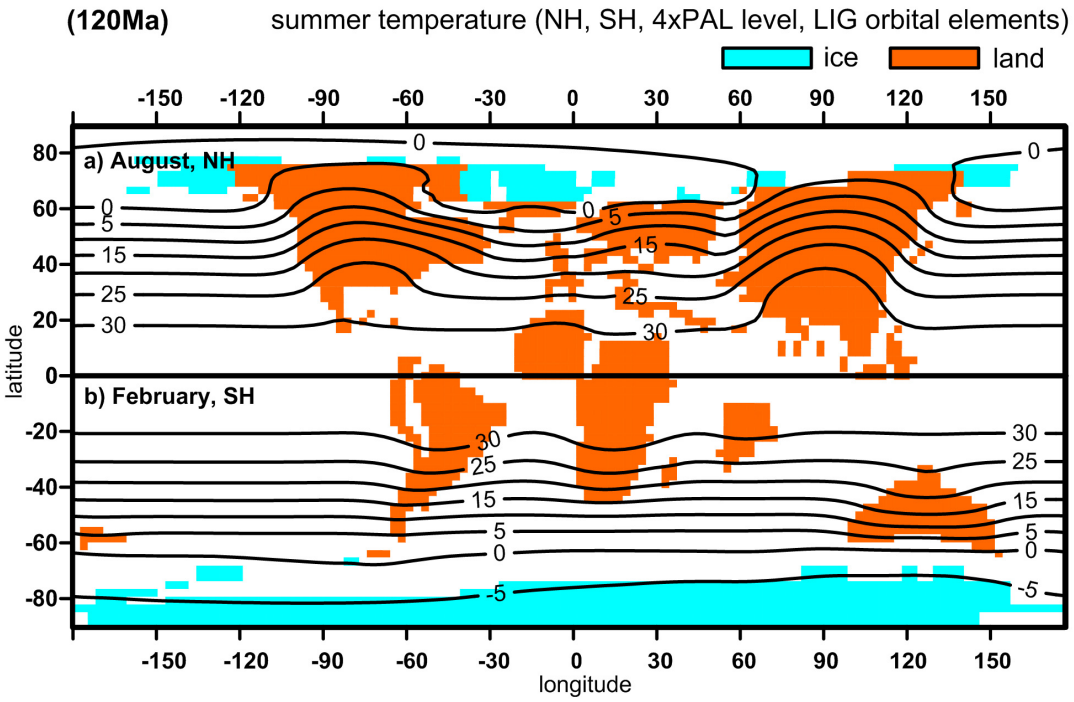

Figure 16. Glacial scenario and summer temperature in 120Ma. Isotherms are in 5ºC intervals. NH and SH refer to the Northern Hemisphere and Southern Hemisphere respectively. Under 4x PAL CO_2 levels and LIG orbital elements, little ice occurs in the NH; whereas SH has about 12 million km^2 of ice.

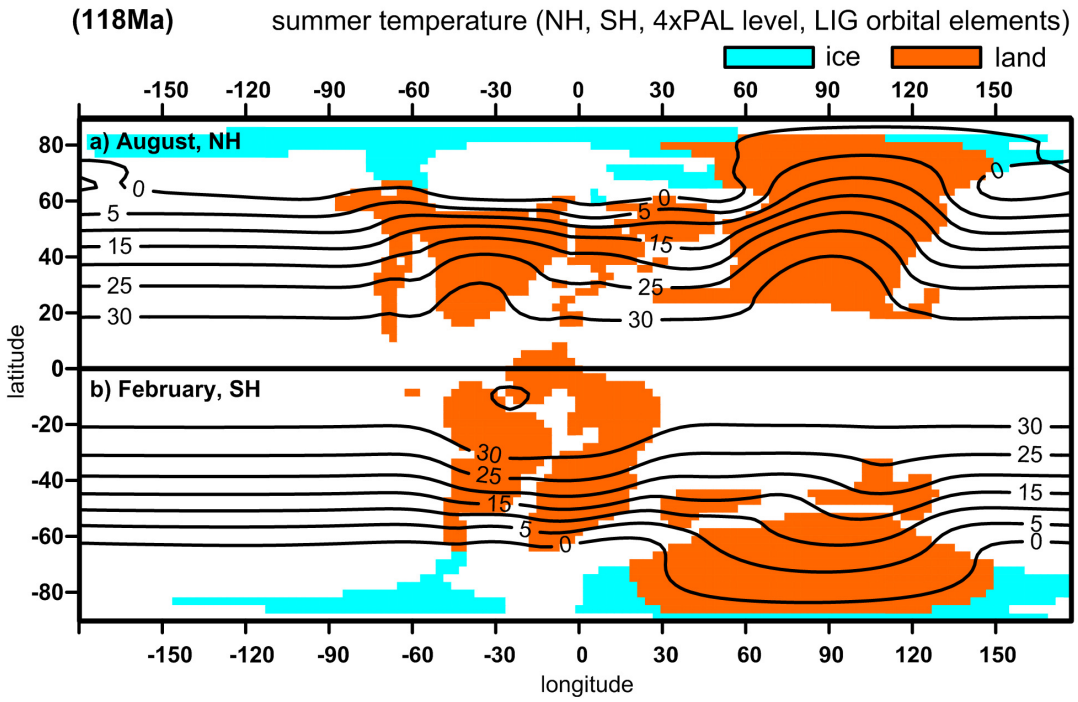

Figure 17. Glacial scenario and summer temperature in 118Ma. Isotherms are in 5ºC intervals. NH and SH refer to the Northern Hemisphere and Southern Hemisphere respectively. Under 4x PAL CO_2 levels and LIG orbital elements, ice occurs in NH and SH with a total area of about 7 million km^2.

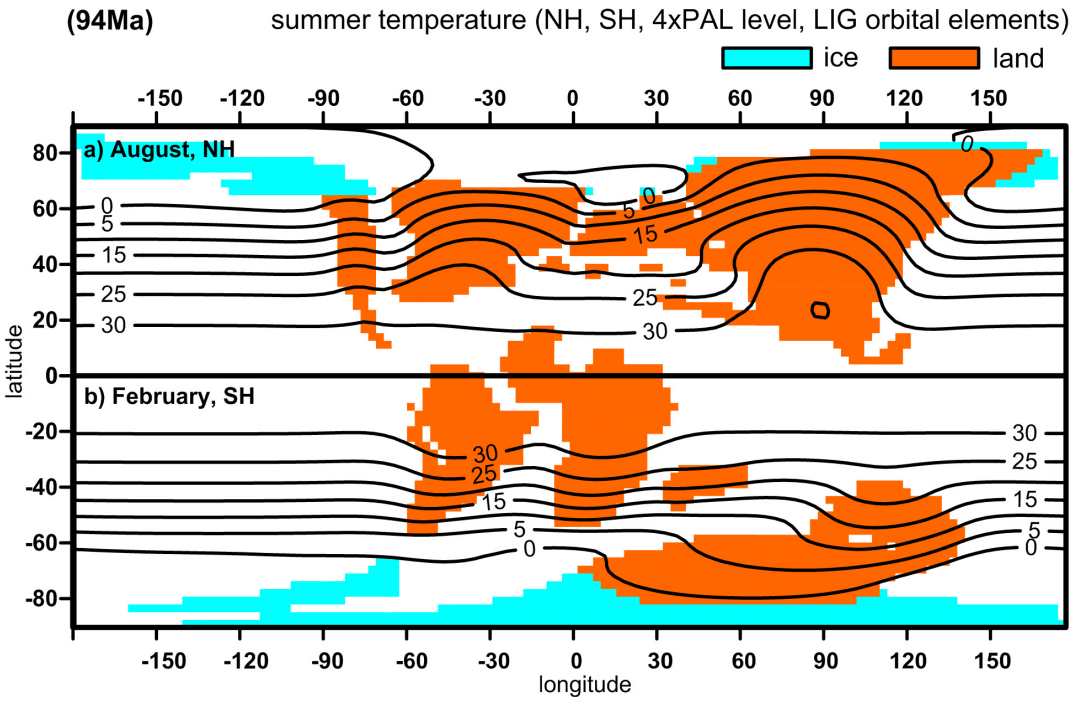

Figure 18. Glacial scenario and summer temperature in 94Ma. Isotherms are in 5ºC intervals. NH and SH refer to the Northern Hemisphere and Southern Hemisphere respectively. Under 4x PAL CO_2 levels and LIG orbital elements, little ice occurs in the NH; whereas NH has about 7 million km^2 of ice.

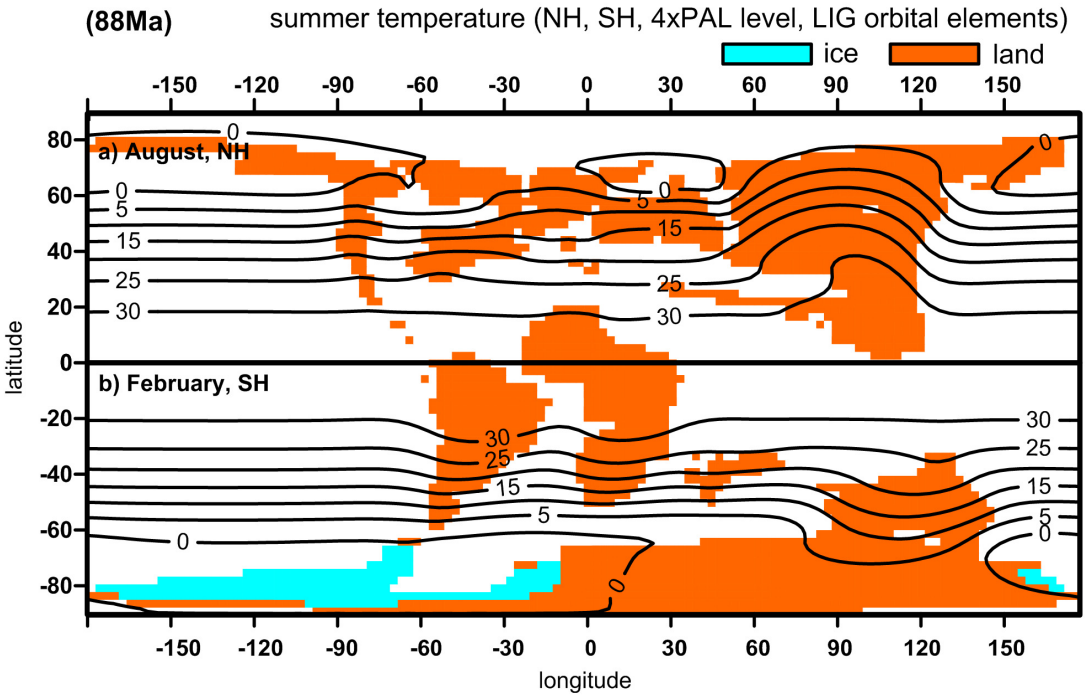

Figure 19. Glacial scenario and summer temperature in 88Ma. Isotherms are in 5ºC intervals. NH and SH refer to the Northern Hemisphere and Southern Hemisphere respectively. Under 4x PAL CO_2 levels and LIG orbital elements, little ice occurs in the SH; whereas NH is ice-free.

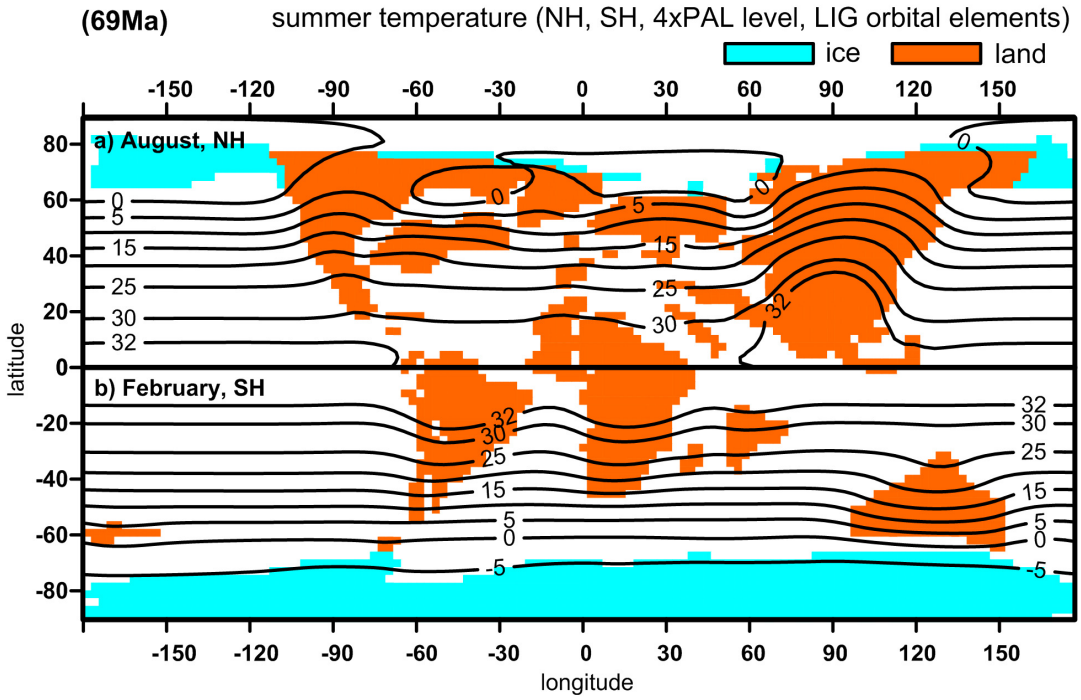

Figure 20. Glacial scenario and summer temperature in 69Ma (ºC). Isotherms are in 5ºC intervals. NH and SH refer to the Northern Hemisphere and Southern Hemisphere respectively. Under 4xPAL CO_2 levels and LIG orbital elements, great ice sheets occur in Antarctica, SH; whereas NH has about 6 million km^2 of ice.

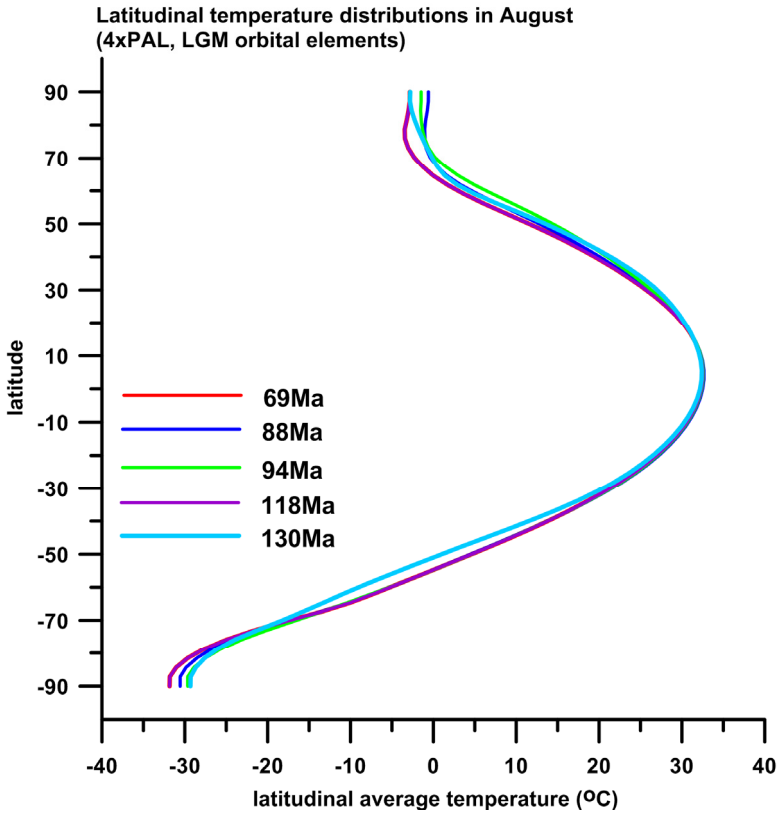

Figure 21. Latitudinal summer temperature distributions under 4x PAL and LGM orbital conditions. All these are the final equilibrium states from the initial ice-free geography. The high latitudinal areas exhibit a different temperature pattern that results from different areas of ice sheet coverage.

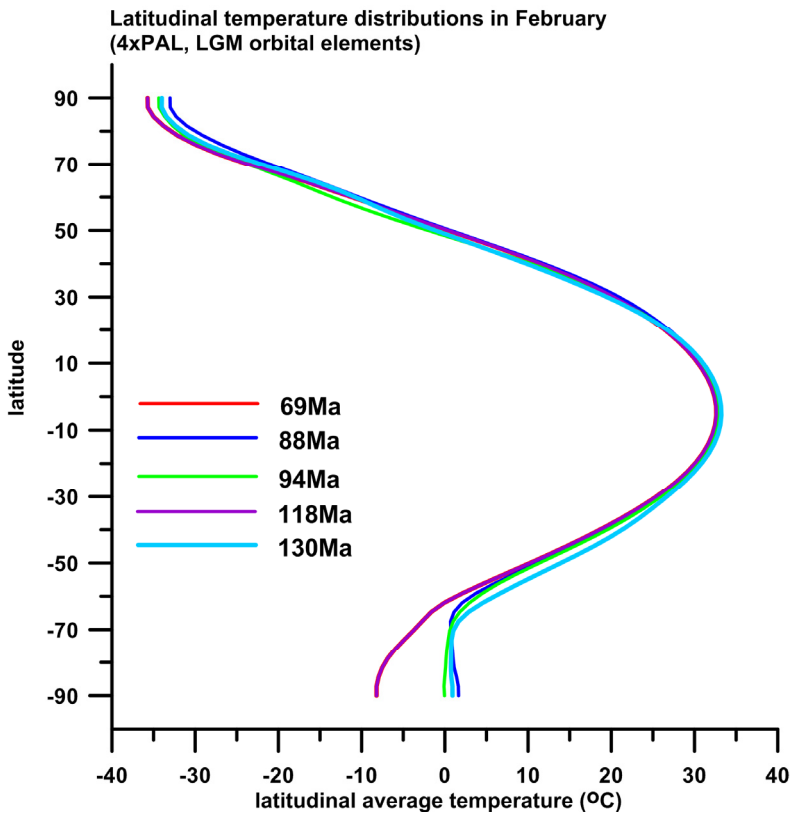

Figure 22. Latitudinal winter temperature distributions under 4x PAL and LGM orbital conditions. All these are the final equilibrium states from the initial ice-free geography. The high latitudinal areas exhibit a different temperature pattern that results from different areas of ice sheet coverage.

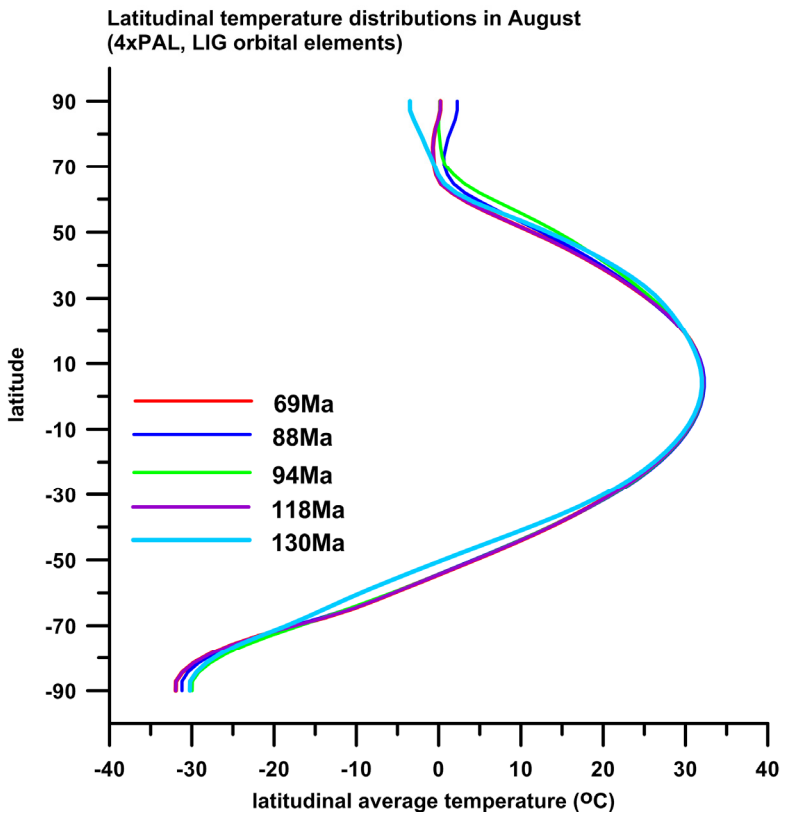

Figure 23. Latitudinal summer temperature distributions under 4x PAL and LIG orbital conditions. All these are the final equilibrium states from the initial ice-free geography. The high latitudinal areas exhibit a different temperature pattern that results from different areas of ice sheet coverage.

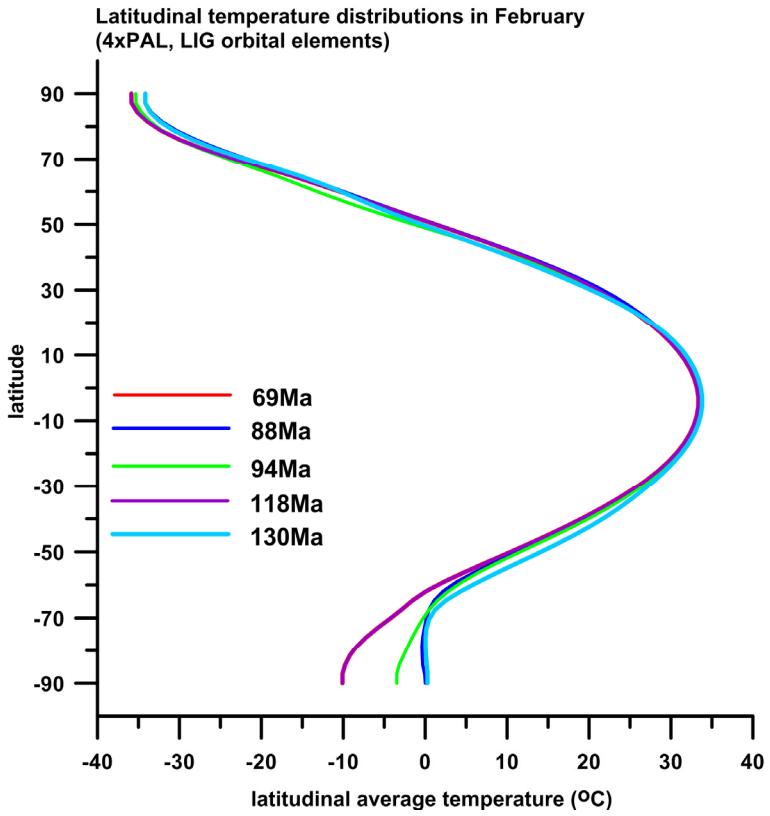

Figure 24. Latitudinal winter temperature distributions under 4x PAL and LIG orbital conditions. All these are the final equilibrium states from the initial ice-free geography. The high latitudinal areas exhibit a different temperature pattern that results from different areas of ice sheet coverage.

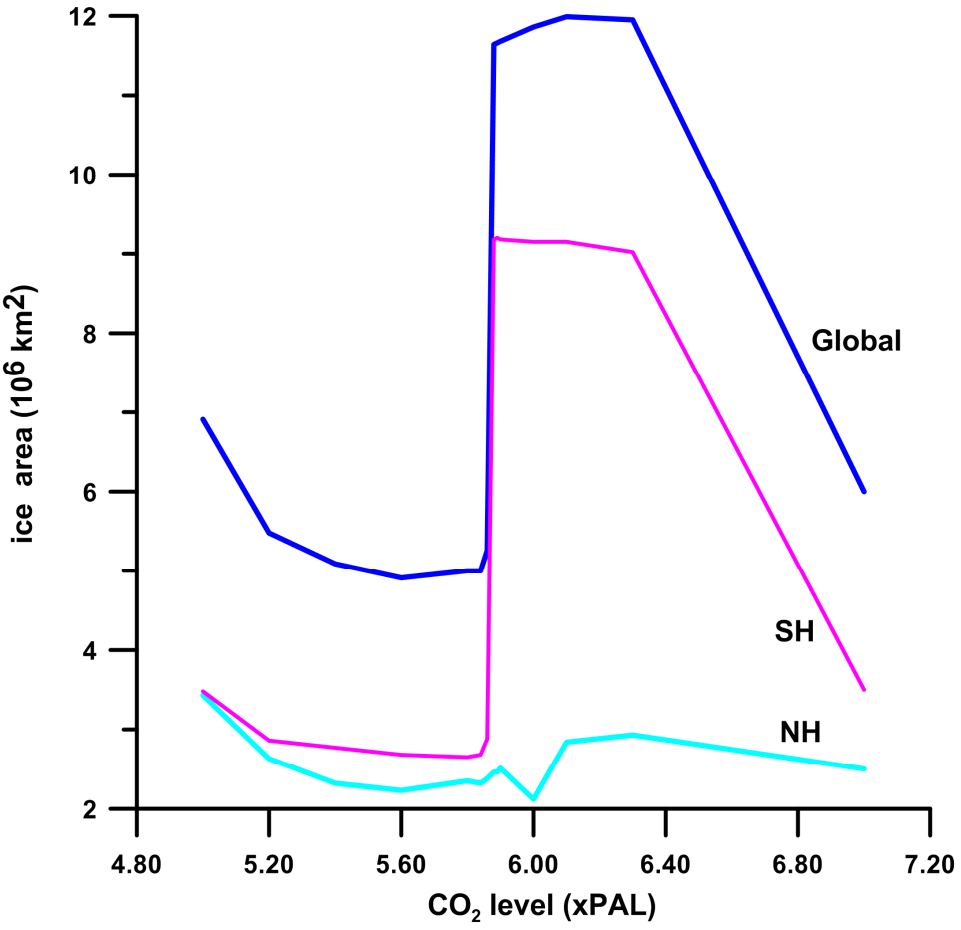

Figure 25. Abrupt ice sheet changes at 88Ma with LIG orbital elements. Global, NH, SH refer to the whole earth, Northern Hemisphere and Southern Hemisphere, respectively. An abrupt change happens in the 5.86x to 5.88x PAL interval. Ice area shifts from less than 3 to 9 $\times 10^6$ km^2. The CO2 level change is only equal to change in radiative forcing of 0.02 Wm^{-2}.

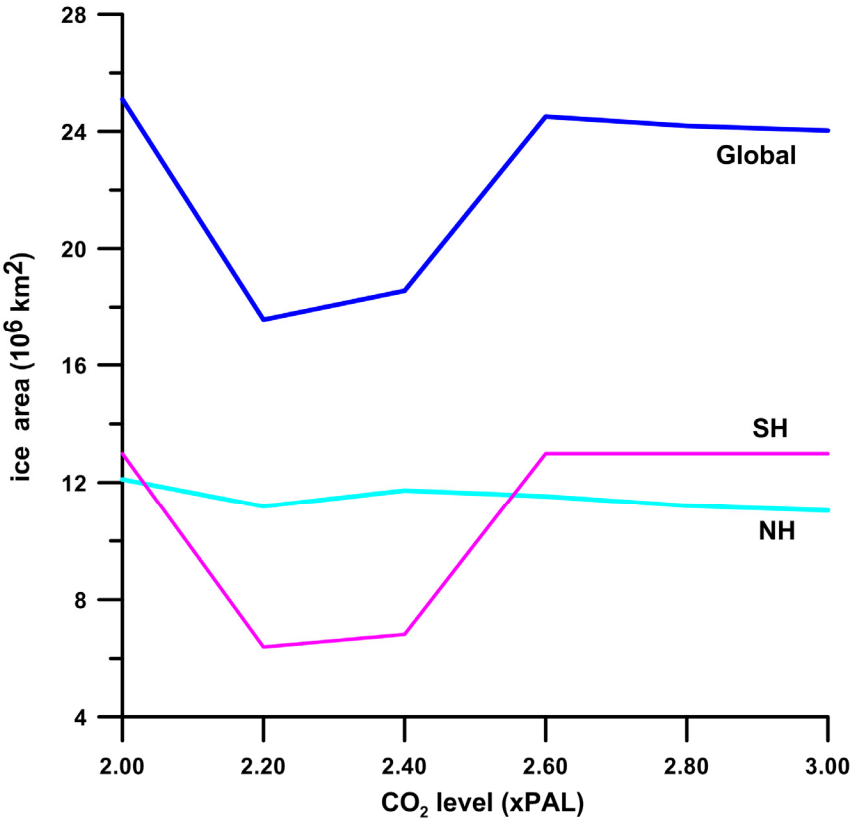

Figure 26. Abrupt ice sheet changes at 69Ma with LGM orbital elements. Global, NH, SH refer to the whole earth, Northern Hemisphere and Southern Hemisphere, respectively. An abrupt change happens in the 2.40x to 2.60x PAL interval. Ice area shifts from 6.8 to 13 $\times 10^6$ km^2. The CO_2 level change is only equal to a change in radiative forcing of 0.56 Wm^{-2}.

At 4x PAL CO_2 level and LIG orbital elements, climates in 69Ma and 120Ma make Antarctica completely glaciated (Table 2; Fig. 16 and Fig. 20); however, during other periods, such as 130Ma, 118Ma, 94Ma, and 88 Ma, with the same conditions Antarctica is only partially ice-covered.

At some geologic time and orbital elements, climates exhibit abrupt changes in characteristics. Such phenomena are well demonstrated in 69Ma with LGM orbital elements (Fig. 26), 88Ma with LIG orbital elements (Fig. 25), and 118Ma with LIG orbital elements. Only a slight change of CO_2 levels in 88Ma from 5.86x to 5.88x PAL, which is equal to 0.02 Wm^{-2} in radiative forcing, results in an abrupt change of glaciated area in Antarctica from less than 3 to 9 $\times 10^6$ km^2 (Fig. 13). Similar features are also found in 69Ma. When CO_2 levels increase from 2.40x to 2.60x PAL, ice area in Antarctica jumps from 6.8 to 13 $\times 10^6$ km^2. At the same time with opposite orbital elements, such as at 69Ma with LIG orbital elements, 88Ma with LGM orbital elements, and 118Ma with LGM orbital elements, only gradual change of ice area occurs without any abrupt changes.

Discussion

CO_2 levels are indispensable in controlling the initiation ice sheets. Orbital elements only are not sufficient to account for the buildup of ice sheets. The simulations of this study have shown that ice sheets exist in the Cretaceous given particular CO_2 levels and

orbital elements. CO_2 levels and orbital elements are two important agents in the construction of ice sheets. At low CO_2 levels (1x - 6x PAL), ice sheets exist in all the six simulation periods no matter LGM or LIG orbital elements. At high CO_2 levels (>7x PAL), however, ice sheets are rarely present except at 69Ma with LIG orbital elements. If CO_2 level is >12x, no ice sheets occur (Tables 1 and 2; Fig. 14).

Stoll and Schrager (1996) proved that the fluctuations of Sr, δ^{13}Cand δ^{18}O isotopes coincided with two sea level drops of >50m (125-126Ma and 128-129Ma) in Brriasian-Valanginian. A sea level change of 50m is roughly equal to 8~9 $\times 10^6$ km^2 of ice sheet following the empirical formula of Paterson (1994). Based on simulations of this study, the CO_2 level should be within 2.5x PAL (<700 ppmv) which was supported by a moderately low value of 650 ppmv after the cool event (135Ma) by Royer (2006).

Many geological studies revealed three brief global cooling events, the Campanian-Maastrichtian boundary (71.6 - 69.6Ma), mid-Maastrichtian (67.5 - 66.6Ma), and end-Maastrichtian (65.6 - 65.5Ma) (Haq et al., 1987; Miller et al., 1999; Miller et al., 2003; Miller et al., 2004; Miller et al., 2005; Royer, 2006). Their data inferred a complete glaciation of Antarctica. A coupled GCM - ice sheet model also supported this idea (DeConto and Pollard, 2003; Pollard and DeConto, 2005). The simulation results of this study confirm this occurrence up to 6x PAL CO_2 level.

CO_2 level during the Aptian (125.0-112Ma) is more variable and several cool intervals correspond with a low CO_2 pulse (Royer, 2006). The continental geography also changed significantly during this period, especially in polar areas. CO_2 level and geography enhance the fluctuations of glaciation during this time. Figures 16 and 17 demonstrate that at the same CO_2 level and orbital elements, geography plays a crucial role in the buildup of ice sheets. These two paleogeography maps are from different authors. The paleogeography map of Figure 16 is from Scotese and Golonka (1992) and the base map of Figure 17 from Blakey (2008). One can see different reconstructions of paleogeography result in different glacial scenarios. Hence a precise paleogeography map is very important in modeling and affects the accuracy of paleoclimate reconstruction.

Under certain orbital elements, a slight change of CO_2 level causes remarkable fluctuations in the coverage of ice sheets which might be a possible mechanism of sea level drop. 88Ma and 69Ma are convincing in this regard (Figures 13 and 14) and might be used to explain the rapid change of sea level in Haq et al. (1987).

In addition to above mentioned mechanisms, the Milankovitch cycles play an important role in adjusting the waxing and waning of ice sheets in given CO_2 levels and continental geography. Figure 27 shows that at 69Ma and 88Ma areas of ice sheets differ greatly from LGM and LIG orbital elements which might be a mechanism to explain the rapid change of glacial scenarios with slight change of CO_2 levels.

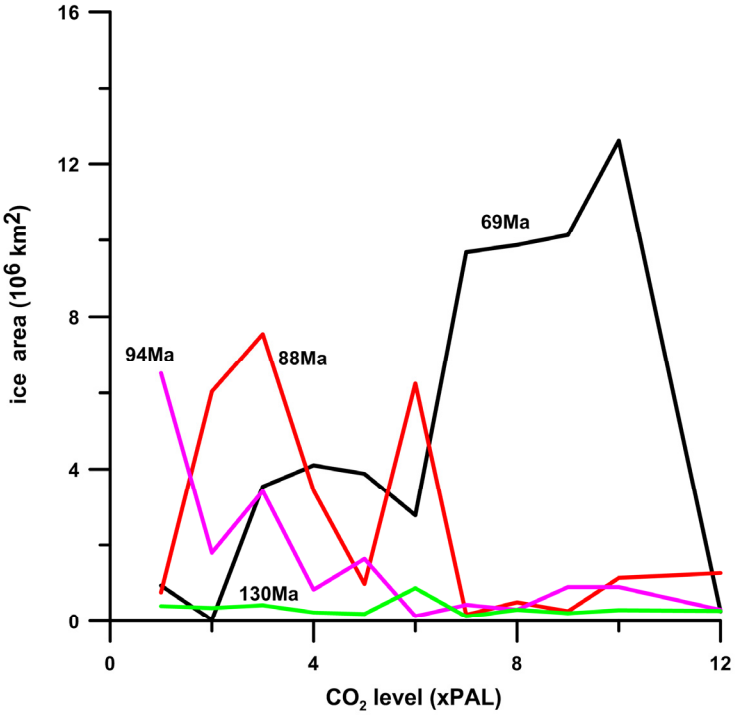

Figure 27. Difference in area of ice sheets between LGM and LIG orbital elements. Remarkable fluctuations of area of ice sheets occur at the same CO_2 level with different orbital elements and paleogeography maps. At high CO_2 levels, difference in glacial areas at 88Ma, 94Ma, and 130Ma is not significant. But this different is distinct at 69Ma which might be a mechanism to explain the rapid change of glacial scenarios with slight change of CO_2 levels.

CO_2 levels are indispensable in controlling the initiation of ice sheets. Orbital elements alone are insufficient to account for the buildup of ice sheets. The simulations of this

study have shown that ice sheets exist in the Cretaceous given particular CO_2 levels and orbital elements.

CO_2 level and continental geography enhance the fluctuations of glaciation during this time. Under certain orbital elements, a slight change of CO_2 level causes remarkable fluctuations of ice sheet coverage which is a possible mechanism of sea level drop (Fig. 27). In addition to the above mentioned mechanisms, Milankovitch cycles play an important role in adjusting the waxing and waning of ice sheets in given CO_2 level and geography.

CHAPTER V

HYSTERESIS OF GLACIATIONS IN THE PERMO-CARBONIFEROUS

Synopsis

Recent studies have revealed that the Permo-Carboniferous was characterized by three non-overlapping glaciations with ice-free lacuna. The simulation results based on the energy balance model with a simple empirical ice-sheet scheme are presented to explain such hysteresis of glaciations. Gondwanaland reached its glacial maximum when CO_2 level was roughly the same or slightly higher than the preindustrial value. If the CO_2 level was three to four times of the preindustrial value, glaciation was only distributed along coasts of Gondwanaland. With a further increase of CO_2, deglaciation dominates and results in an ice free state. The simulation agrees well with recent geological evidence.

Introduction

Recent studies have revealed that the Permo-Carboniferous was characterized by three non-overlapping glaciations with ice-free lacuna (Isbell et al., 2003; Jones and Fielding, 2004). Gondwanaland experienced three glacial successions – Glacial I (Frasnian to possible Tournasian), Glacial II (Namurian to earliest Westphalian) and Glacial III (Stephanian to Artinskian). Two non-glacial intervals made the three glacial strata

distinct (Fig. 28). The inferred shifts in CO_2 agreed well with ice volume and the unstable climate (Crowley and Berner, 2001; Berner, 2006; Royer, 2006; Montanez et al., 2007) though the climate dynamics remained enigmatic (Montanez et al., 2007). The problem here is what is the real mechanism between CO_2-forced climate and the change in volume of the ice sheets?

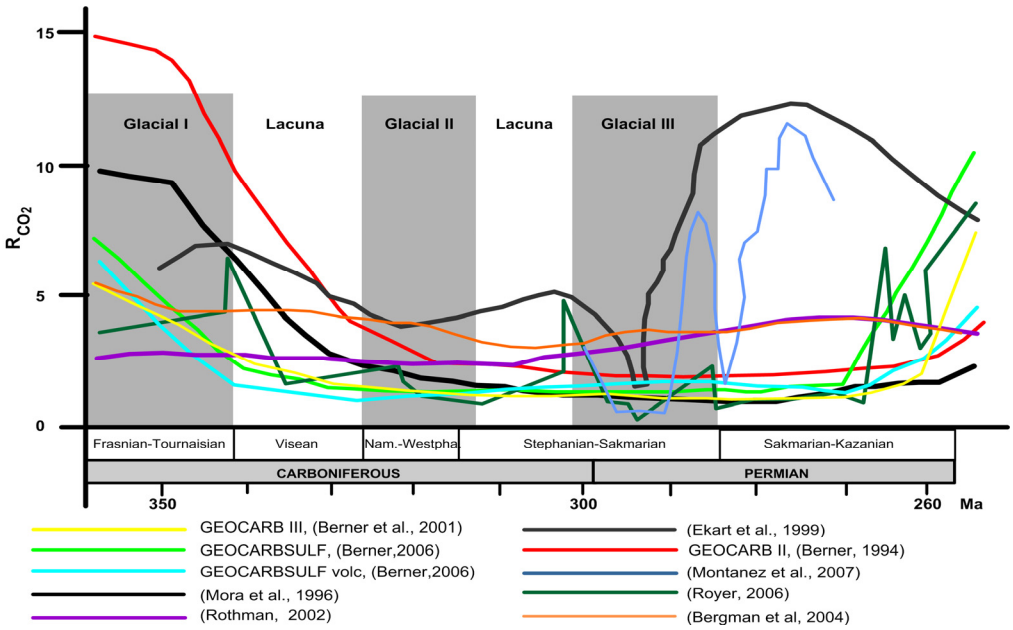

Figure 28. CO_2 in the Permo-Carboniferous. R_{CO2} is the rate to the preindustrial level of 280ppm. The shaded rectangles were three non-overlapping glacials (Isbell et al., 2003).

North (1984) theoretically deduced the small ice cap instability (SICI) based on the zonally symmetric mean annual energy balance model (EBM) and put forward as a mechanism for abrupt climate change (Mengel et al, 1988; Crowley and North, 1988; Lin and North, 1990; Huang and Bowman, 1992; Matteucci, 1993; Marqueda et al., 1998). SICI means that ice caps less than a certain size are unstable (North, 1984). The EBMs and general circulation model (GCMs) have found such phenomenon (Crowley et al, 1994; Held et al., 1981). Baum and Crowley (1991) found a similar bifurcation point using two-dimensional seasonal EBM with the realistic continental geography of 300Ma to explain the initiation of glaciation and glacial oscillation with varied solar luminosity. But no simulations with altered CO_2 were run in their work. Pollard and DeConto (2005) and Ogura and Abe-Ouchi (2001) also employed similar theory to investigate the hysteresis of the Cenozoic glaciations by GCMs.

More and more geological evidence has shown a direct link between climate and CO_2 (e.g., Crowley and Berner, 2001; Kump, 2002; Holbourn et al., 2005; Tripati et al., 2009). If the realistic Permo-Carboniferous continental geography and CO_2 shifts are incorporated into a climate model, could the hysteresis of glaciations be reconstructed for that time?

Glacial and Deglacial Simulations

Here a seasonal two-dimensional EBM (Stevens and North, 1996) with a simple ice sheet scheme is extended to simulate the glacial and deglacial Permo-Carboniferous. Calculating the seasonal cycle as a function of solar input, longwave radiation and continental geography, EBM has been successfully applied in paleoclimatology (e.g., North et al., 1983; Crowley and North, 1991; Baum and Crowley, 1991; Hyde et al., 1990). CO_2 is put as an important radiative forcing with a formula introduced by Myhre et al. (1998). This simple scheme to ice sheet buildup is similar to Hyde et al. (1990). Any land with a monthly average temperature less than -2ºC is defined as ice covered; meanwhile, any sea with monthly average temperature less than -4ºC is stipulated as having sea ice. A stability threshold of 5ºC for delglaciation is added for this study. Based on the deglaciation study since the last glacial maximum, the equatorward edge of ice sheets is found to conform closely to the 5ºC summertime isotherm. Once ice or sea ice formed, it remains relatively stable within the 5ºC isotherm of each month and implies the effects of topography, precipitation, and ice thickness because EBMs do not consider these explicitly. This asymmetry of the ice sheet scheme will make the accumulation of ice sheet severer but its melting milder, which is more significant to test whether Gondwanaland is capable of intense glaciation and enduring deglaciation longer.

The orbital elements of the last glacial maximum (LGM) and the last interglacial (LIG) are chosen to represent the astronomical parameters of warm and cold climates,

respectively (Berger, 1978). The highest (24.65º) and lowest (21.65º) values of obliquity are also taken into consideration. Using the eccentricity, longitude of the perihelion, and obliquity of the last glacial maximum was termed ColdMd. If LGM obliquity is replaced by 24.65º, then the set is termed ColdHi. Similarly, if LGM obliquity is replaced by 21.65º, ColdLo is created. Things are similar to the LIG and they are termed WarmHi, WarmMd, and WarmLo, respectively. Hence two sets of experiments are created with three individual tests for each set. Each test starts with the given continental geography, orbital elements, and CO_2-forced radiative forcing. For each test, an equilibrium state is reached if the difference of global average temperature for two consecutive runs was within 0.0001ºC. The monthly albedo and changed continental geography are determined from the geography and monthly temperature of previous run. This iteration process continues until the final equilibrium state is achieved. The CO_2 levels are tested in a package with 1.0x, 1.5x, 2.0x, 3.0x, 4.0x, 6.0x, 10.0x PAL in which PAL is the preindustrial CO_2 level of 280 ppmv. The package was individually put into the six different runs. Zero ice state is the given geography for glacial test and the geological reconstruction of glaciation (Scotese et al., 1992) is the initial geography for deglacial test.

To gain a fine picture of glaciation three-dimensionally, a coupled general circulation model (GCM) - ice sheet model is employed. The Global and Environmental and Ecological Simulation of Interactive Systems global climate model (GENESIS version 3.0) is used for the research. It has been developed at the National Center for

Atmospheric Research (NCAR) with emphasis on terrestrial physical, biophysical, and cryospheric processes for the purpose of performing greenhouse and paleoclimatic experiments (e.g., Thompson and Pollard, 1997) with a resolution of spectral T31 (3.75° latitude × 3.75° longitude) and 18 levels for the atmospheric GCM, and 2° latitude × 2° longitude for the surface models. Version 3.0 has been improved for radiation calculation adapted from the Community Climate System Model (CCSM 3.0).

The model SICOPOLIS (Simulation Code for Polythermal Ice Sheets) is used to couple with GENESIS to better simulate ice buildup and decay during geologic time. It can simulate the large-scale dynamics and thermodynamics of ice sheets three-dimensionally and as a function of time (Greve, 2005). The model has been used to reconstruct glaciation since the Last Interglacial in the northern hemisphere and Greenland and reconciled with paleoclimate data (Greve et al, 1999; Greve, 2005). Start with zero ice state and given radiative forcing, an equilibrium state is reached from GENESIS modeling and the simulation results of GENESIS are input into the SICOPOLIS model to reach an ice or no-ice state. Then a revised paleogeography based on the simulation from SICOPOLIS is input into the GENESIS modeling. The simulation results from GENESIS again are input into SICOPOLIS until the final equilibrium state is achieved.

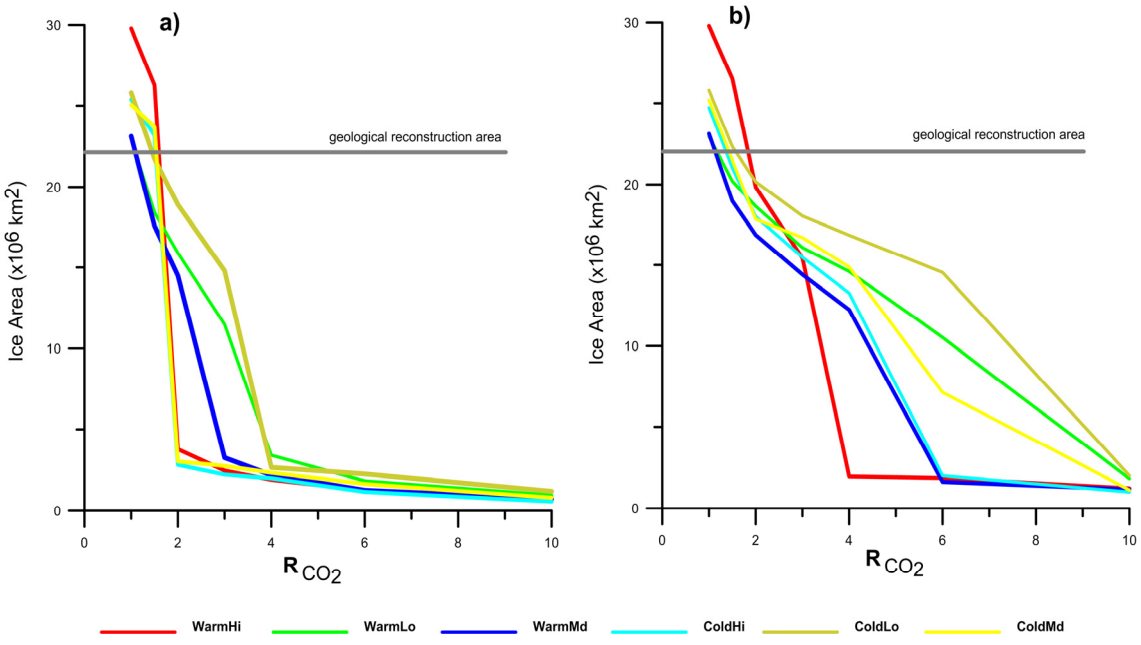

Figure 29. Sensitivity tests of possible ice area in different CO_2 levels. a) Glacial tests. These series of tests start from an ice-free state. At low CO_2 levels up to 2x PAL, great ice sheets occur in Gondwanaland; b) Deglacial tests. These series of tests start from the geologically glacial maximum. Ice sheets can endure higher CO_2 levels than the glacial tests.

The distinctive character of this calculation is that the area of ice sheets has a sudden decrease with an increase of CO_2 levels (Tables 3 and 4; Fig. 29). For glaciations, this phenomenon happened around 3x to 4x PAL; for deglaciation, it took place around 4x to 6x PAL.

Table 3

Glacial simulation results.

CO2	WarmHi	WarmMd	WarmLo	ColdHi	ColdMd	ColdLo
1.00x	29.79	30.80	30.62	33.85	33.41	34.39
1.50x	26.27	23.44	24.56	30.87	31.60	28.96
2.00x	3.77	19.32	21.20	3.75	4.03	25.21
3.00x	2.46	4.33	15.29	2.96	3.66	19.72
4.00x	1.90	2.92	4.53	2.65	3.11	3.54
6.00x	1.25	1.68	2.44	1.55	2.19	3.01
10.00x	0.84	1.00	1.29	0.77	1.08	1.60

CO_2 levels in PAL, ice sheet area in 10^6 km^2.

Table 4

Deglacial simulation results.

CO2	WarmHi	WarmMd	WarmLo	ColdHi	ColdMd	ColdLo
1.00x	29.79	30.80	30.57	32.96	33.60	34.39
1.50x	26.52	25.31	26.94	28.02	28.65	29.75
2.00x	19.84	22.49	24.87	24.01	23.80	26.89
3.00x	15.43	19.21	21.44	20.64	22.27	24.07
4.00x	1.95	16.29	19.46	17.67	19.83	22.47
6.00x	1.85	2.15	14.02	2.66	9.52	19.38
10.00x	1.22	1.54	2.41	1.33	1.49	2.66

CO_2 levels in PAL, ice sheet area in 10^6 km^2.

Glacial and deglacial simulations have demonstrated that if the CO_2 level is kept relatively the same or a little greater than the present level (1.0x - 1.5x PAL), Gondwanaland was covered with an ice sheet of $23x10^6$ km^2 (Fig. 30b). If CO_2 levels were three or four times of the present level, ice sheets were distributed around the coastal areas (Fig 30c) with an area of about $4x10^6$ km^2. Or if the great ice sheet reached its maximum at a low CO_2 rate of 1.0x - 1.5x PAL, it remained relatively stable even when a higher CO_2 environment of 3x - 4x PAL was introduced; Ice sheets melted almost completely, however, at 6x PAL.

The GENESIS-SICOPOLIS tests also show the occurrence of glaciations in the Permo-Carboniferous. Figure 31 is the glacial scenario from SICOPOLIS with full extent of ice sheets in GENESIS and Figure 32 is the SICOPOLIS equilibrium scenario with only half the size of the full extent of ice sheets in GENESIS. Both of them are at WarmLo 1.5x PAL conditions.

Discussion

CO_2 level estimate in the Permo-Carboniferous is uncertain and varied greatly based on geochemical models or proxy data (Fig. 28). For example, at 300Ma some authors inferred as similar values as presented by GEOCARB III (Berner and Kothavala, 2001), GEOCARBSULF (Berner, 2006), or pedogenic carbonate and organic matter (Mora et al, 1996). GEOCARB II (Berner, 1994), Ekart et al. (1999), Rothman (2002), Bergman et al.

(2004), and Royer (2006), however, gave a much higher estimate of 3x to 5x modern values. Obviously, such CO_2 level reconstruction uncertainty is climatically significant. Hyde et al. (2006) applied an inverse climate model to constrain paleoclimate estimates and predicted a lower limit of CO_2 than geochemical model from 360 to 340 Ma, and a greater value of CO_2 for 280Ma than GEOCARBSULF.

To make things more complicated, geologists have different views toward the expanse of ice coverage in the Permo-Carboniferous. Previous reconstructions of glaciations suggested a continuous waxing and waning of ice sheets in this period without a significant deglacial interval since 340Ma after the early Carboniferous (e.g., Veevers and Powell, 1987; Frakes and Francis, 1988; Crowell, 1999). Recent studies have demonstrated that three lacuna of deglacials occurred intercalated with three glacials since 340Ma (Isbell et al., 2003; Royer, 2006; Montanez et al., 2007). The incessant versus intermittent glacial history has different significance in paleoclimatology.

Baum and Crowley (1991) demonstrated the seasonal snowline instability in the Carboniferous. Only a perturbation of $0.002 Wm^{-2}$ of solar luminosity would result in a rapid change of ice coverage from 0 to 26.0×10^6 km^2 in a cold summer orbit. They proposed a mechanism for the glaciation and deglaciation of the Carboniferous. If the solar luminosity is below the threshold of $329.663 Wm^{-2}$, a great glaciation occurs, but above that limit, an ice free state exists. It well explained the rapid oscillations of

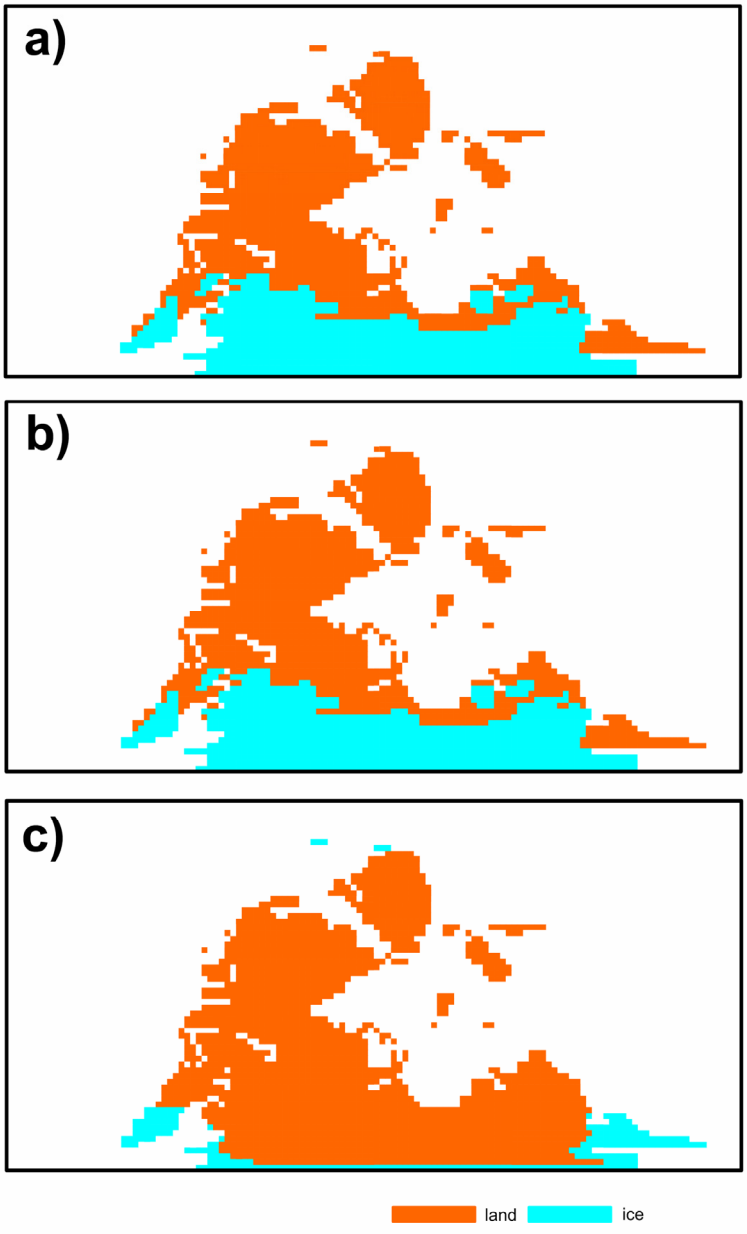

Figure 30. Geological reconstruction and numerical simulations of the Permo-Carboniferous. a) geological reconstructions; b) WarmMd in 1.5x PAL; c) ColdMd in 3xPAL.

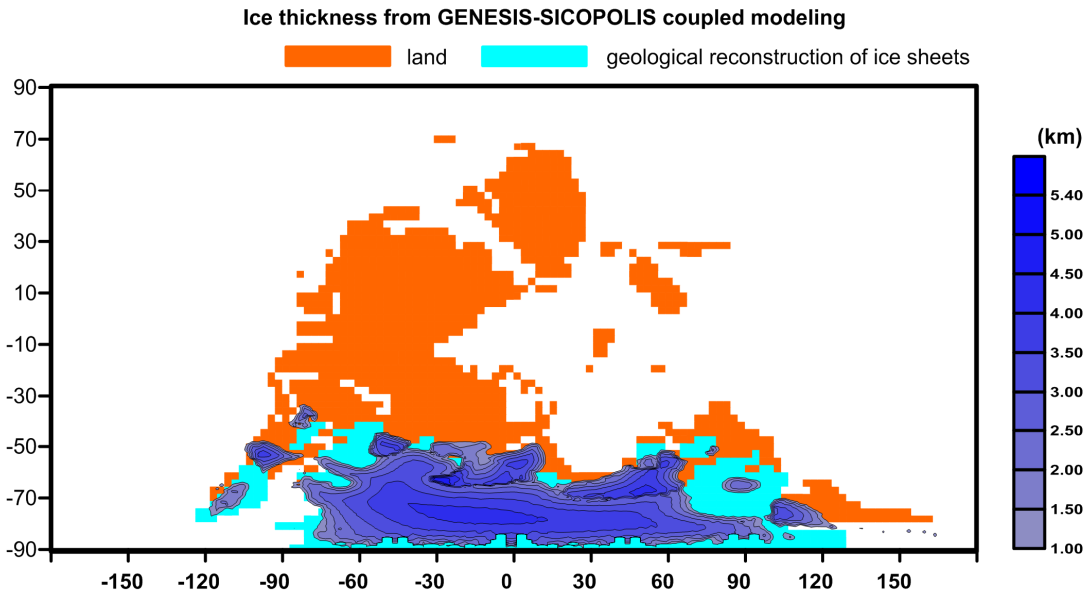

Figure 31. Maximum thickness of ice sheets of the equilibrium state of SICOPOLIS after iterations from an initial ice-free state. The temperature and precipitation input parameters are the results of GENESIS modeling with full ice sheet extent from geological reconstruction.

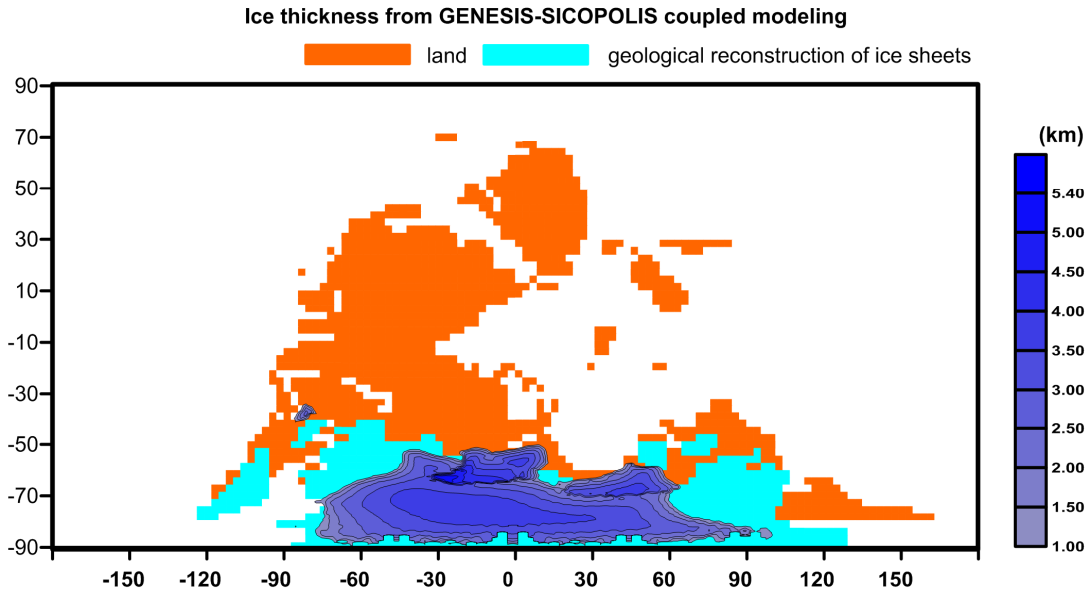

Figure 32. Thickness of ice sheets of the equilibrium state of SICOPOLIS after iterations from an initial ice-free state. The temperature and precipitation input parameters are the results of GENESIS modeling with half of the size of the ice sheets from geological reconstruction.

glaciations and deglaciations. Their study proposed a constant value of CO_2 which is the same as PAL but never addressed this issue in a varied CO_2 scenario.

The EBM simulation revealed that if the CO_2 level in the Permo-Carboniferous was the same or little higher than present levels (1x -1.5x PAL), Gondwanaland was covered with about $26x10^6$ km^2 of ice (Fig. 30b), which agrees well with geological reconstruction (Fig. 30a; Ziegler et al., 1997). The GENESIS-SICOPOLIS tests support the EBM simulation. If CO_2 level is 3 - 4x PAL, Gondwanaland would have a relatively smaller ice coverage near coast (Fig. 30c) reflecting the influence of nearby marine ice and large seasonal cycle over land (Crowley et al., 1987) because of different length scale over water (about 400km) than over land (about 2000km) (Hyde et al., 1990; Baum and Crowley, 1991). If CO_2 increased further, Gondwanaland was in lacuna of deglaciation. After the deglaciation and since the glacial maximum on Gondwanaland, the ice sheet remained relatively stable in a higher CO_2 level (e.g. 3x PAL) which is impossible for initial glaciation because of the nonlinear snow/ice albedo feedback (North, 1984; Hyde et al., 1990; Baum and Crowley, 1991). But it would completely deglaciate above 6x-10x PAL depending on the orbital elements (Fig. 29). Again, if CO_2 decreased to the present level, Gondwanaland would be glaciated once more and start a new cycle of glaciation and deglaciation.

Isbell et al. (2003) considered Gondwanaland glacial I and II were local and narrowly distributed. If CO_2 levels at that periods were 3x - 4x PAL, the simulation of this study

exhibited two ice sheets on both flanks of Gondwanaland. It is generally agreed that Glacial III had a low CO_2 the same or roughly higher than present level (1.0x -1.5x PAL; Fig. 28), and Gondwanaland reached its glacial maximum (Fig. 30b). With the increase of CO_2 levels after three glacial periods, Gondwanaland was deglaciated (Isbell et al., 2003; Montanez et al., 2007).

The essence of SICI is that a slight reduction in insolation, CO_2 level, or even stochastic variations results in a permanent ice cover initially in a small area (e.g., North, 1984; Mengel et al., 1988; Hyde et al., 1990; Lin and North, 1990; Baum and Crowley, 1991; Huang and Bowman, 1992). If CO_2 is lower than 3.0x PAL depending on different orbital elements (Fig. 29a), Gondwanaland was covered with large ice sheets. But if CO_2 level is slightly larger than this threshold, no ice existed in the Gondwanaland hinterland. SICI is applicable to the glaciation of Gondwanaland. Similarly, with an increase in insolation, the CO_2 level brings about an abrupt deglaciation when Gondwanaland reached its glacial maximum. If CO_2 levels were 4x-6x PAL, the glaciated Gondwanaland became ice free, or this phenomenon can be viewed as large ice cap instability (LICI) expounded by Held et al. (1981). SICI and LICI agreed with the three non-overlapping glacials in the Permo-Carboniferous in the CO_2-forced climate.

Changes of CO_2 levels provided an example for SICI and LICI on Gondwanaland in the Permo-Carboniferous. If CO_2 level is the same or slightly higher than present level, Gondwanaland was covered with the greatest ice sheets similar to Glacial III. If CO_2

levels were 3x - 4x PAL, only small ice sheets were found near coasts of Gondwanaland as Glacial I and II (Isbell et al., 2003; Montanez et al., 2007). If CO_2 increased further after glaciation, deglaciation dominated Gondwanaland and if CO_2 levels were between 4x -10 x PAL depending on the orbital elements, lacuna of deglacials occurred.

CHAPTER VI

OCCURRENCE AND STABILITY OF GLACIATIONS IN GONDWANALAND

Synopsis

Gondwanaland is characterized by intervals of continental glaciations and periods of minimal or no ice in geologic time. Five paleogeography maps of the Pre-Cambrian, Cambrian, Ordovician, Silurian, and Triassic are chosen to simulate the occurrence and stability of glaciations in Gondwanaland with a suite combination of CO_2 level and different orbital elements.

A nonlinear EBM model with an empirical ice sheet scheme is used to investigate the occurrence of glaciation on Gondwanaland. The simulations reveal that paleogeography, CO_2 levels and the Milankovitch cycles all contribute to the glaciations of Gondwanaland. The net radiative forcing is the predominant factor to initiate the glaciation or deglaciate after the glacial maximum; continental geography, however, plays an even more important role than the net radiative forcing in some special continental configurations. Meanwhile, the Milankovitch cycle probably causes an abrupt change in a given CO_2 level and continental geography like the Pre-Cambrian. Such combinations of geography, CO_2 levels and solar constant change, and the

Milankovitch cycle complicate the glacial history of Earth. The simulation agrees well with geological evidence.

Introduction

Earth is characterized by intervals of continental glaciations and periods of minimal or no ice in geologic time (e.g., Frakes, 1979; Fisher, 1982; Frakes et al., 1988; Crowley and North, 1991; Frakes et al., 1992; Crowell, 1999; Veizer et al., 2000; Crowley and Berner, 2001). Many theories have been proposed to explain glaciations, such as the Milankovitch cycle, radiative forcing change including solar output and greenhouse effect, polar land shifts, biogeochemical interplay and even bolide impacts (e.g., Hays et al, 1976; Berger, 1978; Imbrie and Imbrie, 1980; Crowley et al., 1987; Crowley and Baum, 1992; Berner and Kothavala, 2001; Huybers, 2006; Drysdale et al., 2009).

Glaciations interspersed between non-glacial periods are common features of the history of Earth (Fig. 33). Five ice ages have been recognized since the Cambrian, namely the Late Cenozoic Ice Age (since ca. 43Ma until present), the Mesozoic Icy Intervals including the Early Cretaceous (ca. 105 -140Ma) and Jurassic Cold Interval (ca. 160 - 175Ma and ca. 188 - 195Ma), the Late Paleozoic Ice Age (ca. 256 - 338Ma), the Late Devonian-Early Carboniferous Ice Age (ca. 353 - 363Ma), and the Ordovician-Silurian Ice Age (ca. 429 - 445Ma) (Crowell, 1999). Some parameters, including CO_2, net radiative forcing, tropical temperature anomaly, and $\delta^{18}O$ show remarkable changes

between glacial and non-glacial periods (Fig. 33). Since the initial study of Vostok ice core, geoscientists have been refining the link between CO_2 and climate change (e.g., Petit et al., 1999; Holbourn et al, 2005; Tripati et al., 2009) (Fig. 34) and put CO_2 as a primary driver for the Phanerozoic climate (Kump, 2002; Royer et al., 2004; Royer, 2006; Royer et al., 2007).

Climate is the "result of changing tectonobiogeochemical activities rooted within the complex earth-air-ocean system itself" (Crowell, 1999, p. 2). Thus, could we use climate models to reconstruct glaciations in geologic time? Further, could we investigate the possibility and stability of glaciations in geologic time using climate models and have the simulation results consistent with geological evidence? A basic problem here is if net radiative forcing, paleogeography, paleobotany induced albedo, orbital elements, geothermal heat flux and other associated parameters are given, could we reconstruct the glaciation and deglaciation history on Earth and reconcile well with the geologic past?

Significant progress has been made in recent years to simulate glaciation for a specific geological period. Crowley and Baum (1992) reconstructed the Phanerozoic glaciation using energy balance models (EBMs) and they also reconciled the glaciation in the Ordovician with high CO_2 and net radiative forcing (Crowley and Baum, 1995). Crowley and Hyde (2008) coupled EBM with an ice sheet model to simulate the late Pleistocene; Hyde et al. (2000) used EBM and an ice sheet model to reconstruct the "snowball Earth" in the Neoproterozoic. At the same time, general circulation models

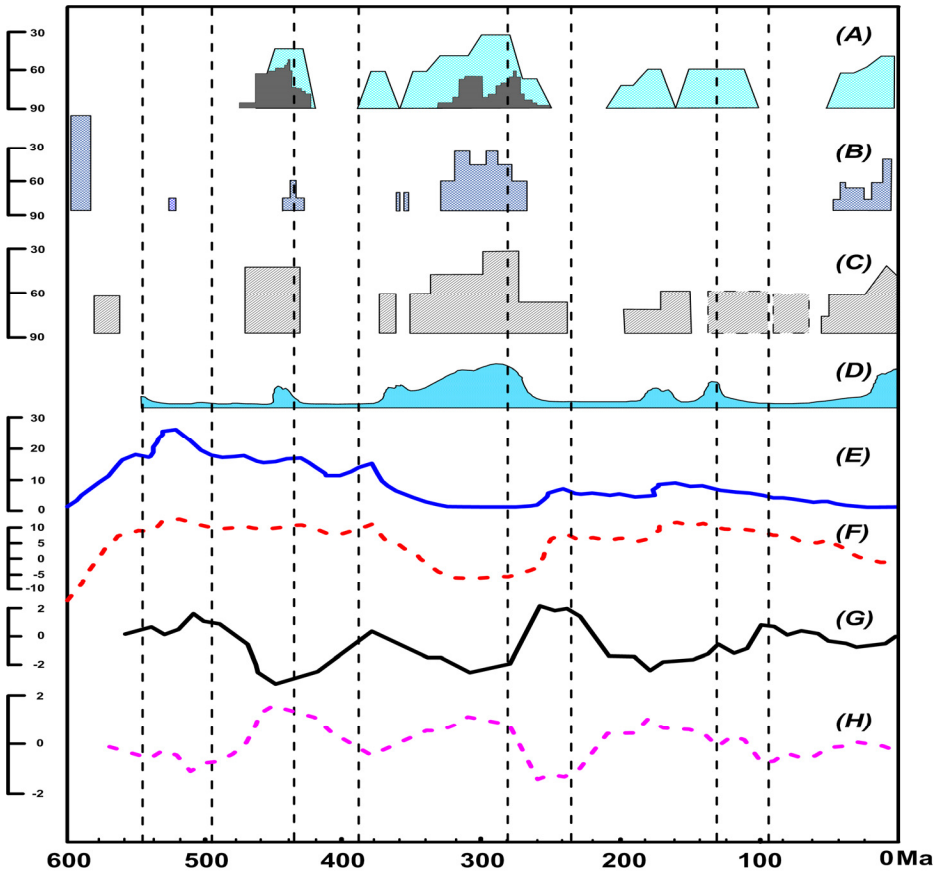

Figure 33. Intervals of glaciations interspersed with times of minimal or no ice in geologic time.

(GCMs) coupled with ice sheet models also made a great leap forward in glaciation modeling. Otto-Bliesner (1996) used GENESIS to discuss the initiation of a continental ice sheet; Pollard and DeConto (2009) reconstructed the growth and collapse of West Antarctic ice sheet through the past five million years using Genesis coupled with a

hydrothermal ice sheet model; Poulsen et al. (2007) explored the tropical climate response to Gondwanan deglaciation using Genesis coupled with a biome model.

Panels A through D in Figure 33 demonstrate glaciation periods from different authors. (A) Veizer et al. (2000), (B) Crowley and Berner (2001), (C) Frakes and Francis (1988), and (D) Crowell (1999) with scales on the left showing the paleolatitude of ice-rafted deposits in degrees. Panels E through G present parameter changes. (E) CO_2 oscillation based on GEOCARB III with scale on the left showing the rate of CO_2 compared with present concentration (Crowley and Berner, 2001; Berner et al., 2001), (F) net radiative forcing based on CO_2 and solar output (Crowley and Berner, 2001) with scale on the left showing change in Wm^{-2}, (G) mean tropical temperature anomaly with scale on the left showing change in ℃(Crowley and Berner, 2001), and (H) detrended calcite $\delta^{18}O$ in ‰ PDB (Veizer et al., 2000). Dashed lines are the interest durations for the ongoing research.

Climate change in geologic time was stepwise or abrupt depending upon the boundary conditions (Crowley and North, 1988; Alley et al., 2003). The small ice cap instability theory (SICI) (North, 1984) was proposed as a possible cause.

North (1984) theoretically deduced the classic snowline instability curve based on a diffusive zonally symmetric mean annual energy balance model (EBM). SICI was also found in the seasonal EBM and GCMs (Held et al., 1981; Mengel et al., 1988; Lin and

North, 1990). Later SICI was confirmed in a realistic geography at 300Ma and applied to the Carboniferous glaciation (Baum and Crowley, 1991; Crowley et al., 1993; Hyde et al., 2006). The question here is: was SICI widespread in geologic time? Is its mechanism a candidate to interpret the abrupt or stepwise climate change?

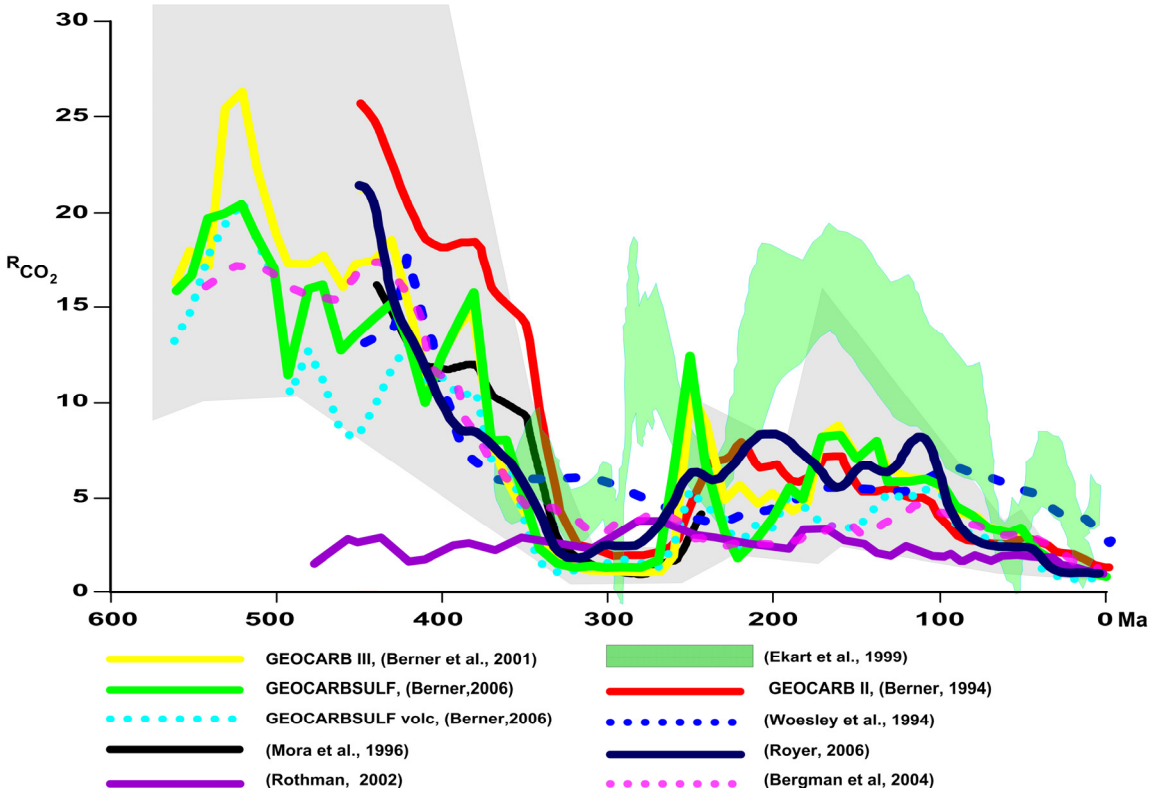

Figure 34. CO_2 levels in the Phanerozoic time. The x-axis is time before present in million years and the y-axis is the CO_2 ratio to the pre-industrial level. The gray shade shows the minimum and maximum CO_2 range of GEOCARB III.

The objective of the this study is to reconstruct the occurrence and stability of glaciations in Gondwanaland by the nonlinear two dimensional energy balance model with seasonal temperature ice sheet scheme under the scenario of various CO_2 levels (Fig. 34).

A suite of realistic geography with orbital elements of the last glacial maximum and the last interglacial with varied CO_2 concentrations (Fig. 34) and solar luminosity will be used in calculations to examine the SICI and discuss the occurrence and stability of glaciations in geologic time.

Methods

A nonlinear EBM from Stevens's version (Stevens and North, 1996) with an empirical ice sheet scheme will be applied to investigate the occurrence and stability of glaciations in geologic time. Six periods are chosen as modeling intervals, namely the pre-Cambrian 600Ma, the early Cambrian 547Ma, the early Ordovician 497Ma, the late Ordovician 430Ma, the late Devonian 370Ma, and the early Triassic 237Ma, respectively.

Calculating the seasonal cycle as a function of solar input, longwave radiation and continental geography, EBM has been successfully applied in paleoclimatology (e.g., North et al., 1983; Hyde et al., 1990; Crowley and North, 1991; Baum and Crowley, 1991). CO_2 was used as an important radiative forcing with a formula introduced by

Myhre et al. (1998). The simple scheme to ice sheet buildup was similar to Hyde et al. (1990). A series of CO_2 levels are applied to the numerical scheme ranging from 1x to 18x PAL. Any land with monthly average temperature less than -2ºC is defined as ice covered; meanwhile, any sea with monthly average temperature less than -4ºC is stipulated as having sea ice. The nonlinear EBM is used with ice sheet feedback mechanism with orbital elements and CO_2, and will test the occurrence and distribution of glaciations with a seasonal ice sheet scheme (Hyde et al., 1990; Hyde et al., 2006).

Five sets of sensitivity tests have been designed to check the occurrence and stability of glaciations: 1) ice albedo is 0.68 and temperature of land-ice transfer threshold is -2ºC; 2) ice albedo is 0.68 and temperature of land-ice transfer threshold is 0ºC; 3) ice albedo is 0.70 and temperature of land-ice transfer threshold is 0ºC; 4) ice albedo is 0.80 and temperature of land-ice transfer threshold is -2ºC; and 5) ice albedo is 0.70 and temperature of land-ice transfer threshold is 1ºC. The purpose of these tests will examine the effects of snow-ice albedo feedback and topographic effects (Crowley and Baum, 1991).

Modeling Results

Simulations have revealed that at low CO_2 levels of 1x - 3x PAL, the six geologic periods have the possibilities of glaciations. Because of the constraints of CO_2 (Fig. 34),

however, these paleogeography maps demonstrate different glacial scenarios under increased CO_2 levels.

The pre-Cambrian 600 Ma experienced glaciations at low CO_2 levels and Figure 35 shows the glaciation picture and its summer temperatures. At LGM orbital condition, the simulation results show an abrupt change point from 1.3x PAL to 1.4x PAL, only a very slight change of radiative forcing, and the glaciated area rapidly changes from 12.31 $x10^6$ km2 to 2.03 $x10^6$ (Fig. 36). At 2x PAL the ice area is less than $1x10^6$ km2 which is deemed to be ice free according to little ice criterion (Hyde et al., 2006). Such abruptness also appears at LIG orbital condition from 1.6x to 1.7x PAL CO_2 levels. A second bifurcation point occurs around 1.9x PAL CO_2 level at LIG condition (Fig. 36). The second abruptness might reveal that at given CO_2 levels the perturbation caused by orbital elements would have remarkable effects on waxing and waning of glaciations. The modeling efforts show that starting from 2x PAL CO_2 levels ice is poorly preserved in the Pre-Cambrian.

The paleogeographies of 430 Ma is chosen to represent the late Ordovician and early Silurian. Figure 37 shows the occurrence and stability of glaciations during this time span. Several sensitivity tests have all proved occurrence of glaciations (Fig. 38 through Fig. 40) at high CO_2 levels. The Milankovitch cycle induced waxing and waning of about 3 x 10^6 km^2 ice sheets.

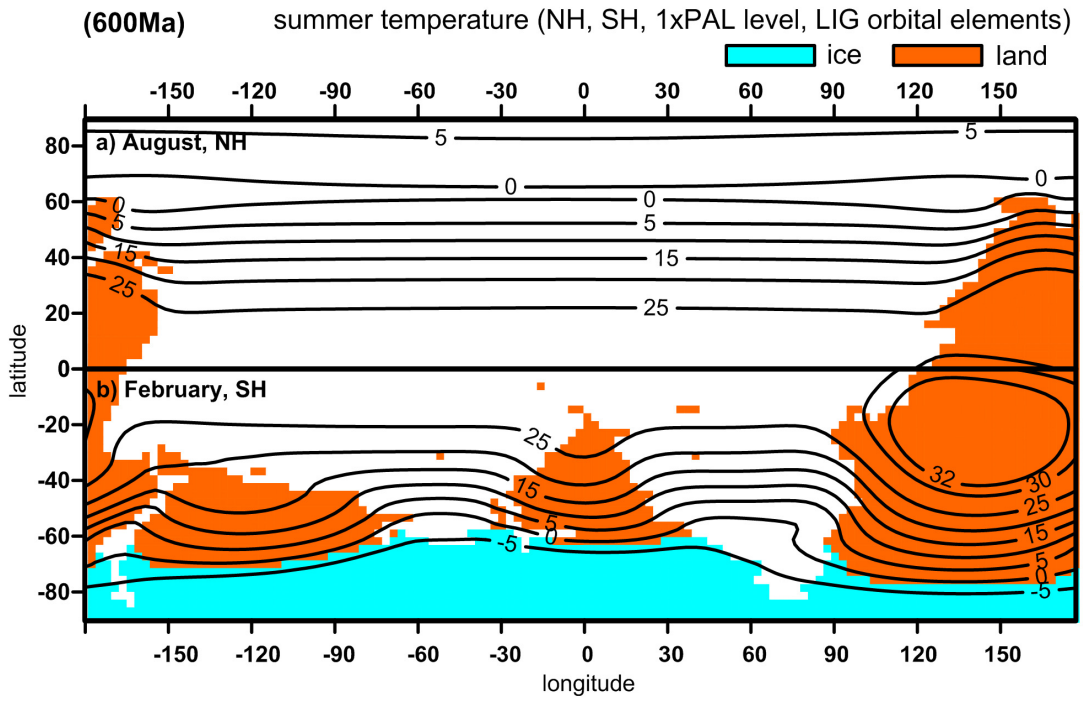

Figure 35. Glacial occurrence in the Pre-Cambrian under low CO_2 levels. Ice sheets remain within the 0ºC isotherm during the summer which shows stability. With a slight increase of CO_2 levels, no ice sheets would appear on the Pre-Cambrian paleogeography.

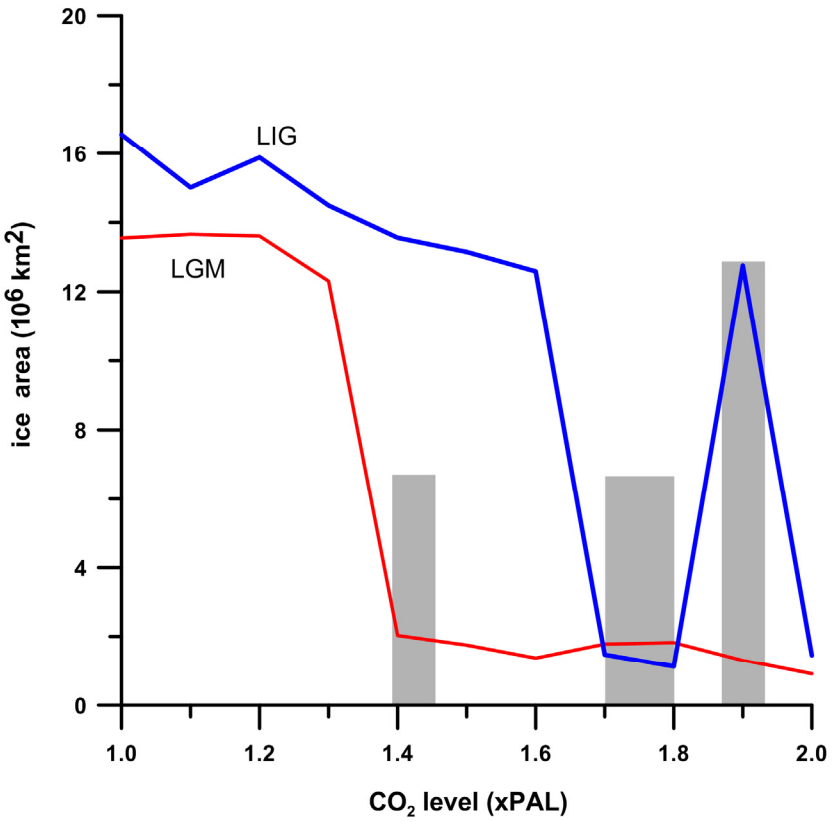

Figure 36. Different glacial scenarios under different CO_2 levels with LIG and LGM orbital elements in 600Ma. Bifurcation points occur for LGM and LIG conditions. The abrupt change takes place from 1.3x to 1.4x PAL CO_2 level for LGM but from 1.6x to 1.7x PAL CO2 level for LIG. A second bifurcation point also occurs for LIG orbital condition at 1.9x PAL CO_2 level.

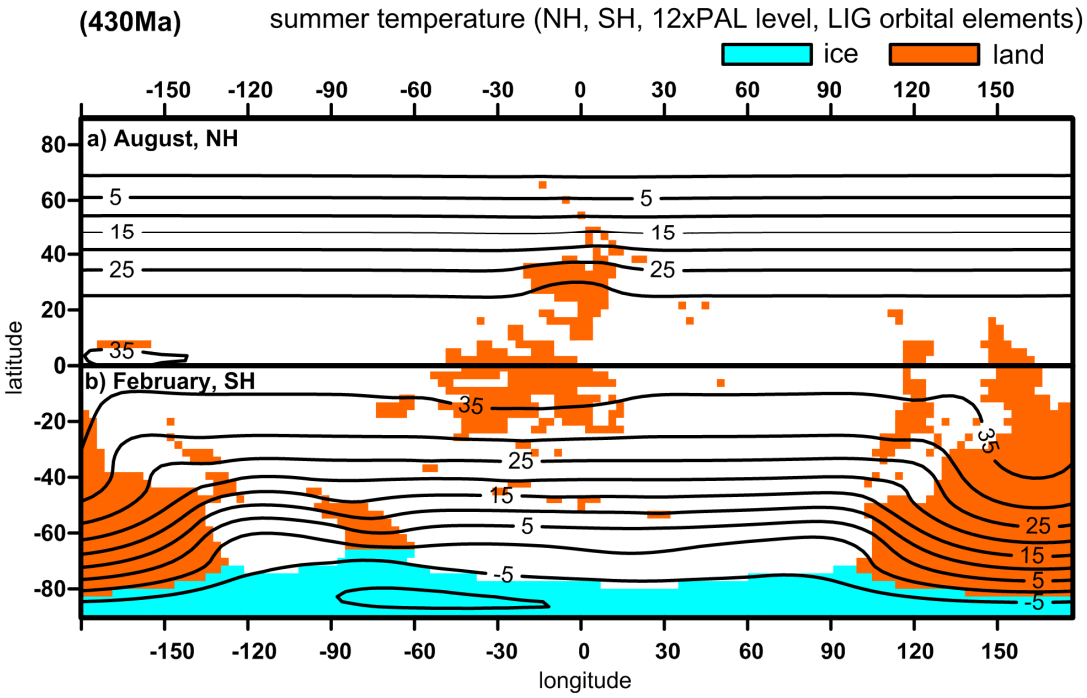

Figure 37. Glacial occurrence in the late Ordovician and early Silurian at high CO_2 levels. Ice sheets remain within the 0ºC isotherm during the summer time which shows stability.

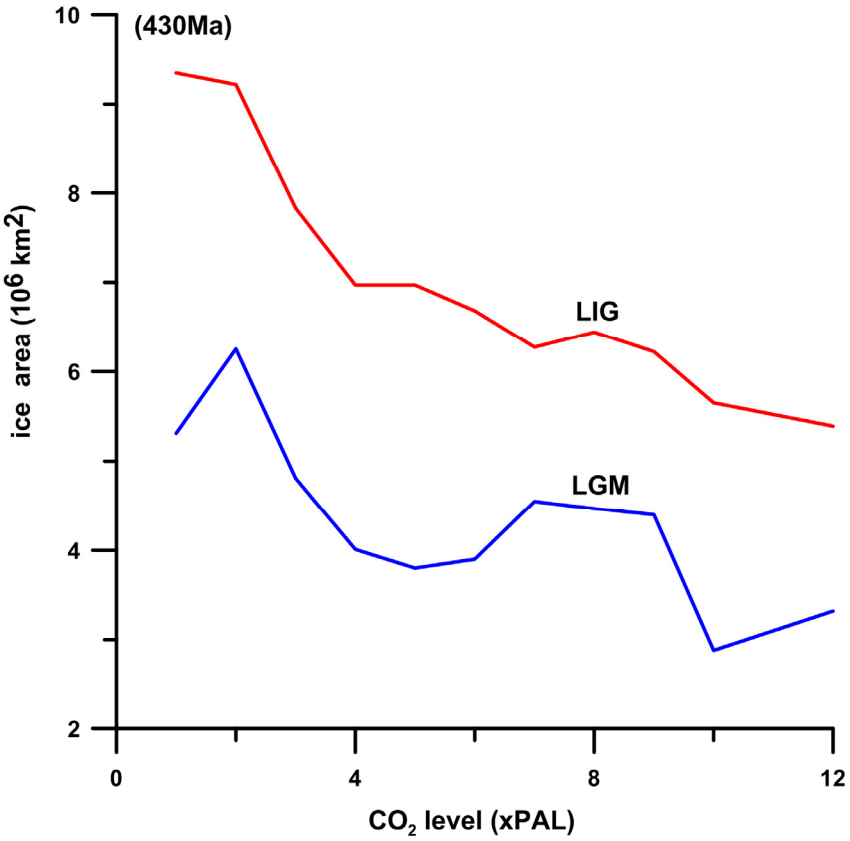

Figure 38. Glacial scenarios under different CO_2 levels at 0ºC land-ice transfer threshold and 0.68 ice albedo. The nonlinear iteration for this sensitivity test is that land-ice transfer threshold is 0ºC and ice albedo is 0.68. Even at very high CO_2 levels ice area remains at 6x 10^6 km^2 for LIG condition and 3x 10^6 km^2 for LGM condition.

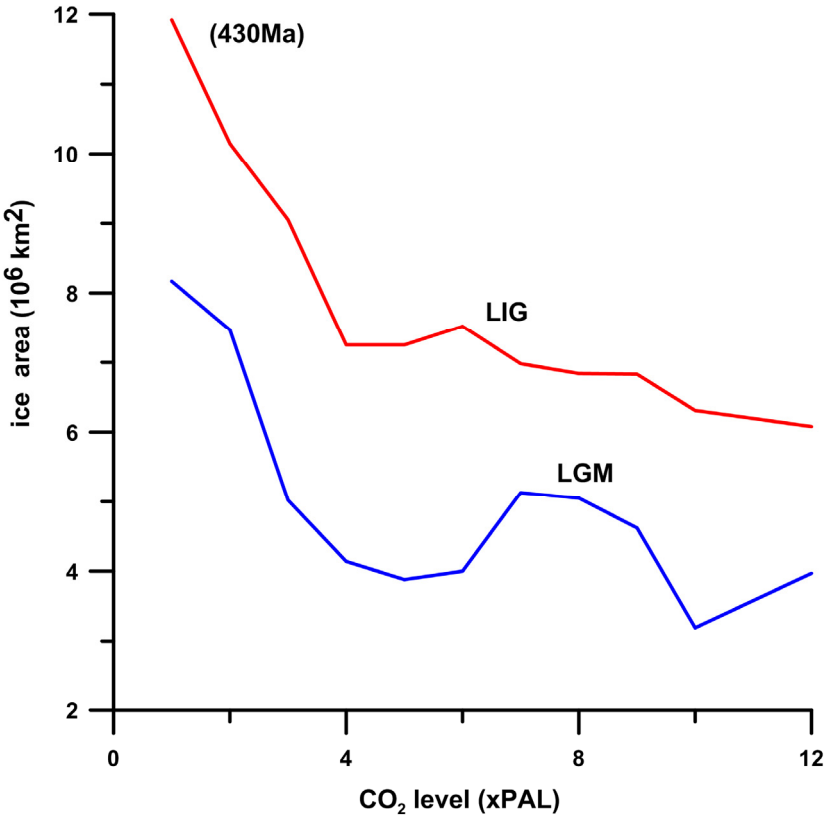

Figure 39. Glacial scenarios under different CO_2 levels at 0ºC land-ice transfer threshold and 0.70 ice albedo. The nonlinear iteration for this sensitivity test is that land-ice transfer threshold is 0ºC and ice albedo is 0.70. Even at very high CO_2 levels ice area remains at 7x 10^6 km^2 for LIG condition and 4x 10^6 km^2 for LGM condition.

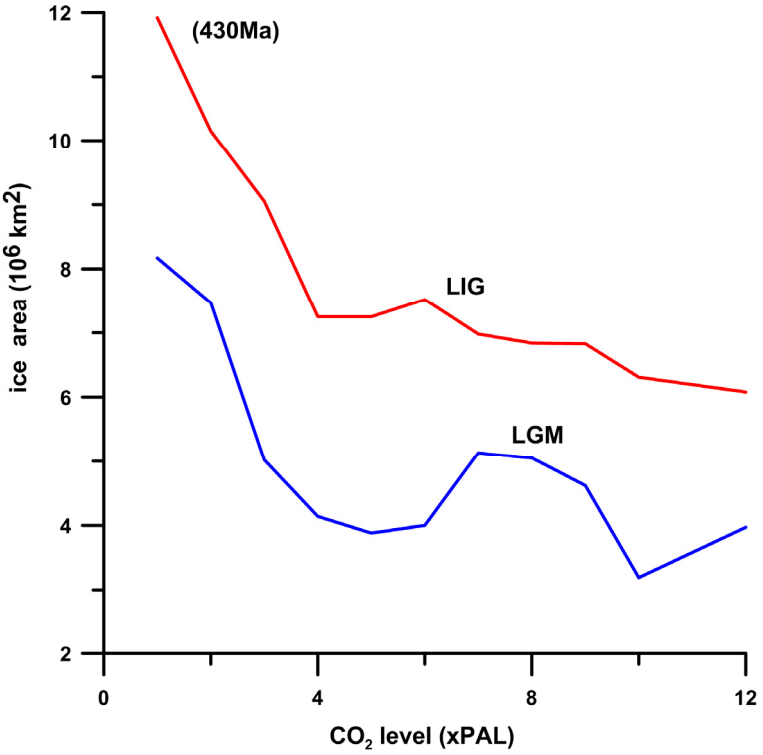

Figure 40. Glacial scenarios under different CO_2 levels at -2ºC land-ice transfer threshold and 0.80 ice albedo. The nonlinear iteration for this sensitivity test is that land-ice transfer threshold is -2ºC and ice albedo is 0.80. Even at very high CO_2 levels ice area remains at 7x 10^6 km^2 for LIG condition and 4x 10^6 km^2 for LGM condition.

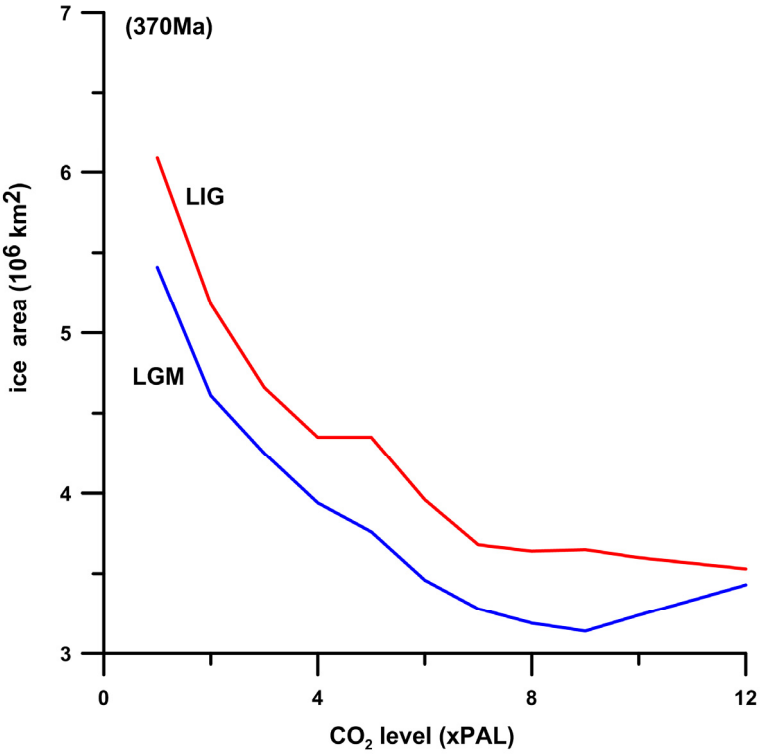

Figure 41. Glacial scenarios under different CO_2 levels at -2ºC land-ice transfer threshold and 0.68 ice albedo. The nonlinear iteration for this sensitivity test is that land-ice transfer threshold is -2ºC and ice albedo is 0.68. Even at very high CO_2 levels ice area remains at 3.4x 10^6 km^2 for LIG condition and 3.5x 10^6 km^2 for LGM condition.

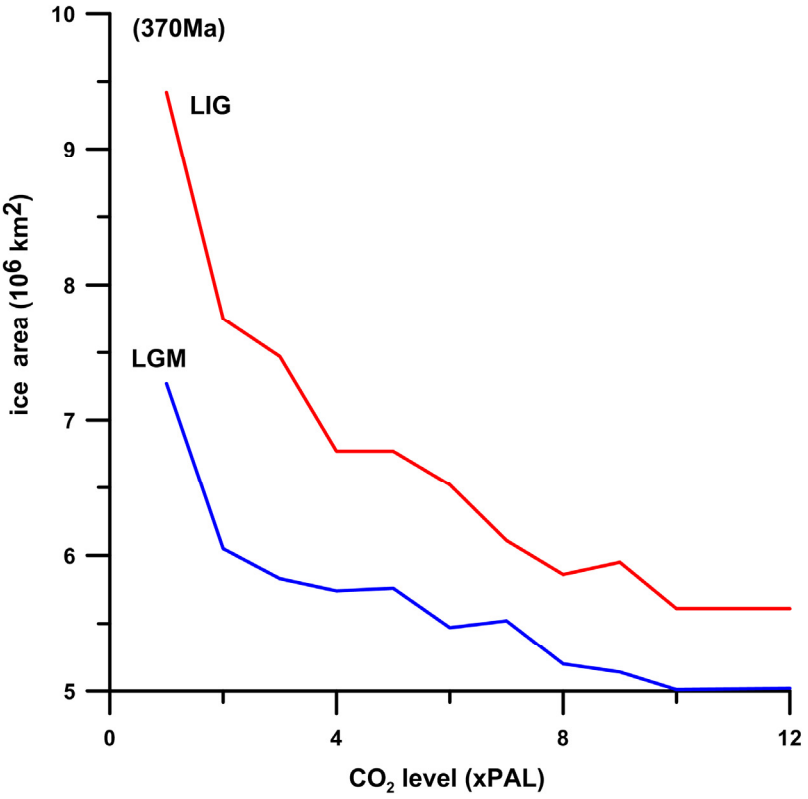

Figure 42. Glacial scenarios under different CO_2 levels at 0ºC land-ice transfer threshold and 0.68 ice albedo. The nonlinear iteration for this sensitivity test is that land-ice transfer threshold is 0ºC and ice albedo is 0.68. Even at very high CO_2 levels ice area remains at 6x 10^6 km^2 for LIG condition and 5x 10^6 km^2 for LGM condition.

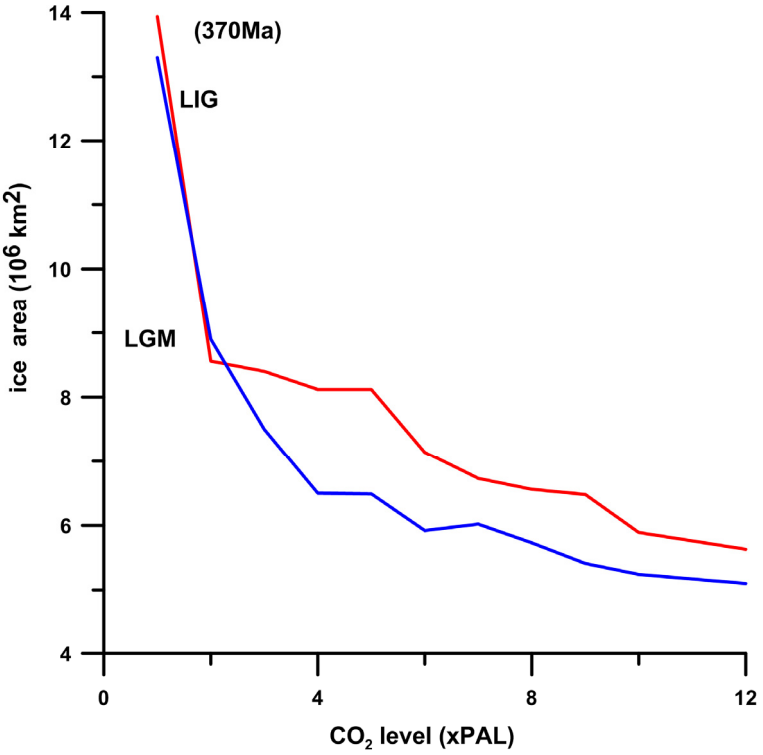

Figure 43. Glacial scenarios under different CO_2 levels at 0ºC land-ice transfer threshold and 0.70 ice albedo. The nonlinear iteration for this sensitivity test is that land-ice transfer threshold is 0ºC and ice albedo is 0.70. Even at very high CO_2 levels ice area remains at 6x 10^6 km^2 for LIG condition and 5x 10^6 km^2 for LGM condition.

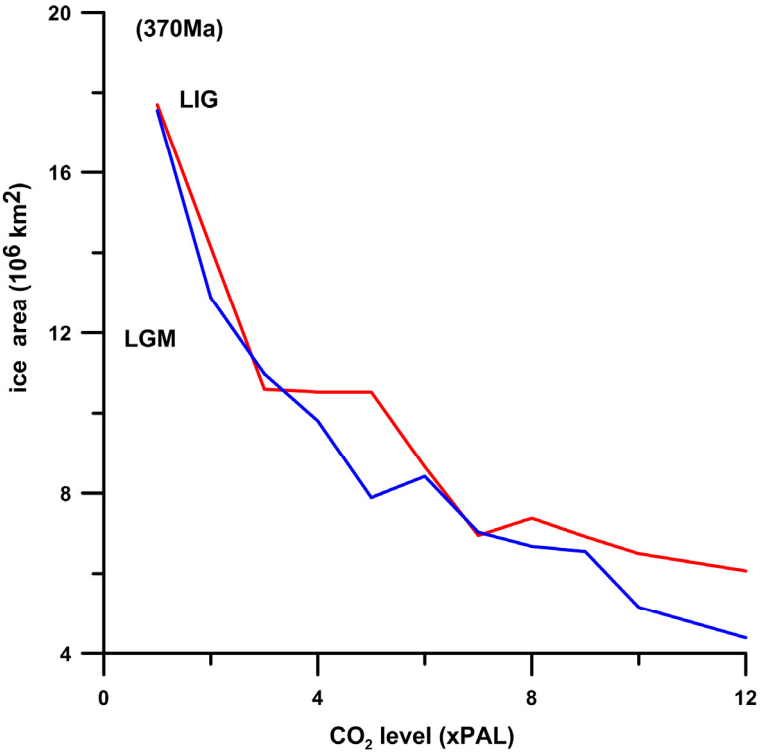

Figure 44. Glacial scenarios under different CO_2 levels at -2ºC land-ice transfer threshold and 0.80 ice albedo. The nonlinear iteration for this sensitivity test is that land-ice transfer threshold is -2ºC and ice albedo is 0.80. Even at very high CO_2 levels ice area remains at 6x 10^6 km^2 for LIG condition and 4x 10^6 km^2 for LGM condition.

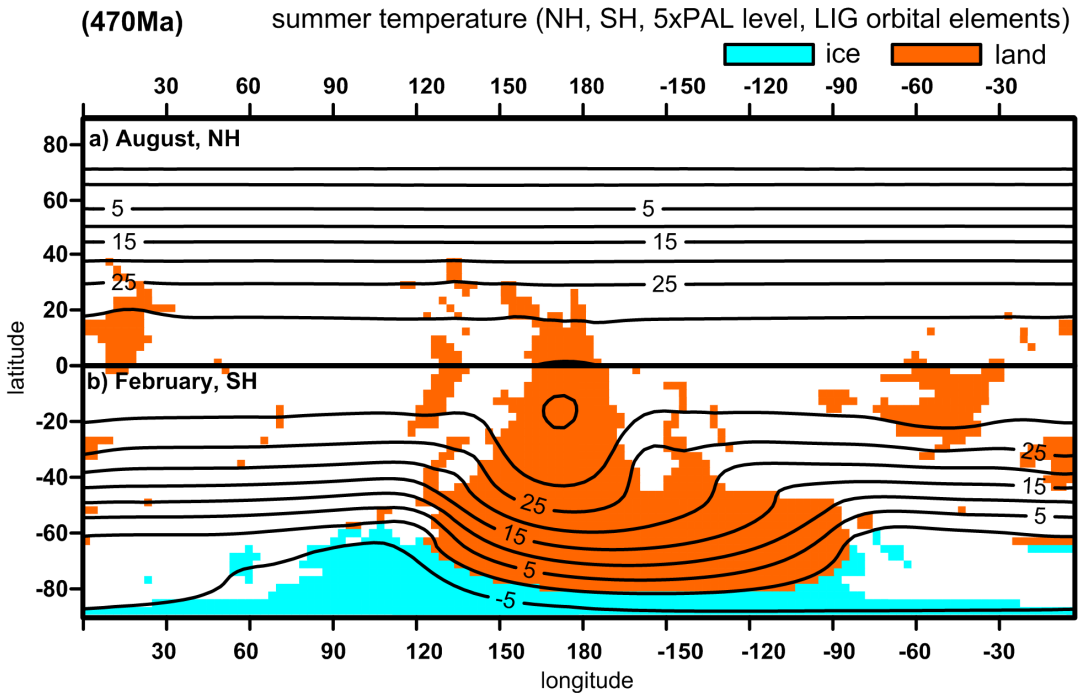

Figure 45. Glacial occurrence in the early Ordovician at an intermediate CO_2 levels. The nonlinear iteration for this sensitivity test is that land-ice transfer threshold is -2ºC and ice albedo is 0.80 with the LIG orbital elements. Ice sheets remain within the 0ºC isotherm during the summer. The simulations show that about 6x 10^6 km^2 of ice sheets occur in the 470Ma paleogeography at 5x PAL CO_2 level.

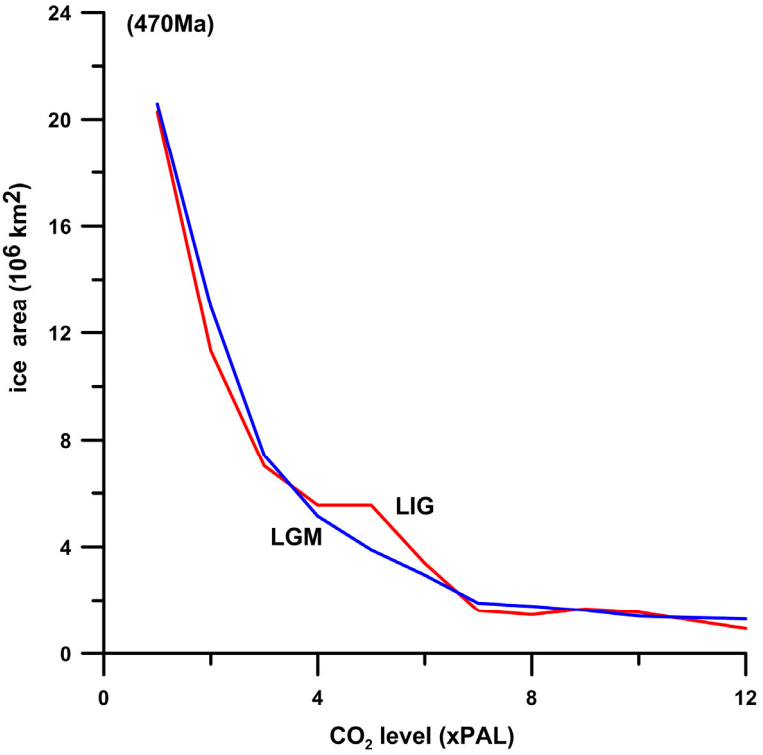

Figure 46. Glacial scenarios under different CO_2 levels at -2ºC land-ice transfer threshold and 0.80 ice albedo. The nonlinear iteration for this sensitivity test is that land-ice transfer threshold is -2ºC and ice albedo is 0.80. Even at very high CO_2 levels ice area remains at 2x 10^6 km^2 for LIG condition and 2x 10^6 km^2 for LGM condition.

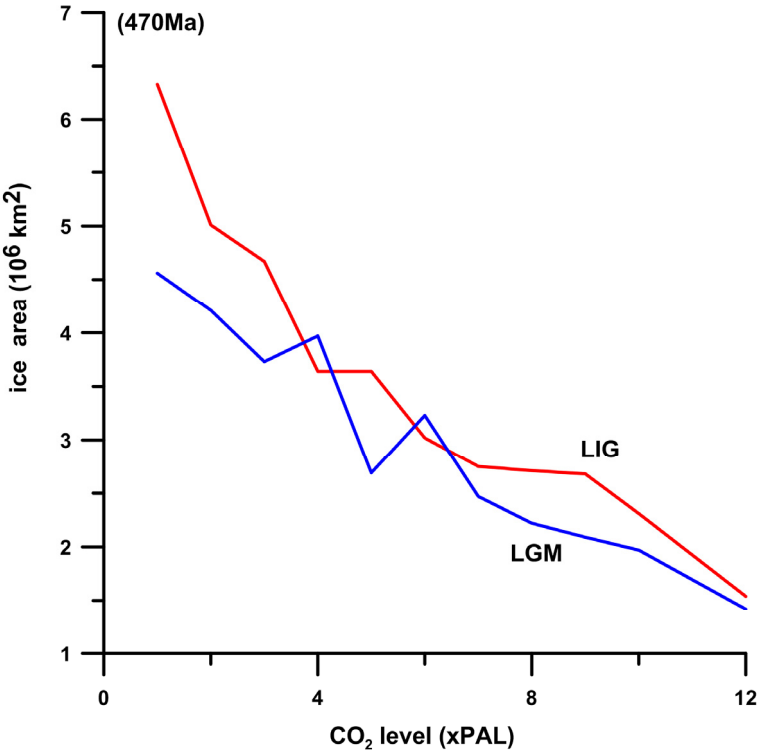

Figure 47. Glacial scenarios under different CO_2 levels at 0ºC land-ice transfer threshold and 0.70 ice albedo. The nonlinear iteration for this sensitivity test is that land-ice transfer threshold is 0ºC and ice albedo is 0.70. Even at very high CO_2 levels ice area remains at 3x 10^6 km^2 for LIG condition and 2x 10^6 km^2 for LGM condition.

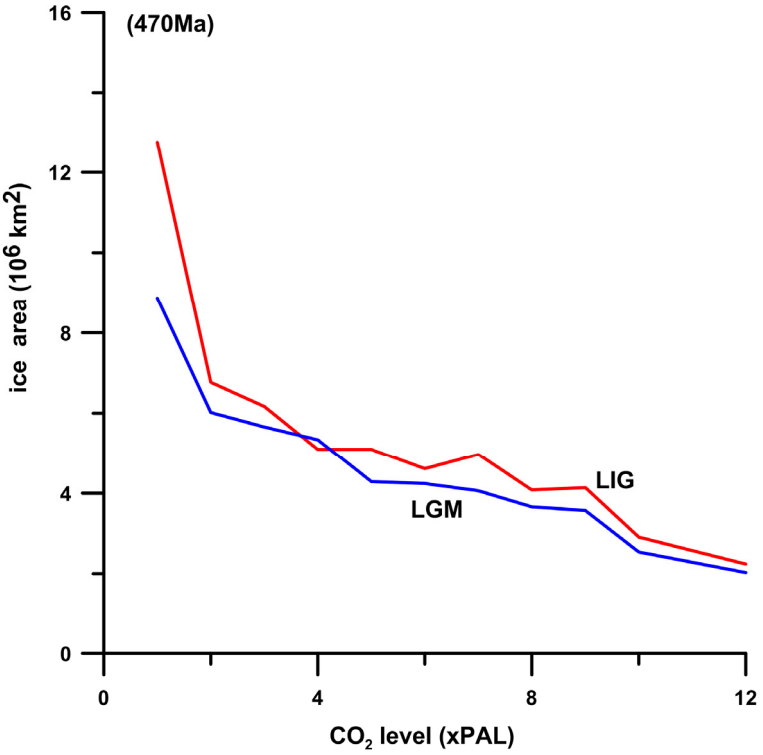

Figure 48. Glacial scenarios under different CO_2 levels at 1ºC land-ice transfer threshold and 0.70 ice albedo. The nonlinear iteration for this sensitivity test is that land-ice transfer threshold is 1ºC and ice albedo is 0.70. Even at very high CO_2 levels ice area remains at 4x 10^6 km^2 for LIG condition and 4x 10^6 km^2 for LGM condition.

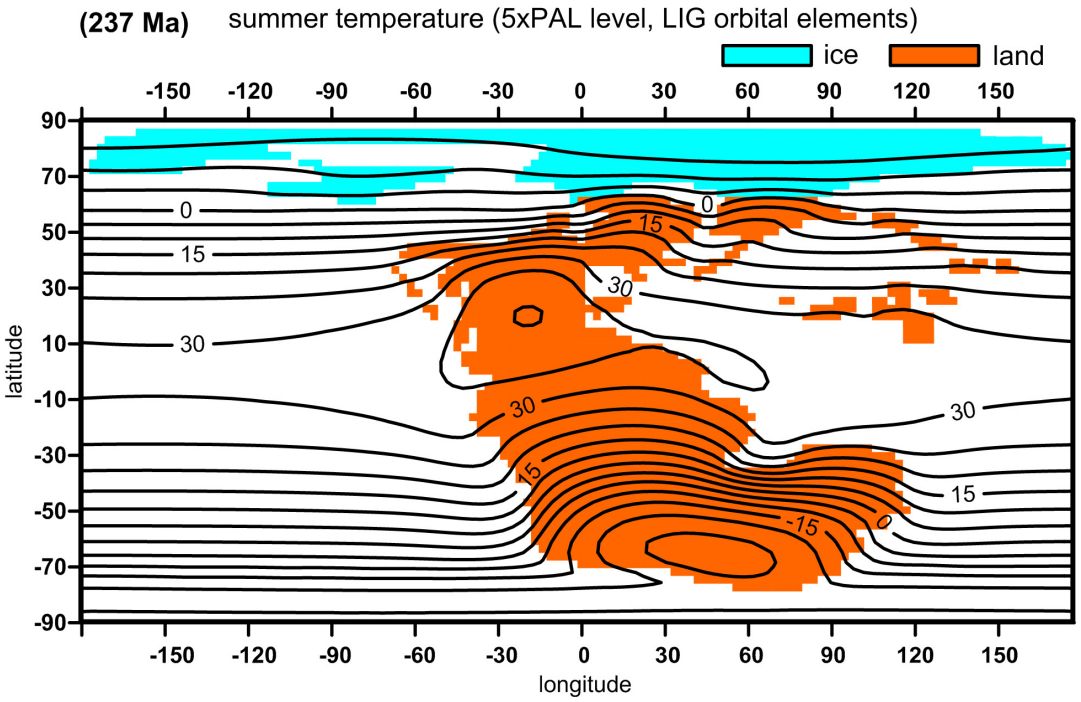

Figure 49. Glacial occurrence in the early Triassic at an intermediate CO_2 level. The nonlinear iteration for this sensitivity test is that land-ice transfer threshold is -2ºC and ice albedo is 0.80 with the LIG orbital elements. Ice sheets remain within the 0ºC isotherm during the summer. The simulations show that about 13x 10^6 km^2 of ice sheets occur in the 237Ma paleogeography at 5x PAL CO_2 level.

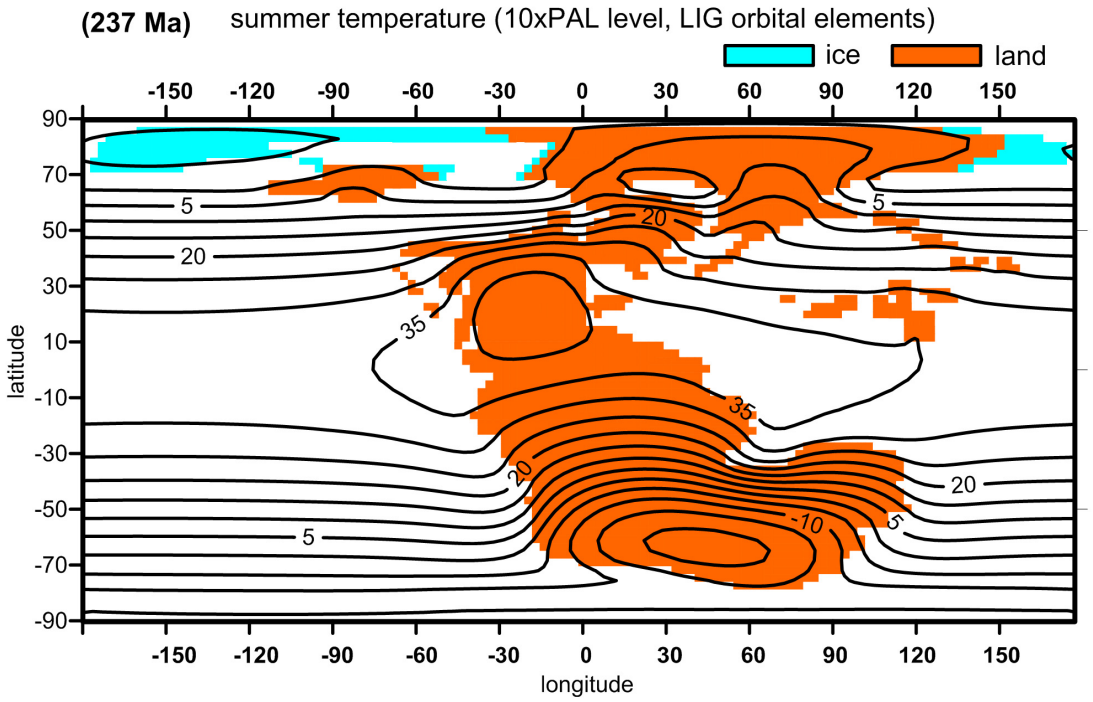

Figure 50. Glacial occurrence in the early Triassic at a high CO_2 level. The nonlinear iteration for this sensitivity test is that land-ice transfer threshold is -2ºC and ice albedo is 0.80 with the LIG orbital elements. Ice sheets remain within the 0ºC isotherm during the summer. The simulations show that little ice occurs in the 470Ma paleogeography at 10x PAL CO_2 level which means that at high CO_2 levels no ice sheets exist in the Triassic.

The paleogeography of 370Ma is chosen to represent the late Devonian. Several sensitivity tests also have all proved occurrence of glaciations (Fig. 41 through Fig. 44) at high CO_2 levels. The Milankovitch cycle induced waxing and waning of about 2×10^6 km^2 ice sheets.

Simulations from 470Ma paleography exhibits that glaciations happen at intermediate CO_2 levels (Fig. 45); however, with the increase of CO_2 levels, no ice can endure the increasing radiative forcing (Fig. 46 through Fig. 48). So if CO_2 levels were high at that time, no glaciations were expected. Similar patterns can also find in the early Triassic (237Ma) in different CO_2 levels (Fig. 49 and Fig. 50).

Discussion

Continental geography plays a more decisive role than CO_2 although the CO_2 paradigm still holds in some special Gondwanaland cases. Because of the strong seasonal variability of Gondwanaland (Crowley et al., 1986; Crowley et al., 1987), glaciations usually need low CO_2 levels to develop; however, the simulation shows that both paleogeography and CO_2 levels have played important roles in the occurrence and intensity of glaciation. Glaciation only happens in Pre-Cambrian 600Ma at low CO_2 levels if the CO_2 level is slightly greater than 1.4x PAL for LGM and 1.7x PAL for LIG orbital elements. Ice sheets could exist at low CO_2 levels in late Cambrian 497Ma which is contrary to the high CO_2 levels at that time (Figure 34). On the other hand, some

paleogeographic reconstructions support glaciations at high CO_2 levels, such as late Ordovician to early Silurian 430Ma and late Devonian 370Ma, which agrees well with the simulation results of Crowley and Baum (1991).

Geological evidence has proved that glaciations existed in the pre-Cambrian, late Ordovician especially the Hirnantian stages, early Silurian, and late Devonian (Caputo, 1985; Hambrey, 1985; Brenchley et al, 1994; Brenchley et al, 1999; Crowell, 1999; Kump et al., 1999; Sutcliffe et al., 2000; Brenchley et al, 2003; Melchin and Holmden, 2006; Delabroye and Vecoli, 2010). Reconstructions of CO_2 level (Figure 34) combined with the simulations support for the CO_2 paradigm. The Milankovitch cycle is not the only factor for the inception and demise of glaciations although the Milankovitch cycle does play significant roles in waxing and waning of ice sheets. The Milankovitch cycle alone is not sufficient to initiate the glaciation. It still needs an appropriate CO_2 level. If CO_2 can not reach the threshold, no glaciation will develop even the orbital elements are optimal.

Paleogeography, CO_2 levels and the Milankovitch cycle all contribute to the glaciations of Gondwanaland. The net radiative forcing is the predominant factor to initiate the glaciation or deglaciate after the glacial maximum; however, continental geography is even more important than the net radiative forcing such as the serial simulations have shown. Meanwhile, the Milankovitch cycle probably causes an abrupt change in given CO_2 level and geography like the Pre-Cambrian (Fig. 36). Such combinations of

geography, CO_2 levels and solar constant change, and the Milankovitch cycle complicate the glacial history of Earth.

CHAPTER VII

SUMMARY

Glaciations interspersed between non-glaciations are common features of the history of Earth. Using climate models, this study investigates the occurrence and stability of glaciations in geologic time, reconstructs the glacial and deglacial history, and reconciles the simulation results with the geologic evidence.

The nonlinear EBM model with an empirical ice sheet scheme proved to be robust. The simulations have shown that at each iteration step the ice sheet remains within the 0℃ isotherms of summer temperature and it is capable of applying to the study of occurrence and stability of glaciations in geologic time.

The CO_2 level and the Milankovitch cycles contribute to the glaciation process. Lower CO_2 lowers the global temperature and the nonlinear iteration finally builds up the ice sheets from ice-albedo feedback. The high ice albedo enhanced the growth of ice sheets. Net radiative forcing caused by greenhouse gases, such as CO_2 and solar constant change are the primary drivers to glacial inception or demise. The Milankovitch cycles adjust the waxing and waning of ice sheets.

A simple linear two dimensional energy balance model is applied to present, the LGM, 15ka, 12ka and 9ka BP, respectively, with corresponding continental geography, albedo,

greenhouse gas concentrations, and orbitally forced changes in seasonal insolation. The simulation results show that the summertime thawline conformed closely to the equatorward edge of the ice sheets and implies the relative stability toward deglaciation.

Many geological studies have revealed the three brief global cooling events in the Cretaceous, the Campanian-Maastrichtian boundary, mid-Maastrichtian, and end-Maastrichtian. The data inferred a possible whole glaciation of Antarctica. The simulation results support the idea of glaciation during this time of supergreenhouse. About half to a full size of the modern Antarctic ice sheet has been reconstructed corresponding with 20~40m of sea level change which agrees well with recent isotopic discoveries.

The modeling shows that ice sheets exist in the Cretaceous given CO_2 levels and orbital elements. At low CO_2 levels (1x-6x PAL), ice sheets exist in all the simulation periods no matter LGM or LIG orbital elements. At high CO_2 levels (>7x PAL) ice sheets are rarely present except at 69Ma with LIG orbital elements. If the CO_2 level is >12x PAL, no ice sheets will form.

Recent studies have demonstrated that the Permo-Carboniferous was characterized by three non-overlapping glacial episodes with ice-free lacuna. The simulation results based on the energy balance model with a simple empirical ice-sheet scheme are presented to explain such hysteresis of glaciations. Gondwanaland reached its glacial maximum when

CO_2 level was roughly the same or slightly higher than the preindustrial value. If the CO_2 level was three to four times of the preindustrial value, glaciation was only distributed along coasts of Gondwanaland. With a further increase of CO_2, deglaciation dominates and results in an ice free state. Again, if CO_2 decreased to the present level, Gondwanaland would be glaciated once more and start a new cycle of glaciation and deglaciation. Changes of CO_2 levels provided an example for SICI and LICI on Gondwanaland in the Permo-Carboniferous. The simulation agrees well with recent geological evidence.

Gondwanaland is characterized by intervals of continental glaciations and periods of minimal or no ice in geologic time. Five paleogeography maps of the Pre-Cambrian, Cambrian, Ordovician, Silurian, and Triassic are chosen to simulate the occurrence and stability of glaciations in Gondwanaland with a suite combination of CO_2 level and different orbital elements.

The simulations reveal that paleogeography, CO_2 levels and the Milankovitch cycles all contribute to the glaciations of Gondwanaland. The net radiative forcing is the predominant factor to initiate the glaciation or deglaciate after the glacial maximum; continental geography, however, plays an even more important role than the net radiative forcing in some special continental configurations. Meanwhile, the Milankovitch cycle probably causes an abrupt change in a given CO_2 level and continental geography like the Pre-Cambrian.

This study shows that orbital elements alone are insufficient to account for the evolution of ice sheets. Net radiative forcing caused by greenhouse gases, such as CO_2 and solar constant change are the primary drivers to glacial inception or demise. Continental geography, CO_2 levels, solar constant change, and the Milankovitch cycles complicate the glacial history of Earth.

REFERENCES

Alley, R.B., Marotzke, J., Nordhaus, W.D., Overpeck, J.T., Peteet, D.M., Peilke Jr., R.A., Pierrehumbert, R.T., Rhines, P.B., Stocker, T.F. , Talley, L.D., Wallace, J.M., 2003. Abrupt climate change. Science 299, 2005-2010.

Ando, A., Huber, B.T., MacLeod, K.G., Ohta, T., Khim, B-K., 2009. Blake Nose stable isotopic evidence against the mid-Cenomanian glaciation hypothesis. Geology 37, 451-454.

Barnola, J.M., Raynaud, D., Korotkevich, Y.S., Lorius, C., 1987. Vostok ice core provides 160,000-year record of atmospheric CO_2. Nature 329, 408-414.

Baum, S.K., Crowley, T.J., 1991. Seasonal snowline instability in a climate model with realistic geography: application to Carboniferous (~300Ma) glaciation. Geophysical Research Letters 18, 1719-1722.

Berger, A.L., 1978. Long-term variations of daily insolation and Quaternary climatic changes. Journal of the Atmospheric Sciences 35, 2362-2367.

Bergman, N.M., Lenton, T.M., Watson, A.J., 2004. COPSE: a new model of biogeochemical cycling over Phanerozoic time. American Journal of Science 304, 397-437.

Berner, R. A., 1991. A model for atmospheric CO_2 over Phanerozoic time. American Journal of Science 291, 339-376.

Berner, R.A., 1994. GEOCARB II: a revised model of atmospheric CO2 over Phanerozoic time. American Journal of Science 294, 56-91.

Berner, R.A., 2006. GEOCARBSULF: a combined model for Phanerozoic atmospheric O_2 and CO_2. Geochimica et Cosmochimica Acta 70, 5653-5664.

Berner, R.A., Kothavala, Z., 2001. GEOCARB III: a revised model of atmospheric CO_2 over Phanerozoic time. American Journal of Science 301, 182-204.

Blakey, R.C., 2008. Gondwana paleogeography from assembly to breakup: a 500 m.y. Odyssey. In: Fielding, C.R., Frank, T.D., and Isbell, J.L., (Eds.), Resolving the Late Paleozoic Ice Age in Time and Space. Boulder, Colorado, Geological Society of America Special Paper 441, pp. 1-28.

Bowman, K.P., Huang, J., 1991. A multigrid solver for the Helmholtz equation on a semiregular grid on the sphere. Monthly Weather Review 119, 769-775.

Breecker, D.O., Sharp, Z.D., McFadden, L.D., 2010. Atmospheric CO2 concentrations during ancient greenhouse climates were similar to those predicted for A.D. 2100. Proceedings of the National Academy of Sciences of the United States of America 107, 576-580.

Brenchley, P.J., Marshall, J.D., Carden, G.A.F., Robertson, D.B.R., Long, D.G.F., Meidla, T., Hints, L., Anderson, T.F., 1994. Bathymetric and isotopic evidence for a short-lived late Ordovician glaciation in a greenhouse period. Geology 22, 295-298.

Brenchley, P.J., Carden, G.A., Hints, L., Kaljo, D., Marshall, J.D., Martma, T., Meidla, T., Nolvak, J., 2003. High-resolution stable isotope stratigraphy of upper Ordovician sequences: constraints on the timing of bioevents and environmental changes associated with mass extinction and glaciation. Geological Society of America Bulletin 115, 89-104.

Budyko, M.I., 1969. The effect of solar radiation on the climate of the Earth. Tellus 21, 611-619.

Caputo, M.V., 1985. Late Devonian glaciation in South America. Palaeogeography, Palaeoclimatology, Palaeoecology 51, 291-317.

CLIMAP project members, 1976. The surface of the ice-age earth. Science 191, 1131-1136.

CLIMAP project members, 1981. Seasonal reconstruction of the earth's surface at the last glacial maximum. GSA Map and Chart Series, MC-36.

Crowell, J.C., 1999. Pre-Mesozoic ice ages: their bearing on understanding the climate system. Memoir 192, Geological Society of America, Boulder, Colorado, pp. 106.

Crowley, T.J., 2000. CLIMAP SSTs re-visited. Climate Dynamics 16, 241-255.

Crowley, T.J., Short, D.A., Mengel, J.G., North, G.R., 1986. Role of seasonality in the evolution of climate during the last 100 million years. Science 231, 579-584.

Crowley T.J., Mengel, J.G., Short, D.A., 1987. Gondwanaland's seasonal cycle. Nature 329, 803-807.

Crowley, T.J., North, G.R., 1988. Abrupt climate change and extinction events in Earth history. Science 240, 996-1002.

Crowley, T.J., Hyde, W.T., Short, D.A., 1989. Seasonal cycle of variations on the supercontinent of Pangea. Geology 17, 457-460.

Crowley, T.J., North, G.R., 1990. Modeling onset of glaciation. Annals of Glaciology 14, 39-42.

Crowley, T.J., Baum, S.K., 1991. Estimating Carboniferous sea-level fluctuations from Gondwanan ice extent. Geology 19, 975-977.

Crowley, T.J., North, G.R., 1991. Paleoclimatology. Oxford University Press, New York.

Crowley, T.J., Baum, S. K., 1992. Modeling late Paleozoic glaciation. Geology 20, 507-510.

Crowley, T.J., Yip, K.J., Baum, S.K., 1994. Snowline instability in a general circulation model: application to Carboniferous glaciation. Climate Dynamics 10, 363-376.

Crowley, T.J., Baum, S. K., 1995. Toward reconciliation of late Ordovician (~440Ma) glaciation with very high CO_2 levels. Journal of Geophysical Research 96, 22597-22610.

Crowley, T.J., Berner, R.A., 2001. CO_2 and climate change. Science 292, 870-872.

Crowley, T.J., Hyde, W.T., 2008. Transient nature of late Pleistocene climate variability. Nature 456, 226-230.

De Lurio, J.L., Frakes, L.A., 1999. Glendonites as a paleoenvironmental tool: implications for early Cretaceous high latitude climates in Australia. Geochimica et Cosmochimica Acta 63, 1039-1048.

DeConto, R.M., Pollard, D., 2003. Rapid Cenozoic glaciation of Antarctica induced by declining atmospheric CO_2. Nature 421, 245-249.

Delabroye, A., Vecoli, M., 2010. The end-Ordovician glaciation and the Hirnantian Stage: a global review and questions about late Ordovician event stratigraphy. Earth-Science Reviews 98, 269-282.

Drysdale, R.N., Hellstrom, J.C., Zanchetta, G., Fallick, A.E., Goni, M.F.S., Couchoud, I., McDonald, J., Maas, R., Lohmann, G., Isola, I., 2009. Evidence for obliquity forcing of glacial termination II. Science 325, 1527-1531.

Ekart, D.D., Cerling, T.E., Montanez, I.P., Tabor, N.J., 1999. A 400 million year carbon isotope record of pedogenic carbonate: implications for paleoatmospheric carbon dioxide. American Journal of Science 299, 805-827.

Fisher, A.G., 1982. Long-term climatic oscillations recorded in stratigraphy. In: Berger, W.H., Crowell, J.C., (Eds.), Climate in Earth History. National Academy Press, Washington, D.C., pp. 97-104.

Frakes, L.A., 1979. Climate through geologic time. Elsevier, Amsterdam.

Frakes, L.A., Francis, J.E., 1990. Cretaceous paleoclimate. In: Ginsburg, R.N., Beaudoin, B., (Eds.), Cretaceous Resources, Events and Rhythms. Kluwer Academic Publishers, Dordrecht, pp. 273-287.

Frakes, L.A., Francis, J.E., 1988. A guide to Phanerozoic cold polar climates from high-latitude ice rafting in the Cretaceous. Nature 333, 546-549.

Frakes, L.A., Francis, J.E., Syktus, J.I., 1992. Climate Modes of the Phanerozoic. Cambridge University Press, Cambridge.

Galeotti, S., Rusciadelli, G., Sprovieri, M., Lanci, L., Gaudio, A., Pekar, S., 2009. Sea-level control on facies architecture in the Cenomanian–Coniacian Apulian margin (Western Tethys): a record of glacio-eustatic fluctuations during the Cretaceous greenhouse? Palaeogeography, Palaeoclimatology, Palaeoecology 276, 196–205.

Greve, R., Wyrwoll, K-H., Eisenhauer, A., 1999. Deglaciation of the northern hemisphere at the onset of the Eemian and Holocene. Annals of Glaciology 28, 1-8.

Greve, R., 2005. Relation of measured basal temperature and spatial distribution of the geothermal heat flux for the Greenland ice sheet. Annals of Glaciology 42, 424-432.

Hallam, A., 1992. Phanerozoic Sea-Level Changes. Columbia University Press, New York.

Hambrey, M.J., 1985. The late Ordovician: early Silurian glacial record. Palaeogeography, Palaeoclimatology, Palaeoecology 51, 273-289.

Haq, B.U., Hardenbol, J., Vail, P.R., 1987. Chronology of fluctuating sea levels since the Triassic. Science 235, 1156-1167.

Hays, J.D., Imbrie, J., Shackleton, N.J., 1976. Variations in the Earth's orbit: pacemaker of the ice ages. Science 194, 1121-1132.

Held, I.M., Linder, D.I., Suarez, M.J., 1981. Albedo feedback, the meridional structure of the effective heat diffusivity: results from dynamic and diffusive models. Journal of the Atmospheric Sciences 38, 1911-1927.

Holbourn, A., Kuhnt, W., Schulz, M., Erlenkeuser, H., 2005. Impacts of orbital forcing and atmospheric carbon dioxide on Miocene ice-sheet expansion. Nature 438, 483-487.

Huang, J., Bowman, K.P., 1992. The small ice cap instability in seasonal energy balance models. Climate Dynamics 7, 205-215.

Huybers, P., 2006. Early Pleistocene glacial cycles and the integrated summer insolation forcing. Science 313, 508-511.

Huybers, P, Tziperman, E., 2008. Integrated summer insolation forcing and 40,000-year glacial cycles: the perspective from an ice-sheet/energy-balance model. Paleoceanography 23, PA1208, doi: 10.1029/2007PA001463.

Hyde, W.T., Kim, K.Y., Crowley, T.J., North, G.R., 1989. A comparison of GCM and energy balance model simulations of seasonal temperature changes over the past 18,000 years. Journal of Climate 2, 864-887.

Hyde, W.T., Kim, K.Y., Crowley, T.J., 1990. On the relation between polar continentality and climate: studies with a nonlinear seasonal energy balance model. Journal of Geophysical Research 95, 18653-18668.

Hyde, W.T., Grossman, E.L., Crowley, T.J., Pollard, D., Scotese, C.R., 2006, Siberian glaciation as a constraint on Permian-Carboniferous CO_2 levels. Geology 34, 421-424.

Imbrie, J., Imbrie, J.Z., 1980. Modeling the climate response to orbital variations. Science 207, 943-953.

Isbell, J.L., Miller, M.F., Wolfe, K.L., Lenaker, P.A., 2003. Timing of late Paleozoic glaciation in Gondwana: was glaciation responsible for the development of northern hemisphere cyclothems? In: Chan, M.A., Archer, A.W., (Eds.), Extreme Depositional Environments: Mega End Members in Geologic Time. Boulder, Colorado, Geological Society of America Special Paper 370, pp. 5-24.

Jones, A.T., Fielding, C.R., 2004. Sedimentological record of the late Paleozoic glaciation in Queensland, Australia. Geology 32, 153-156.

Kemper, J.P., 1987. Das Klima der Kreide-Zeit. Geologisches Jahrbuch Reihe A 96, 5-185.

Kim, S., Crowley, T.J., Erickson, D.J., Govindasamy, B., Duffy, P.B., Lee, B.Y., 2007. High-resolution climate simulation of the last glacial maximum. Climate Dynamics 31, 1-16.

Kump, L.R., Arthur, M.A., Patzkowsky, M.E., Gibbs, M.T., Pinkus, D.S., Sheehan, P.M., 1999. A weathering hypothesis for glaciation at high atmospheric Pco2 during the

Late Ordovician. Palaeogeography, Palaeoclimatology, Palaeoecology 152, 173-187.

Kump, L.R., 2002. Reducing uncertainty about carbon dioxide as a climate driver. Nature 419, 188-190.

Kyle, H.L., Weiss, M., Ardency, P., 1995. Cloud, surface temperature, and outgoing longwave radiation for the period from 1979 to 1990. Journal of Climate 8, 2644-2658.

Lin, R.Q., North, G.R., 1990. A study of abrupt climate change in a simple nonlinear climate model. Climate Dynamics 4, 253-261.

Marqueda, M.A.M., Willmott, A.J., Bamber, J.L., Darby, M.S., 1998. An investigation of the small ice cap instability in the Southern Hemisphere with a coupled atmosphere-sea ice-ocean-terrestrial ice model. Climate Dynamics 14, 329-352.

Matteucci, G.M., 1993. Multiple equilibria in a zonal energy balance climate model: the thin ice cap instability. Journal of Geophysical Research 98, D10, 18515-18526.

Melchin M.J., Holmden, C., 2006. Carbon isotope chemostratigraphy in Arctic Canada: sea-level forcing of carbonate platform weathering and implications for Hirnantian

global correlation. Palaeogeography, Palaeoclimatology, Palaeoecology 234, 186-200.

Mengel, J.G., Short, D.A., North, G.R., 1988. Seasonal snowline instability in an energy balance model. Climate Dynamics 2, 127-131.

Miller, K.G., 2009. Broken greenhouse windows. Nature Geoscience 2, 465-466.

Miller, K.G., Barrera, E., Olsson, R.K., Sugarman, P.J., Savin, S.M., 1999. Does ice drive early Maastrichtian eustasy? Geology 27, 783-786.

Miller, K.G., Sugarman, P.J., Browning, J.V., Kominz, M.A., Hernandez, J.C., 2003. Late Cretaceous chronology of large, rapid sea-level changes: glacioeustasy during the greenhouse world. Geology 31, 585-588.

Miller, K.G., Sugarman, P.J., Browning, J.V., Kominz, M.A., Olsson, R.K., Feigenson, M.D., Hernandez, J.C., 2004. Upper Cretaceous sequences and sea-level history, New Jersey coastal plain. Geological Society of America Bulletin 116, 368-393.

Miller, K.G., Kominz, M.A., Browning, J.V., Wright, J.D., Mountain, G.S., Katz, M.E., Sugarman, P.J., Cramer, B.S., Christie-Blick, N., Pekar, S.F., 2005. The Phanerozoic record of global sea-level change. Science 310, 1293-1298.

Montanez, I.P., Tabor, N.J., Niemeier, D., Dimichele, W.A., Frank, T.D., Fielding, C.R., Isbell, J.L., Birgenheier, L. P., Rygel, M. C., 2007. CO_2-forced climate and vegetation instability during late Paleozoic deglaciation. Science 315, 87-91.

Mora, C.I., Driese, S.G., Colarusso, L.A., 1996. Middle to late Paleozoic atmospheric CO_2 levels from soil carbonate and organic matter. Science 271, 1105-1107.

Myhre, G., Highwood, E.J., Shine, K.P., Stordal, F., 1998. New estimates of radiative forcing due to well mixed greenhouse gases. Geophysical Research Letters 25, 2715-2718.

North, G.R., 1984. The small ice cap instability in diffusive climate models. Journal of the Atmospheric Sciences 41, 3390-3395.

North, G.R., Cahalan, R.F., Coakley, J.A., 1981. Energy balance models. Review of Geophysics and Space Physics 19, 91-121.

North, G.R., Mengel, J.G., Short, D.A., 1983. Simple energy model resolving the seasons and the continents: application to the astronomical theory of the ice age. Journal of Geophysical Research 88, 6576-6586.

North, G.R., Wu, Q., 2001. Detecting climate signals using space-time EOFs. Journal of Climate 14, 1839-1863.

Ogura, T., Abe-Ouchi, A., 2001. Influence of the Antarctic ice sheet on southern high latitude climate during the Cenozoic: Albedo vs topography effect. Geophysical Research Letters 28, 587-590.

Otto-Bliesner, B.L., 1996. Initiation of a continental ice sheet in a global climate model (Genesis). Journal of Geophysical Research 101, 16909-16920.

Paterson, W.S.B., 1972. Laurentide ice sheets: estimated volumes during late Wisconsin. Reviews of Geophysics and Space Physics 10, 885-917.

Paterson, W.S.B., 1994. The physics of glaciers. Pergamon, Oxford, UK.

Peltier, W.R., 2004. Global glacial isostasy and the surface of the ice-age earth: the ICE-5G (VM2) model and GRACE. Annual Review of Earth Planetary Sciences 32, 111-149.

Petit, J.R., Jouzel, J., Raynaud, D., Barkov, N.I., Barnola, J-M., Basile, I., Bender, M., Chappellaz, J., Davisk, M., Delaygue, G., Delmotte, M., Kotlyakov, V.M., Legrand, M., Lipenkov, V.Y., Lorius, C., Pepin, L., Ritz, C., Saltzmank, E.,

Stievenard, M.,1999. Climate and atmospheric history of the past 420,000 years from the Vostok ice core, Antarctica. Nature 399, 429-436.

Pollard, D., DeConto, R.M., 2005. Hysteresis in Cenozoic Antarctic ice-sheet variations. Global and Planetary Change 45, 9-21.

Pollard, D., DeConto, R.M., 2009. Modelling West Antarctic ice sheet growth and collapse through the past five million years. Nature 458, 329-333.

Poulsen, C. J., Pollard, D., Montanez, I. P., Rowley, D., 2007. Late Paleozoic tropical climate response to Gondwanan deglaciation. Geology 35, 771-774.

Price, G.D., 1999. The evidence and implications of polar ice during the Mesozoic. Earth-Science Reviews 48, 183-210.

Rothman, D.H., 2002. Atmospheric carbon dioxide levels for the last 500 million years. Proceedings of the National Academy of Sciences 99, 4167-4171.

Royer, D.L., 2006. CO_2-forced climate thresholds during the Phanerozoic. Geochimica et Cosmochimica Acta 70, 5665-5675.

Royer, D.L., 2010. Fossil soils constrain ancient climate sensitivity. Proceedings of the National Academy of Sciences of the United States of America 107, 517-518.

Royer, D.L., Berner, R.A., Montanez, I.P., Tabor, N.J., Beerling, D.J., 2004. CO_2 as a primary driver of Phanerozoic climate. GSA Today 14, 4-10.

Royer, D.L., Berner, R.A., Park, J., 2007. Climate sensitivity constrained by CO_2 concentrations over the past 420 million years. Nature 446, 530-532.

Scotese, C.R., Golonka, J., 1992. PALEOMAP Paleogeographic Atlas, PALEOMAP progress report #20. Department of Geology, University of Texas at Arlington.

Selleck, B.W., Carr, P.F., Jones, B.G., 2007. A review and synthesis of glendonites (pseudomorphs after ikaite) with new data: assessing applicability as recorders of ancient coldwater conditions. Journal of Sedimentary Research 77, 980-991.

Sellers, W.D., 1969. A climate model based on the energy balance of the earth-atmosphere system. Journal of Applied Meteorology 8, 392-400.

Steuber, T., Rauch, M., Masse, J-P., Graaf, J., Malkoc, M., 2005. Low-latitude seasonality of Cretaceous temperatures in warm and cold episodes. Nature 437, 1341-1344.

Stevens, M.J., North, G.R., 1996. Detection of the climate response to the solar cycle. Journal of Atmospheric Sciences 53, 2594-2608.

Stoll, H.M., Schrag, D.P., 1996. Evidence for glacial control of rapid sea level changes in the early Cretaceous. Science 272, 1771-1774.

Stoll, H.M., Schrag, D.P., 2000. High-resolution stable isotope records from the Upper Cretaceous rocks of Italy and Spain: glacial episodes in a greenhouse planet? Geological Society of America Bulletin 112, 308-319.

Sutcliffe, O.E., Dowdeswell, J.A., Whittington, R.J., Theron, J.N., Craig, J., 2000. Calibrating the Late Ordovician glaciation and mass extinction by the eccentricity cycles of Earth's orbit. Geology 28, 967-970.

Thompson, S.L., Pollard, D., 1997. Greenland and Antarctic mass balances for present and doubled CO_2 from the GENESIS v.2 global climate model. Journal of Climate 10, 871-900.

Tripati, A.K., Roberts, C.D., Eagle, R.A., 2009. Coupling of CO_2 and ice sheet stability over major climate transitions of the last 20 million years. Science 326, 1394-1397.

Veevers, J.J., Powell, C.M., 1987. Late Paleozoic glacial episodes in Gondwanaland reflected in transgressive-regressive depositional sequence in Euramerica. Geological Society of America Bulletin 98, 475-487.

Veizer, J., Godderis, Y., Francois, L.M., 2000. Evidence for decoupling of atmospheric CO2 and global climate during the Phanerozoic eon. Nature 408, 698-701.

Worsley, T.R., Moore, T. L., Fraticelli, C. M., Scotese, C. R., 1994. Phanerozoic CO_2 levels and global temperatures inferred from changing paleogeography. In Klein, G. D., (Ed.), Pangea: Paleoclimate, Tectonics, and Sedimentation During Accretion, Zenith, and Breakup of a Supercontinent. Boulder, Colorado, Geological Society of America Special Paper 288, pp. 57-73.

Ziegler, A.M., Hulver, M.L., Rowley, D.B., 1997. Permian world topography and climate, In: Martini, I. P., (Ed.), Late Glacial and Post-Glacial Environmental Changes: Quaternary, Carboniferous-Permian and Proterozoic. Oxford University Press, New York, pp. 111-146.

VITA

Kelin Zhuang received his Bachelor of Science degree in geochemistry from Nanjing University in 1990. He entered Ocean University of China in September 1995 and received his Master of Science degree in marine geology in July 1998. He has directed several marine projects in China Geological Survey since 1998. In January 2007 he began his doctoral studies in geology at Texas A&M University majoring in paleoclimatology and graduated with his Ph.D. in August 2010.

Kelin Zhuang can always be reached at: klzhuang@hotmail.com and his mailing address is: Department of Geology and Geophysics, MS 3115, Texas A&M University, College Station, TX 77843-3115.